TECHNISCHE UNIVERSITÄT WIEN
Vienna | Austria

DIPLOMARBEIT

Investigation of First-Order Corrections in Bistatic Radiative Transfer Models for Remote Sensing of Vegetated Terrain

Ausgeführt am
TU Wien Department of Geodesy and Geoinformation
(Research Group Remote Sensing)
und dem
Atominstitut der Technischen Universität Wien

Unter der Anleitung von
Univ.-Prof. DI Dr. Wolfgang Wagner
und
Univ.-Prof. DI Dr. Franz Josef Maringer

durch

Raphael Ivan Quast

Ort, Datum

Ort, Datum

Abstract

The thesis is carried out in the field of satellite-based active remote sensing of the earth's surface using measurements of scattered radiation in the microwave domain.

Due to the capabilities of microwaves to partially penetrate vegetation, the existence of a vegetation-coverage above a soil-surface introduces additional contributions to the measured backscattered radiation. These contributions are both a benefit and a hindrance since on the one hand they contain valuable information on the vegetation-coverage that are hardly accessible by any other means, while on the other hand they act as a disturbance when studying the properties of the underlying soil-surface. At the present time, most investigations treat the effects of a vegetation-coverage on microwave backscatter measurements via a zero-order expansion of the radiative transfer equation in the scattering coefficient κ_s of the vegetation-layer. While this has been proven to give reasonably good agreement for measurements incorporating sparse vegetation, higher order scattering effects might give considerable contributions to the measured signal for more dense coverages like full-grown agricultural fields or forests. Since at the time of this investigation no general method on how to consistently evaluate higher order scattering contributions has been available, the main target of the following thesis is to develop a method for including (first-order) multiple-scattering effects, focussing on an analytic representation of the scattered radiation in order to allow reasonably fast processing of large datasets.

First, a short review on the successive orders of scattering approximation of the scalar radiative transfer equation is given, highlighting the requirements and constraints of the method. The presented representations of the individual scattering-contributions are kept in a general form suitable for bistatic calculations. The zero-order approximation of this series-expansion is the so-called $\omega - \tau-$model that has widely been used in previous studies to account for vegetation-corrections.
Next, the first-order multiple scattering contribution is investigated in great detail and a method for analytic evaluation of the appearing integrals for specific representations of the vegetation scattering phase-function $\hat{p}$ and the surface bidirectional reflectance distribution function $BRDF$ is presented. The introduced method remains applicable for any combination of $\hat{p}$ and $BRDF$ as long as they can be represented (or approximated) in terms of a power-series in the cosine of a generalized scattering-angle. Chapter 3 then provides a literature-review of possible analytic functions that are both applicable to the method of evaluating first-order contributions as developed in Chapter 2 and have a suitable shape to be used for approximating scattering distribution functions. Finally, some simulation-results are provided in Chapter 4 to show the dynamics of monostatic- and bistatic scattered radiation and the effects of multiple-scattering contributions with respect to changes in the main parameters for a given set of scattering distributions ($\hat{p}$ and $BRDF$).

Kurzfassung

Der folgende Text befasst sich mit der Beschreibung von satellitengestützten Beobachtungen der Erdoberfläche durch Messung der Streuung elektromagnetischer Strahlung im Mikrowellenbereich.

Aufgrund der Tatsache dass Vegetation im Mikrowellenbereich als teilweise transparent betrachtet werden muss, beinhaltet das gestreute Signal einer vegetationsbehafteten Oberfläche sowohl Anteile des Untergrunds, als auch Anteile welche durch Streuung an der Vegetation hervorgerufen werden. Diese Beiträge enthalten einerseits wertvolle Informationen über die Vegetation, fungieren jedoch andererseits als Störung bei der Ermittlung der Eigenschaften des Untergrunds. Aufgrund der hohen Komplexität der Berechnung von vielfachstreueffekten wurden Vegetationskorrekturen meist in Form einer Reihenentwicklung der Strahlungstransport-Gleichung im Streukoeffizienten κ_s verwendet, in welcher sämtliche Vielfachstreueffekte als vernachlässigbar angenommen wurden. Während diese Näherung für dünne Vegetationsschichten gute Übereinstimungen liefert, können Vielfachstreueffekte für dichtere Vegetation wie zum Beispiel Wald oder Agrarflächen nicht mehr vernachlässigbare Beiträge liefern. Da zum Zeitpunkt der Verfassung dieser Arbeit keine Methode zur konsistenten Berücksichtigung von Vielfachstreueffekten bekannt war, wurde der Fokus der folgenden Abhandlung auf die Entwicklung einer Methode zur Berechnung von Streueffekten erster-Ordnung in Form einer allgemein anwendbaren, analytischen Lösung gelegt.

Zu Beginn wird die Reihenentwicklung der Strahlungstransport-Gleichung im Streukoeffizienten des Vegetations-Layers wiederholt und die wesentlichen Bedingungen zur Anwendbarkeit dieser Näherung werden dargelegt. Die präsentierten Darstellungen der einzelnen Beiträge sind dabei allgemein gehalten, und sind somit auch zur Berechnung bistatischer Messungen geeignet. Die Vernachlässigung sämtlicher vielfachstreu-Beiträge führt zum sogenannten $\omega - \tau-$Modell welches weithin zur Berechnung von Vegetationskorrekturen verwended wurde.
Anschließend folgt eine detaillierte Abhandlung zur analytischen Berechnung der Beiträge erster Ordnung für allgemeine Streuphasenfunktionen $\hat{p}$ und Bidirektionale Reflektanzverteilungsfunktion $BRDF$. Die entwickelte Methode ist für beliebige kombinationen von $\hat{p}$ und $BRDF$ anwendbar, solange die verwendeten Funktionen als Potenzreihen im Cosinus eines verallgemeinerten Streuwinkels darstellbar (approximierbar) sind. Eine Auflistung möglicher Funktionen welche sowohl als fit-Funktionen für Streuverteilungen als auch zur Ermittlung der Beiträte erster-Ordnung über die zuvor eingeführte Methode geeignet sind ist in Kapitel 3 gegeben. Abschließend werden in Kapitel 4 einige Simulationen dargestellt um die Dynamik vom monostatischen- und bistatischen Messungen und die Effekte der Beiträge erster-Ordnung zu illustrieren.

Contents

1. Introduction **1**

2. A Scattering Model for Vegetated Terrain **3**
2.1. Vegetation in the Microwave Domain 3
2.2. Radiative Transfer Solution for Two-Layered Media 5
2.2.1. Individual Contributions 6
2.3. An Analytic Solution to the Interaction Term 10
2.4. Evaluation of the f_n coefficients 17
2.4.1. Existence of the f_n coefficients 17
2.4.2. An Algorithm for Coefficient Retrieval 21

3. Phase Functions **22**
3.1. Volume-Scattering Phase Functions 22
3.1.1. The Asymmetry Parameter g 23
3.1.2. The Isotropic Phase Function: 24
3.1.3. The Rayleigh Phase Function: 24
3.1.4. The Forward-Scattering Phase Function 24
3.1.5. Henyey Greenstein Phase Function 25
3.1.6. Henyey Greenstein Rayleigh Phase Function 25
3.1.7. Gaussian Peak 26
3.1.8. Gegenbauer Kernel Phase Function 27
3.2. Surface-BRDF's 28
3.2.1. Ideally Rough (*Lambertian*) Surface: 30
3.2.2. Cosine Lobes (*Phong Model*) 31
3.2.3. Generalized Cosine Lobes (*Lafortune Model*) 31
3.3. Further possibilities 32

4. Simulation results **34**
4.1. Connection between I_s and σ_0 34
4.2. Example specification 35
4.2.1. Surface parametrization 35
4.2.2. Covering layer parametrization 36
4.3. Example Results 37
4.3.1. Plot descriptions 37
4.3.2. Bistatic scattering distributions 38
4.3.3. Tau variations (Isotropic) 40
4.3.4. Tau variations (Rayleigh) 41

4.3.5. Tau variations (Henyey Greenstein $t = 0.2$) 43
4.3.6. Tau variations (Henyey Greenstein $t = 0.4$) 44
4.3.7. Contributions (Isotropic) 46
4.3.8. Contributions (Rayleigh) 47
4.3.9. Contributions (Henyey Greenstein $t = 0.2$) 48
4.3.10. Contributions (Henyey Greenstein $t = 0.4$) 49

A. Appendix **50**
A.1. Used symbols and definitions 50
A.2. Mathematical Methods 52
A.2.1. Cauchy Principal Value: 52
A.2.2. Exponential Integral Function $Ei(x)$ 53
A.3. Auxiliary Calculations 54
A.3.1. Solutions for Chapter 2.4.1 and 2.4.2 54
A.3.2. Legendre-expansion of the Gaussian Peak 56
A.3.3. Nadir hemispherical reflectance of Henyey-Greenstein Function 59

B. Published Paper **60**

References **68**

List of Figures

2.1. Schematic illustration of the considered geometry. 3
2.2. Idealization of the problem geometry 5
2.3. Illustration of the used variables and problem-geometry 6
2.4. Separation of up-and downwelling angles 6
2.5. Illustration of the reciprocity of the $BRDF$. 10
2.6. Illustration of the reciprocity of $\hat{p}$. 11

3.1. Isotropic- and Rayleigh phase function 24
3.2. Henyey-Greenstein function 25
3.3. HG-Rayleigh function 25
3.4. Gaussian peak 26
3.5. Lambertian BRDF 30
3.6. Cosine lobes of power L 31
3.7. Comparison Lafortune/Cosine-lobe 31
3.8. Linear combination of generalized Henyey-Greenstein phase-functions 33
3.9. Linear combination of BRDFs 33

4.1. Henyey Greenstein function used as BRDF approximation function . 35
4.2. Illustration of volume scattering phase functions 36
4.3. Illustration of the bistatic scattering coefficient - 01 38
4.4. Illustration of the bistatic scattering coefficient - 02 39
4.5. Tau variations (Isotropic) - 01 40
4.6. Tau variations (Isotropic) - 02 40
4.7. Tau variations (Isotropic) - 03 41
4.8. Tau variations (Rayleigh) - 01 41
4.9. Tau variations (Rayleigh) - 02 42
4.10. Tau variations (Rayleigh) - 03 42
4.11. Tau variations (Henyey Greenstein t=0.2) - 01 43
4.12. Tau variations (Henyey Greenstein t=0.2) - 02 43
4.13. Tau variations (Henyey Greenstein t=0.2) - 03 44
4.14. Tau variations (Henyey Greenstein t=0.4) - 01 44
4.15. Tau variations (Henyey Greenstein t=0.4) - 02 45
4.16. Tau variations (Henyey Greenstein t=0.4) - 03 45
4.17. Contributions (Isotropic) - 01 46
4.18. Contributions (Isotropic) - 02 46
4.19. Contributions (Isotropic) - 03 46

4.20. Contributions (Rayleigh) - 01 47
4.21. Contributions (Rayleigh) - 02 47
4.22. Contributions (Rayleigh) - 03 47
4.23. Contributions (Henyey Greenstein t=0.2) - 01 48
4.24. Contributions (Henyey Greenstein t=0.2) - 02 48
4.25. Contributions (Henyey Greenstein t=0.2) - 03 48
4.26. Contributions (Henyey Greenstein t=0.4) - 01 49
4.27. Contributions (Henyey Greenstein t=0.4) - 02 49
4.28. Contributions (Henyey Greenstein t=0.4) - 03 49

1. Introduction

Satellite based observations of the earth's surface using microwave radar measurements have been widely used to provide global-scale biophysical parameters like *soil-moisture*, *vegetation biomass*, etc.. Considering the temporal dynamics of the gained estimates, such measurements provide a basis for monitoring of *drought*, *desertification* and various other effects that are assumed to be crucial indicators of climate-change.

The retrieval process leading from actual measurements of (currently mostly monostatic) scattered intensity to the final model-parameter however is affected by various assumptions that are necessary in order to be able to describe the complicated measurement-setup within a reasonably simple theoretical framework.

To name a few obvious examples:

Surface-scattering dependencies:

- effective roughness of the soil surface in the considered frequency range
- penetration depth of the signal
  - → homogeneity of the soil-layer
  - → consideration of a subsurface dielectric profile
- response of the scattered intensity to a change in dielectric properties
- etc.

Vegetation-scattering dependencies:

- percentage of vegetation-coverage within the radar footprint
- composition of the individual vegetation constituents
- scattering characteristics of the vegetation constituents
  - → homogenity of the vegetation-layer
  - → dielectric properties of the vegetation constituents
- etc.

Within current remote-sensing retrieval models, most of the dependencies are either addressed via empirical relations or modelled theoretically by applying extensive simplifications.

The reason for this stems mainly from the following limitations:

1) most of the dependencies are only barely explored due to a lack of available measurements in the specific frequency range used within the experiments

2) the overall specification of the problem suffers from under-determination since mostly only monostatic observations from a single satellite are used within the retrieval-process. Without simultaneous acquisition of auxiliary data, the properties of the soil-surface and the state of the vegetation-coverage can only be specified via empirical relations or by incorporating assumptions that appear reasonable for the region of interest.

3) global-scale retrieval models generally allow only a limited complexity due to computational limitations because of the immense amount of data that has to be processed in reasonable times

The intention of the following thesis is therefore to provide a reasonably simple theoretical framework for modelling the effects induced by a vegetative coverage above a rough soil-surface for observations in the microwave domain. The focus of the investigation hereby is not the discussion on actual parametrization of real soil- and vegetation samples, but rather the development of a general method that is capable of evaluating the scattered intensity for given combinations of soil- and vegetation characteristics. The provided model is therefore not limited to the microwave-domain, but could equally well be used for describing completely different setups to which a treatment via the successive orders of scattering approximation of the *Radiative Transfer Equation* can be applied. However, since the intention of this thesis originates from studies in the field of microwave remote sensing, the nomenclature will mostly follow the remote-sensing terminology.

2. A Scattering Model for Vegetated Terrain

2.1. Vegetation in the Microwave Domain

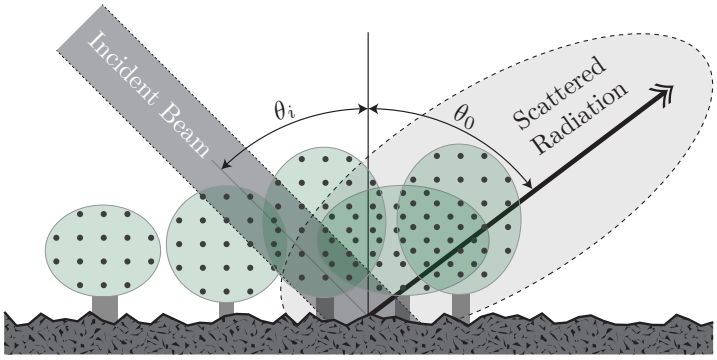

Figure 2.1.: Schematic illustration of the considered geometry.

Fig.2.1 shows a schematic illustration of the problem-geometry we are dealing with in the following, consisting of a rough surface covered by various types of vegetation that is illuminated by a beam of radiation at frequencies in the microwave domain.

In order to be able to formulate a reasonably simple model for the scattered radiation of a vegetation-covered surface, the description of both the vegetation and the soil-surface has to be carried out in a drastically simplified manner.

For scatterometer-observations using radiation in the microwave band (8-18GHz) it has been shown by *Attema and Ulaby* in 1978 that moderately dense vegetation can successfully be modelled as a **water-cloud** [1]. The underlying assumption hereby is, that moderate vegetation in the microwave domain has a low scattering coefficient[1] ($\kappa_s << 1$), leading to the fact that multiply scattered radiation within the canopy is assumed to be negligible.

[1]The scattering coefficient describes the fraction of radiation that is being scattered (as opposed to being absorbed or undergoing no interaction at all) when a beam of radiation impinges on a vegetation-constituent.

In other words, using this assumption, one considers only the following contributions when calculating the scattered radiation:

- radiation scattered directly from the ground surface
  (attenuated due to the absorptive properties of the vegetation-layer)
- radiation scattered once within the vegetation layer
  (again attenuated while propagating through the vegetation-layer)

Thus, all terms that involve intermediate scattering-events within the vegetation layer are neglected.

Even though this approach is a rather extreme simplification of the description of vegetation, it proved very successful when deriving surface soil-moisture over moderately vegetated terrain and was therefore implemented in numerous retrieval algorithms for active remote sensing observations [2].

However, as soon as the vegetation density increases or vegetation-constituents such as stems and trunks become more dominant, the assumption that intermediate scattering events yield negligible contributions is no longer justified as can be seen from the discussions in [3, 4, 5].

Consideration of multiple scattering effects however is an ongoing research field. The reason for this is mainly twofold:
First, there is a lack of reasonably simple models that are capable of accounting for first- and higher order scattering effects with a feasible computational effort, and second, there is a great lack of availability of the parameters that would be needed in order to fully parametrize the multiple-scattering problem since a consideration of multiple scattering contributions requires knowledge on the bistatic scattering characteristics of both the surface and the vegetation layer.

Within this thesis, it will be shown that first-order scattering effects can be expressed in an analytical manner by assuming certain reasonable restrictions on the functions used to describe the bistatic scattering distributions.

The gained solution for the first-order contributions is kept in a very general way, allowing it to be used for a great variety of possible scattering distributions.

The second problem, namely the specification of possible candidates for scattering distributions as well as their parametrization will then briefly be addressed in section 3. A detailed discussion on possible model-parametrizations that might be applied to certain types of vegetation or terrain however is beyond the scope of this thesis and is intended to be conducted within further investigations.

The method for evaluating the first-order interaction contribution which is at the core of this thesis was already published at the *OSA Journal of Applied Optics*. The resulting paper [6] is attached in Appendix B.

2.2. Radiative Transfer Solution for Two-Layered Media

Within the following chapter, the formulation of a *Radiative Transfer Model* describing the scattered radiation from a uniformly illuminated rough surface covered by a tenuous distribution of particulate media is reviewed.

For detailed information on the origin of the presented formulas the reader is referred to the preceding project thesis [7] in which the derivation of the successive orders of scattering approximation to the *Radiative Transfer Equation* is presented in great detail. The following section therefore serves just as a listing of results that are important for subsequent discussions. A survey of the used symbols and definitions is given in Appendix A.1.

In order to be able to treat the problem of a vegetation covered soil-surface, the initially very complicated problem is simplified drastically as shown in Fig.2.2, i.e.: it is assumed that the vegetation-cover can be described (for radiation within the microwave domain) as a homogeneous layer of particulate scattering- and absorbing media [1] described by a scattering coefficient κ_s and an extinction coefficient κ_{ex} together with a scattering phase-function that accounts for the directionality of the scattered radiation.

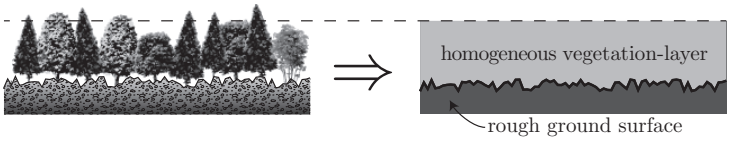

Figure 2.2.: Idealization of the problem geometry. (image taken from [7])

If we now consider a beam of radiative Intensity I, propagating within such a scattering- and absorbing media[2], the equation governing the attenuation of the intensity along it's ray-path is given by[3]:
(Detailed derivations and explanations can be found in [8], [9] or numerous other books covering the formulation of *Radiative Transfer Theory*)

$$\cos(\theta)\frac{\partial I_f(\mathbf{r},\Omega)}{\partial r} = -\kappa_{ex} I_f(\mathbf{r},\Omega) + \kappa_s \iint\limits_{\Omega'=4\pi} I_f(\mathbf{r},\Omega')\hat{p}(\Omega'\to\Omega)d\Omega' \tag{2.1}$$

$\mathbf{r}\ldots$	distance within the object	$\theta\ldots$	incidence-angle
$\Omega\ldots$	incident-direction $\Omega\equiv(\theta,\phi)$	$d\Omega=\sin(\theta)d\theta d\phi\ldots$	differential solid angle
$I_f\ldots$	intensity at frequency f	$\hat{p}(\Omega'\to\Omega)\ldots$	scattering phase function
$\kappa_{ex}\ldots$	extinction-coefficient	$\kappa_s\ldots$	scattering-coefficient

[2] Since the following discussion focusses on active remote sensing, the emission-properties of the media are assumed to give an negligible contribution to the measured signal.

[3] dr denotes the penetration depth within the object, i.e. $dr=\cos(\theta)\ ds \quad\Rightarrow\quad \frac{\partial I}{\partial s}=\cos(\theta)\frac{\partial I}{\partial r}$ (The problem geometry is illustrated in Fig.2.3)

Applying the assumption that the scattering-coefficient is small ($\kappa_s << 1$), the intensity emerging from the top of the canopy I_{em} in direction of the detector Ω_{em} can be found in terms of a series-expansion in κ_s, leading to a solution of the form:

$$I_{tot}(\Omega_{em}) = \overbrace{I_s(\Omega_{em}) + \underbrace{I_v(\Omega_{em})}}^{\text{cloud-model}} + \overbrace{\underbrace{I_{sv}(\Omega_{em}) + I_{vs}(\Omega_{em})}_{\propto\kappa_s} + I_{svs}(\Omega_{em})}^{1^{st}\text{order interaction}} + \mathcal{O}(\kappa_s^2) \quad (2.2)$$

The above representation of the solution to the *Radiative Transfer Equation* is usually referred to as *successive orders of scattering series*, since each appearing term ($I_s, I_v, I_{sv}, I_{vs}, I_{svs}$) represents a contribution due to a specific scattering event. The exact form of the appearing contributions and the assumptions used within the derivation is summarized briefly within the following section. The term I_{svs} represents a 2^{nd}-order scattering event and will therefore be omitted in the following.

2.2.1. Individual Contributions

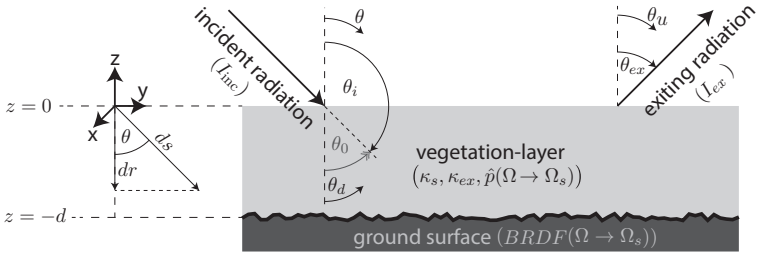

Figure 2.3.: Illustration of the used variables and problem-geometry as applied in the solution of the *Radiative Transfer Equation.* (image taken from [7])

The definition of the used variables is shown in Fig.2.3. In order to be able to introduce the boundary condition of a reflecting surface, the *Radiative Transfer Equation* (Eq. 2.1) is split into a set of two coupled integro-differential equations, one for upwelling and one for downwelling radiation. [7]

This separation is achieved by splitting the radiative intensity into an upwelling and downwelling part via:

$$I^+(\theta_u, \phi) = I_f(\theta_u, \phi) \qquad \theta_u \in \left[0, \frac{\pi}{2}\right]$$
$$I^-(\theta_d, \phi) = I_f(\pi - \theta_d, \phi) \qquad \theta_d \in \left[\frac{\pi}{2}, 0\right]$$

The resulting representation of Eq.2.1 in terms of an upwelling angle θ_u and a downwelling angle θ_d (measured counter-clockwise) is given by:

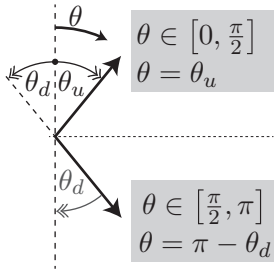

Figure 2.4.: Separation of up-and downwelling angles

$$\mu_u \frac{\partial I^+(\mu_u)}{\partial r} + \kappa_{ex} I^+(\mu_u) = F^+(\mu_d) \qquad \mu_u \in [1,0] \tag{2.3}$$

$$-\mu_d \frac{\partial I^-(\mu_d)}{\partial r} + \kappa_{ex} I^-(\mu_d) = F^-(\mu_d) \qquad \mu_d \in [0,1] \tag{2.4}$$

with $\mu_u = \cos(\theta_u), \quad \mu_d = \cos(\theta_d)$ and:

$$F^{\pm}(\mu_{\substack{u\\d}}) = \kappa_s \int_{\phi'=0}^{2\pi} \int_{\mu'=0}^{1} \Big[I^+(\mu') \hat{p}(\mu' \to \pm\mu_{\substack{u\\d}}) + I^-(\mu') \hat{p}(-\mu' \to \pm\mu_{\substack{u\\d}}) \Big] d\mu' d\phi' \tag{2.5}$$

Even though the right hand sides of Eq.2.3 and Eq.2.4 still contain the unknown up- and downwelling intensities $I^{\pm}(\mu_{\substack{u\\d}})$, the above equations can be used as a starting-point for deriving a successive orders of scattering series for the upwelling radiation by solving the equations with the assumption that the source-terms $F^{\pm}(\mu_{\substack{u\\d}})$ are known a priori. Using the method of variation of constants to solve the inhomogeneous differential equations, one arrives at the following *"formal"* solutions:

$$I^+(z,\mu_u) = I^+(-d,\mu_u) e^{-\frac{\kappa_{ex}}{\mu_u}(z+d)} + \int_{-d}^{z} \frac{1}{\mu_u} e^{-\frac{\kappa_{ex}}{\mu_u}(z-z')} F^+(z',\mu_u) dz' \tag{2.6}$$

$$I^-(z,\mu_d) = I^-(0,\mu_d) e^{\frac{\kappa_{ex}}{\mu_d} z} + \int_{z}^{0} \frac{1}{\mu_d} e^{-\frac{\kappa_{ex}}{\mu_d}(z-z')} F^-(z',\mu_d) dz' \tag{2.7}$$

The necessary boundary conditions to specify the appearing boundary-terms $I^+(-d,\mu_u,\phi)$ and $I^-(0,\mu_u,\phi)$ can now be introduced by assuming that the top of the vegetation-canopy is uniformly illuminated at a single incidence-angle $\mu_0 = \cos(\theta_0)$ and furthermore that radiation impinging on the ground surface is reflected upwards according to a given *Bidirectional Reflectance Distribution Function* $BRDF(\Omega \to \Omega_s)$.

The used boundary-conditions are thus given by:

$$I^-(0,\theta_d) = I_{\text{inc}} \delta(\mu_d - \mu_0) \delta(\phi_d - \phi_0) \tag{2.8}$$

$$I^+(-d,\mu_u) = \int_{\phi=0}^{2\pi} \int_{\mu_d=0}^{1} \mu_d \; BRDF(-\mu_d \to \mu_u) \; I^-(-d,\mu_d) \; d\mu_d d\phi \tag{2.9}$$

Once the boundary-conditions have been specified, a series-expansion of the upwelling radiation with respect to the scattering coefficient κ_s can be obtained by successively inserting the representations Eq.2.6 and 2.7 into the unknown source-terms $F^{\pm}(\mu_{\substack{d\\u}})$ and sorting the appearing terms with respect to κ_s.

The individual contributions appearing in the successive orders of scattering expansion of the upwelling intensity when considering only first order interaction events are given by:

τ hereby denotes the *Optical Depth* of the canopy, which has been introduced as:

$$\tau = \kappa_{ex} d \tag{2.10}$$

Surface-Contribution:
Radiation scattered once by the ground-surface

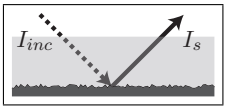

At a distance $z \in [-d, 0]$ within the canopy:

$$I_s^+(z, \mu_0, \mu_{ex}) = I_{inc}\, e^{-\frac{\kappa_{ex} d}{\mu_0}} e^{-\frac{\kappa_{ex}(z+d)}{\mu_{ex}}}\ \mu_0\ BRDF(-\mu_0 \to \mu_{ex})$$

At the top of the canopy ($z = 0$):

$$I_s^+(\mu_0, \mu_{ex}) = I_{inc}\, e^{-\frac{\tau}{\mu_0}} e^{-\frac{\tau}{\mu_{ex}}}\ \mu_0\ BRDF(-\mu_0 \to \mu_{ex}) \tag{2.11}$$

Volume-Contribution
Radiation scattered once by the vegetation-canopy

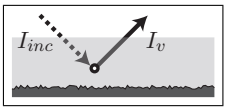

At a distance $z \in [-d, 0]$ within the canopy:

$$I_v^+(\Omega) = I_{inc}\ \omega\ \frac{\mu_0}{\mu_0 + \mu_{ex}} \Big(e^{-\frac{\kappa_{ex} z}{\mu_0}} - e^{-\frac{\kappa_{ex} d}{\mu_0}} e^{-\frac{\kappa_{ex}(z+d)}{\mu_{ex}}} \Big) \hat{p}(-\mu_0 \to \mu_{ex})$$

At the top of the canopy ($z = 0$):

$$I_v^+(\Omega) = I_{inc}\ \omega\ \frac{\mu_0}{\mu_0 + \mu_{ex}} \Big(1 - e^{-\frac{\tau}{\mu_0}} e^{-\frac{\tau}{\mu_{ex}}} \Big) \hat{p}(-\mu_0 \to \mu_{ex}) \tag{2.12}$$

Surface-Volume-Contribution
Radiation scattered first by the surface, and then by the vegetation-canopy

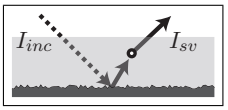

At a distance $z \in [-d, 0]$ within the canopy:

$$I_{sv}^+ = I_{inc}\, \omega\, e^{-\frac{\kappa_{ex} d}{\mu_0}} \mu_0 \int_0^{2\pi} \int_0^1 \frac{\mu'}{\mu_{ex} - \mu'} \Big(e^{-\frac{\kappa_{ex}(z+d)}{\mu_{ex}}} - e^{-\frac{\kappa_{ex}(z+d)}{\mu'}} \Big) BRDF(-\mu_0 \to \mu') \hat{p}(\mu' \to \mu_{ex}) d\mu' d\phi'$$

At the top of the canopy ($z = 0$):

$$I_{sv}^+ = I_{inc}\, \omega\, e^{-\frac{\tau}{\mu_0}} \mu_0 \int_0^{2\pi} \int_0^1 \frac{\mu'}{\mu_{ex} - \mu'} \Big(e^{-\frac{\tau}{\mu_{ex}}} - e^{-\frac{\tau}{\mu'}} \Big) BRDF(-\mu_0 \to \mu') \hat{p}(\mu' \to \mu_{ex}) d\mu' d\phi' \tag{2.13}$$

Volume-Surface-Contribution
Radiation scattered first by the vegetation-canopy, and then by the surface.

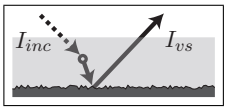

At a distance $z \in [-d, 0]$ within the canopy:

$$I_{vs}^{+} = I_{inc}\,\omega\, e^{-\frac{\kappa_{ex}(d+z)}{\mu_{ex}}}\mu_0 \int_0^{2\pi}\int_0^{1} \frac{\mu'}{\mu_0-\mu'}\left(e^{-\frac{\kappa_{ex}d}{\mu_0}} - e^{-\frac{\kappa_{ex}d}{\mu'}}\right)\hat{p}(-\mu_0 \to -\mu')BRDF(-\mu' \to \mu_{ex})\,d\mu' d\phi'$$

At the top of the canopy ($z = 0$):

$$I_{vs}^{+} = I_{inc}\,\omega\, e^{-\frac{\tau}{\mu_{ex}}}\mu_0 \int_0^{2\pi}\int_0^{1} \frac{\mu'}{\mu_0-\mu'}\left(e^{-\frac{\tau}{\mu_0}} - e^{-\frac{\tau}{\mu'}}\right)\hat{p}(-\mu_0 \to -\mu')BRDF(-\mu' \to \mu_{ex})\,d\mu' d\phi' \tag{2.14}$$

As one can see from the above equations, both the direct surface term (Eq. 2.11) and the direct volume term (Eq. 2.12) are already given explicitly if the vegetation *scattering phase-function* $\hat{p}$ and the *Bidirectional Reflectance Distribution Function* $BRDF$ of the underlying ground surface are known.

Furthermore, considering the monostatic case (i.e. $\theta_{ex} = \theta_0$ and $\phi_{ex} = \phi_0 + \pi$), this means that a simple qualitative description of the backscattering properties is sufficient as long as a zero-order approximation is used, and one does not have to bother on the bistatic scattering properties of both the surface and the vegetation layer. However, as soon as higher order interaction-terms become relevant, knowledge on the bistatic scattering distributions is necessary in order to solve the remaining integrals in the surface-volume and volume-surface contribution.

As already mentioned, unfortunately very sparse information on how to analytically approximate the bistatic scattering characteristics of vegetation- and rough soil surfaces in the microwave region is currently available. To overcome this problem, it will be shown in the following that the first-order interaction integrals can be solved analytically by expressing the surface- and vegetation scattering distributions as polynomial expansions in the scattering angle. In section 2.4, it will then be proven that such polynomial approximations exist for a wide range of possible analytic distribution functions that can be used to approximate the scattering behaviour of both the ground-surface and the vegetation coverage.

In chapter 3, a listing of possible analytic functions that might be used as fit-functions to given bistatic measurements is provided together with their polynomial expansions as needed in order to evaluate the associated first-order interaction contribution.

2.3. An Analytic Solution to the Interaction Term

From Eq.2.13 and Eq.2.14 one can see, that the remaining integrals that have to be solved are given by:

Surface-Volume Term:

$$F_{int}^{sv}(\mu_0, \mu_{ex}) = \int_0^{2\pi}\int_0^1 \frac{\mu'}{\mu_{ex} - \mu'}\left(e^{-\frac{\tau}{\mu_{ex}}} - e^{-\frac{\tau}{\mu'}}\right) BRDF(-\mu_0 \to \mu')\hat{p}(\mu' \to \mu_{ex})\ d\mu' d\phi' \tag{2.15}$$

Volume-Surface Term:

$$F_{int}^{vs}(\mu_0, \mu_{ex}) = \int_0^{2\pi}\int_0^1 \frac{\mu'}{\mu_0 - \mu'}\left(e^{-\frac{\tau}{\mu_0}} - e^{-\frac{\tau}{\mu'}}\right) BRDF(-\mu' \to \mu_{ex})\hat{p}(-\mu_0 \to -\mu')\ d\mu' d\phi' \tag{2.16}$$

In the following we restrict ourselves to $BRDF$ and *volume-phase functions* obeying reciprocity, and use the following identities to find that the remaining integrals are actually related via a simple change of variables.

A function is said to be reciprocal if it is *invariant under a change of incoming and outgoing directions.*

In Fig.2.5 and Fig.2.6 the geometry for the reciprocity conditions of both the $BRDF$ and $\hat{p}$ is shown. It is important to notice that for the $BRDF$ we have to distinguish between upwelling and downwelling radiation since each scattering event transforms downwelling to upwelling radiation and their angular description is different according to the separation introduced in Fig.2.4 .

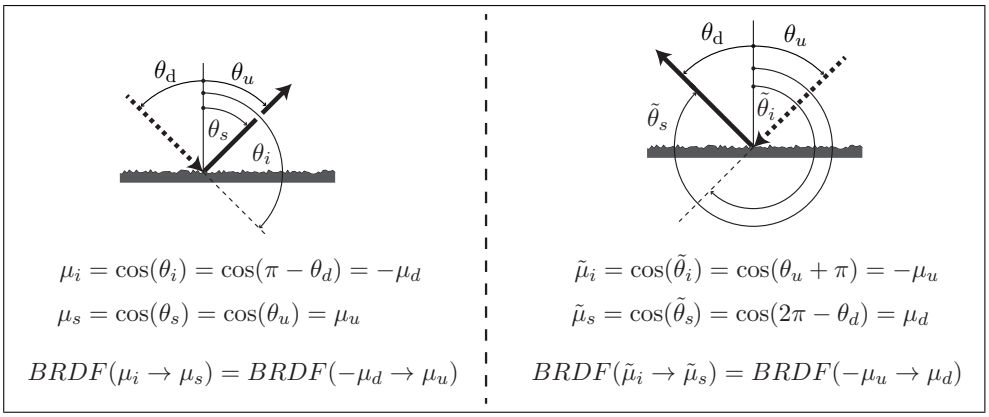

Figure 2.5.: Illustration of the reciprocity of the $BRDF$.

From Fig. 2.5 we can thus deduce that the reciprocity condition for the BRDF is given by:

$$BRDF(-\mu_d \to \mu_u) = BRDF(-\mu_u \to \mu_d) \tag{2.17}$$

For $\hat{p}$ we do not need to consider such a transformation since for both *volume-surface* and *surface-volume* interaction contributions the volume-scattering is either (upwelling) → (upwelling) or (downwelling) → (downwelling).

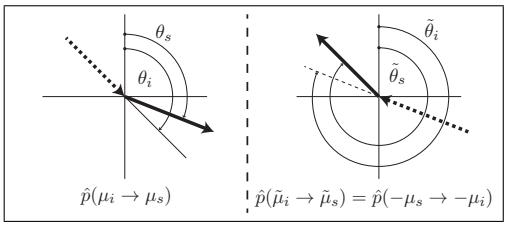

Figure 2.6.: Illustration of the reciprocity of $\hat{p}$.

Thus, the reciprocity condition for $\hat{p}$ is given by:

$$\hat{p}(\mu_i \to \mu_s) = \hat{p}(-\mu_s \to -\mu_i) \tag{2.18}$$

Inserting those conditions in Eq. 2.15 and Eq. 2.16 we find:

$$\Rightarrow \qquad F_{int}^{sv}(\mu_0, \mu_{ex}) = F_{int}^{vs}(\mu_{ex}, \mu_0) := F_{int}(\mu_0, \mu_{ex}) \tag{2.19}$$

In order to solve the remaining integral, we will assume that the following (approximately finite) series-expansion is known:

$$\int_0^{2\pi} BRDF(-\mu_0 \to \mu)\hat{p}(\mu \to \mu_{ex})\, d\phi \approx \sum_{n=0}^{N_{max}} f_n(\mu_0, \mu_{ex})\, \mu^n \tag{2.20}$$

The existence of the expansion-coefficients f_n and methods of it's evaluation will be discussed in section 2.4.

Expanding the product of the $BRDF$ and $\hat{p}$ in terms of a series as defined in Eq.(2.20), the integral simplifies to:

$$\begin{aligned} F_{int}(\mu_0, \mu_{ex}) &= \sum_{n=0}^{N_{max}} f_n(\mu_0, \mu_{ex}) \left\{ \left[e^{-\frac{\tau}{\mu_{ex}}} \int_0^1 \frac{(\mu')^{n+1}}{\mu_{ex} - \mu'} d\mu' \right] - \left[\int_0^1 \frac{(\mu')^{n+1}}{\mu_{ex} - \mu'} e^{-\frac{\tau}{\mu'}} d\mu' \right] \right\} \\ &= \sum_{n=0}^{N_{max}} f_n(\mu_0, \mu_{ex}) \left[e^{-\frac{\tau}{\mu_{ex}}} A(n+1) - B(n+1) \right] \end{aligned} \tag{2.21}$$

Where the remaining integrals $A(N), B(N)$ are given by:

$$A(N) = \int_0^1 \frac{(\mu')^N}{\mu_{ex} - \mu'} d\mu' \qquad B(N) = \int_0^1 \frac{(\mu')^N}{\mu_{ex} - \mu'} e^{-\frac{\tau}{\mu'}} d\mu' \tag{2.22}$$

In order to solve those integrals, we expand the fraction within the integrals as follows: (the validity can readily be proven by means of complete induction)

$$\frac{(\mu')^N}{\mu_{ex}-\mu'} = \frac{\mu_{ex}^N}{\mu_{ex}-\mu'} - \sum_{k=1}^{N} \mu_{ex}^{N-k}(\mu')^{k-1} \tag{2.23}$$

Inserting this expansion, we are thus left with:

$$A(N) = \underbrace{\int_0^1 \frac{\mu_{ex}^N}{\mu_{ex}-\mu'} d\mu'}_{A_1} - \sum_{k=1}^{N} \underbrace{\int_0^1 \mu_{ex}^{N-k}(\mu')^{k-1} d\mu'}_{A_2} \tag{2.24}$$

$$B(N) = \underbrace{\int_0^1 \frac{\mu_{ex}^N}{\mu_{ex}-\mu'} e^{-\frac{\tau}{\mu'}} d\mu'}_{B_1} - \sum_{k=1}^{N} \underbrace{\int_0^1 \mu_{ex}^{N-k}(\mu')^{k-1} e^{-\frac{\tau}{\mu'}} d\mu'}_{B_2} \tag{2.25}$$

$\mathbf{A}_1$:

Before solving the integral A_1, we notice that the integrand encounters a singularity for $\mu' = \mu_{ex}$. Since $\mu_{ex} \in (0,1)$, we know that this singularity is definitely located within the integration-interval, and therefore the value of the integral is only meaningful in terms of its Cauchy Principal Value (see Appendix A.2.1). Thus, we write:

$$\int_0^1 \frac{\mu_{ex}^N}{\mu_{ex}-\mu'} d\mu' \quad \Rightarrow \quad \lim_{\epsilon\to 0}\left(\int_0^{\mu_{ex}-\epsilon} \frac{\mu_{ex}^N}{\mu_{ex}-\mu'} d\mu' + \int_{\mu_{ex}+\epsilon}^1 \frac{\mu_{ex}^N}{\mu_{ex}-\mu'} d\mu' \right)$$

In order to evaluate the limit, we first have to find the general solution to the integral which is readily obtained via:

$$\int \frac{\mu_{ex}^N}{\mu_{ex}-\mu'} d\mu' = \left| \begin{array}{l} u = \mu_{ex}-\mu' \\ du = -d\mu' \end{array} \right. = -\mu_{ex}^N \int \frac{1}{u} du = -\mu_{ex}^N \ln(u) = -\mu_{ex}^N \ln(\mu_{ex}-\mu')$$

Inserting this solution in the definition of the Cauchy Principal Value we find:

$$\begin{aligned} \oint_0^1 \frac{\mu_{ex}^N}{\mu_{ex}-\mu'} d\mu' &= \lim_{\epsilon\to 0}\left(-\mu_{ex}^N\Big[\ln(\epsilon)-\ln(\mu_{ex})\Big] - \mu_{ex}^N\Big[\ln(\mu_{ex}-1)-\ln(-\epsilon)\Big]\right) \\ &= \mu_{ex}^N\Big(\ln(\mu_{ex})-\ln(\mu_{ex}-1)\Big) + \mu_{ex}^N \lim_{\epsilon\to 0}\Big(\ln(-\epsilon)-\ln(\epsilon)\Big) \end{aligned}$$

Using the fact that $\ln(-\epsilon) = \ln(-1) + \ln(\epsilon)$, the limit can directly be evaluated, and therefore we find:

$$\begin{aligned}\fint_0^1 \frac{\mu_{ex}^N}{\mu_{ex} - \mu'} d\mu' &= \mu_{ex}^N \Big(\ln(\mu_{ex}) - \ln(\mu_{ex} - 1) + \ln(-1) \Big) = \mu_{ex}^N \Big(\ln(\mu_{ex}) - \ln(1 - \mu_{ex}) \Big) \\ &= \mu_{ex}^N \ln\left(\frac{\mu_{ex}}{1 - \mu_{ex}} \right)\end{aligned}$$

$\mathbf{A}_2$:

The second integral A_2 can directly be evaluated, and we get:

$$\int_0^1 \mu_{ex}^{N-k} (\mu')^{k-1} d\mu' = \mu_{ex}^{N-k} \left. \frac{\mu'^k}{k} \right|_{\mu'=0}^1 = \frac{\mu_{ex}^{N-k}}{k}$$

Thus, a solution to $A(N)$ is given by:

$$A[N] = \mu_{ex}^N \ln\left(\frac{\mu_{ex}}{1 - \mu_{ex}} \right) - \sum_{k=1}^{N} \frac{\mu_{ex}^{N-k}}{k} = \mu_{ex}^N \left[\ln\left(\frac{\mu_{ex}}{1 - \mu_{ex}} \right) - \sum_{k=1}^{N} \frac{\mu_{ex}^{-k}}{k} \right] \tag{2.26}$$

$\mathbf{B}_1$:

A solution for the B_1-integral can again be obtained in terms of its Cauchy principal value as follows:

$$\int_0^1 \frac{\mu_{ex}^N}{\mu_{ex} - \mu'} e^{-\frac{\tau}{\mu'}} d\mu' = \mu_{ex}^N \fint_0^1 \frac{1}{\mu_{ex} - \mu'} e^{-\frac{\tau}{\mu'}} d\mu'$$

Since the integrand already looks quite similar to an exponential integral (see Eq.(A.3)), we try to split the multiplier, i.e.:

$$\frac{1}{\mu_{ex} - \mu'} = -\frac{1}{\mu'} + X \qquad \Rightarrow \qquad X = \frac{\mu 0}{\mu'(\mu_{ex} - \mu')}$$

$$\Rightarrow \qquad B_1 = \underbrace{-\mu_{ex}^N \fint_0^1 \frac{1}{\mu'} e^{-\frac{\tau}{\mu'}} d\mu'}_{\mu_{ex}^N Ei(-\tau)} - \mu_{ex}^N \fint_0^1 \left(-\frac{\mu_{ex}}{\mu'(\mu_{ex} - \mu')} \right) e^{-\frac{\tau}{\mu'}} d\mu'$$

In order to solve the remaining integral, we try to identify it as $Ei(f(x))$, thus we

search for a function $f(x)$ that satisfies (see Eq.(A.2)): [4]

$$\frac{df(\mu')}{d\mu'} = -\frac{\mu_{ex}}{\mu'(\mu_{ex}-\mu')} f(\mu')$$

Using the Ansatz $f(\mu') = e^{g(\mu')} \quad \Rightarrow \quad \frac{df(\mu')}{d\mu'} = f(\mu') \, \frac{dg(\mu')}{d\mu'}$, the equation can directly be solved to yield:

$$\frac{dg(\mu')}{d\mu'} = -\frac{\mu_{ex}}{\mu'(\mu_{ex}-\mu')} = -\frac{1}{\mu'} + \frac{1}{\mu'-\mu_{ex}}$$

$$\Rightarrow g(\mu') = -\ln(\mu') + \ln(\mu'-\mu_{ex}) \qquad \Rightarrow \qquad f(\mu') = \frac{\mu'-\mu_{ex}}{\mu'} = 1 - \frac{\mu_{ex}}{\mu'}$$

It shall be noted here that the found candidate $f(\mu')$ is not unique since multiplying the gained result with an arbitrary constant will still lead to the same multiplier. Therefore we can shape the function such that it fits to the argument of the exponential-function as appearing in the B_1-integral (i.e.: $\frac{\tau}{\mu'}$) by choosing:

$$\tilde{f}(\mu') = \frac{\tau}{\mu_{ex}} f(\mu') = \frac{\tau}{\mu_{ex}} - \frac{\tau}{\mu'} \qquad \Rightarrow \qquad \text{we still have:} \quad \frac{\tilde{f}'}{\tilde{f}} = -\frac{\mu_{ex}}{\mu'(\mu_{ex}-\mu')}$$

Using $\tilde{f}(\mu')$ we can now finally transform the integral to the desired shape:

$$B_1: \qquad \mu_{ex} Ei(-\tau) - \mu_{ex} \int_0^1 \left(-\frac{\mu_{ex}}{\mu'(\mu_{ex}-\mu')} \right) e^{-\frac{\tau}{\mu'}} d\mu' =$$

$$\mu_{ex} Ei(-\tau) - \mu_{ex} \, e^{-\frac{\tau}{\mu_{ex}}} \int_0^1 \left(-\frac{\mu_{ex}}{\mu'(\mu_{ex}-\mu')} \right) e^{\frac{\tau}{\mu_{ex}} - \frac{\tau}{\mu'}} d\mu'$$

In order to identify this integral as exponential integral function, we have to check the necessary conditions as derived in Eq.(A.4) which are readily shown to be true:

$$\lim_{\mu' \to 0} \left(\frac{\tau}{\mu_{ex}} - \frac{\tau}{\mu'} \right) \to -\infty \qquad \lim_{\mu' \to 1} \left(\frac{\tau}{\mu_{ex}} - \frac{\tau}{\mu'} \right) = \frac{\tau}{\mu_{ex}} - \tau \in \mathbb{R}$$

[4] The negative sign in the multiplier is introduced since otherwise we would get $f(\mu') = \frac{\mu'}{\mu'-\mu_{ex}}$ which can not directly be related to the argument of the exponential function as appearing in the integral. The reason for this choice will be more evident when the identification of the integral as $Ei(f(x))$ is carried out.

Thus, we can identify the integral as $Ei(\tilde{f}(1))$ with $\tilde{f}(\mu') = \frac{\tau}{\mu_{ex}} - \frac{\tau}{\mu'}$, and so the Cauchy principal value of the integral B_1 is finally given by:

$$\begin{aligned}\int_0^1 \frac{\mu_{ex}^N}{\mu_{ex} - \mu'} e^{-\frac{\tau}{\mu'}} d\mu' &= \mu_{ex}^N Ei(-\tau) - \mu_{ex}^N e^{-\frac{\tau}{\mu_{ex}}} Ei\left(\frac{\tau}{\mu_{ex}} - \tau\right) \\ &= \mu_{ex}^N \left[Ei(-\tau) - e^{-\frac{\tau}{\mu_{ex}}} Ei\left(\frac{\tau}{\mu_{ex}} - \tau\right)\right]\end{aligned}$$

$\mathbf{B_2}$:

The B_2-integral can now be identified as a generalized exponential-integral-function $E_n(x)$ which is defined in the NIST Handbook of Mathematical Functions [10] as:

$$E_n(x) := \int_1^\infty \frac{e^{-xt}}{t^n} dt \qquad \text{for} \quad x > 0 \tag{2.27}$$

The identification can be performed via:

$$\begin{aligned}\int_0^1 \mu_{ex}^{N-k} (\mu')^{k-1} e^{-\frac{\tau}{\mu'}} d\mu' &= \mu_{ex}^{N-k} \int_0^1 (\mu')^{k-1} e^{-\frac{\tau}{\mu'}} d\mu' = \left| \begin{array}{l} u = \frac{1}{\mu'} \\ d\mu' = -\mu'^2 du \end{array} \right. \\ &= -\mu_{ex}^{N-k} \int_\infty^1 (\mu')^{k+1} e^{-\tau u} du = \mu_{ex}^{N-k} \int_1^\infty \frac{e^{-\tau u}}{u^{k+1}} du \\ &= \mu_{ex}^{N-k} E_{k+1}(\tau)\end{aligned}$$

Thus, combining the results, a solution to $B(N)$ is given by:

$$B(N) = \mu_{ex}^N \left[Ei(-\tau) - e^{-\frac{\tau}{\mu_{ex}}} Ei\left(\frac{\tau}{\mu_{ex}} - \tau\right) - \sum_{k=1}^{N} \mu_{ex}^{-k} E_{k+1}(\tau)\right] \tag{2.28}$$

Inserting the obtained solutions for $A(N)$ and $B(N)$ into Eq.(2.21), the general solution to the interaction-integral F_{int} is given by:

$$F_{int}(\mu_0,\mu_{ex}) = \sum_{n=0}^{\infty} f_n(\mu_0,\mu_{ex})\ \mu_{ex}^{n+1}\left[e^{-\frac{\tau}{\mu_{ex}}}\ln\left(\frac{\mu_{ex}}{1-\mu_{ex}}\right) - Ei(-\tau) + e^{-\frac{\tau}{\mu_{ex}}}Ei\left(\frac{\tau}{\mu_{ex}}-\tau\right) + \sum_{k=1}^{n+1}\mu_{ex}^{-k}\left(E_{k+1}(\tau) - \frac{e^{-\frac{\tau}{\mu_{ex}}}}{k}\right)\right] \quad (2.29)$$

$$F_{int}(\mu_0,\mu_{ex}) = \mu_{ex}\left(\sum_{n=0}^{\infty} f_n(\mu_0,\mu_{ex})\mu_{ex}^{n}\right)\left[e^{-\frac{\tau}{\mu_{ex}}}\ln\left(\frac{\mu_{ex}}{1-\mu_{ex}}\right) - Ei(-\tau) + e^{-\frac{\tau}{\mu_{ex}}}Ei\left(\frac{\tau}{\mu_{ex}}-\tau\right)\right] + \sum_{n=0}^{\infty} f_n(\mu_0,\mu_{ex})\sum_{k=1}^{n+1}\mu_{ex}^{n+1-k}\left(E_{k+1}(\tau) - \frac{e^{-\frac{\tau}{\mu_{ex}}}}{k}\right) \quad (2.30)$$

Finally, the interaction-term is given by:

$$I_{int}^{+}(\mu_0,\mu_{ex}) = I_{sv}^{+}(\mu_0,\mu_{ex}) + I_{vs}^{+}(\mu_0,\mu_{ex}) \quad (2.31)$$

$$= I_{inc}\ \mu_0\ \omega\left[e^{-\frac{\tau}{\mu_0}}F_{int}(\mu_0,\mu_{ex}) + e^{-\frac{\tau}{\mu_{ex}}}F_{int}(\mu_{ex},\mu_0)\right] \quad (2.32)$$

Moreover, if we are only interested in monostatic measurements (i.e. $\mu_0 = \mu_{ex}$), the calculation of the interaction-term simplifies drastically and we find:

$$I_{int}^{+}(\mu_0) = 2I_{inc}\ \mu_0\ \omega e^{-\frac{\tau}{\mu_0}}F_{int}(\mu_0,\mu_0) \quad (2.33)$$

2.4. Evaluation of the f_n coefficients

2.4.1. Existence of the f_n coefficients

The existence of the expansion coefficients for arbitrary choices of scattering distributions is not ensured. However, it can be shown that as long as one can express the distributions in terms of a series-expansion in a generalized scattering angle, the coefficients exist and can in principle always be calculated.

The generalized scattering angle Θ_x is defined as the generalized scalar product between an incoming ($\hat{i}$) and an outgoing ($\hat{s}$) direction as shown below:

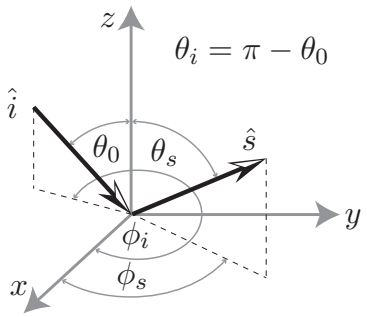

$$\hat{i} = \begin{pmatrix} \sin(\theta_i)\cos(\phi_i) \\ \sin(\theta_i)\sin(\phi_i) \\ \cos(\theta_i) \end{pmatrix} \tag{2.34}$$

$$\hat{s} = \begin{pmatrix} \sin(\theta_s)\cos(\phi_s) \\ \sin(\theta_s)\sin(\phi_s) \\ \cos(\theta_s) \end{pmatrix} \tag{2.35}$$

$$\cos(\Theta_x) = \hat{i}^T \, \mathbf{M}_x \cdot \hat{s} \qquad \text{with} \qquad \mathbf{M}_x = \begin{pmatrix} a_x & 0 & 0 \\ 0 & b_x & 0 \\ 0 & 0 & c_x \end{pmatrix} \tag{2.36}$$

$$\Rightarrow \cos(\Theta_x) = a_x \cos(\theta_i)\cos(\theta_s) + \sin(\theta_i)\sin(\theta_s)\left[b_x \cos(\phi_i)\cos(\phi_s) + c_x \sin(\phi_i)\sin(\phi_s)\right]$$

The diagonal elements (a_x, b_x, c_x) of the weighting-matrix $\mathbf{M}_x$ are hereby to be seen as fitting parameters that allow consideration of off-specular and anisotropic effects as proposed e.g. in [11]. For $a_x = b_x = c_x = 1$ the generalized scattering angle reduced to the standard scattering angle given by:

$$\cos(\Theta) = \cos(\theta_i)\cos(\theta_s) + \sin(\theta_i)\sin(\theta_s)\cos(\phi_i - \phi_s) \tag{2.37}$$

In the following, it will now be proven that as long as both the phase function $\hat{p}$ and the $BRDF$ can be represented in terms of a power-series expansion in terms of a generalized scattering angle $\cos(\Theta_x)$, the expansion-coefficients f_n from Eq. 2.20 exist and can in principle always be calculated.[5]

[5] For the sake of simplicity, we will restrict ourselves to functions that can be represented utilizing a single coefficient matrix $\mathbf{M}_x$, however the following prove can easily be adapted to work also for power series containing multiple choices for $\mathbf{M}_x$

In order to prove the above statement, we assume that the following representations exist and the coefficients p_n and b_n are known:

$$\hat{p} \sim \sum_{n=0}^{\infty} p_n \cos(\Theta_1)^n \qquad\qquad BRDF \sim \sum_{n=0}^{\infty} b_n \cos(\Theta_2)^n \tag{2.38}$$

In order to be able to evaluate the ϕ_s-integral of Eq. 2.20, we first have to find a convenient representation of the product of $(\hat{p} \cdot BRDF)$.

Expanding $\cos(\Theta_x)^n$, we find:

$$\cos(\Theta_x)^n = \left[\tilde{a}_x \cos(\theta_s) + \sin(\theta_s) \underbrace{\{\tilde{b}_x \cos(\phi_s) + \tilde{c}_x \sin(\phi_x)\}}_{\Omega_x} \right]^n \tag{2.39}$$

$$= \sum_{k=0}^{n} \binom{n}{k} \left[\tilde{a}_x \cos(\theta_s)\right]^{n-k} \sin(\theta_s)^k \ \Omega_x^k \tag{2.40}$$

Now that $\cos(\Theta_x)^n$ has been expressed in terms of a series, we can use the following summation-identity to gain a convenient representation for the phase-function $\hat{p}$:

$$\sum_{n=0}^{\infty} \sum_{k=0}^{n} a_{n,k} = \sum_{k=0}^{\infty} \sum_{n=k}^{\infty} a_{n,k} \tag{2.41}$$

Therefore, applying the above identity, we find:

$$\hat{p} \sim \sum_{n=0}^{\infty} p_n \cos(\Theta_1)^n = \sum_{n=0}^{\infty} \sum_{k=0}^{n} p_n \binom{n}{k} \left[\tilde{a}_1 \cos(\theta_s)\right]^{n-k} \sin(\theta_s)^k \ \Omega_1^k$$

$$= \sum_{k=0}^{\infty} \sin(\theta_s)^k \ \Omega_1^k \underbrace{\sum_{n=k}^{\infty} p_n \binom{n}{k} \left[\tilde{a}_1 \cos(\theta_s)\right]^{n-k}}_{\text{pseries}(k)} \tag{2.42}$$

$$= \sum_{k=0}^{\infty} \sin(\theta_s)^k \ \Omega_x^k \ \text{pseries}(k) \tag{2.43}$$

and similarly for the $BRDF$ we get:

$$BRDF \sim \sum_{n=0}^{\infty} b_n \cos(\Theta_2)^n = \sum_{k=0}^{\infty} \sin(\theta_s)^k \ \Omega_2^k \ \text{bseries}(k) \tag{2.44}$$

Since we are interested in finding a representation of the product between the $BRDF$ and $\hat{p}$, we can now use the Cauchy-product formula to express the product of two infinite sums which is given by [12]:

$$\left(\sum_{p=0}^{\infty} a_p\right)\left(\sum_{q=0}^{\infty} b_q\right) = \sum_{n=0}^{\infty} c_n \qquad \text{with} \qquad c_n = \sum_{k=0}^{n} (a_k \ b_{n-k}) \tag{2.45}$$

Thus, using the above formula, we find:

$$\hat{p} \cdot BRDF = \sum_{n=0}^{\infty} \sum_{k=0}^{n} \sin(\theta_s)^n \ \Omega_1^k \ \Omega_2^{n-k} \ \text{pseries}(k) \ \text{bseries}(n-k) \tag{2.46}$$

Now that we have found a convenient representation for $BRDF \cdot \hat{p}$, we can directly evaluate the azimuthal integral as necessary to obtain the f_n coefficients in Eq. 2.20 since the ϕ_s-dependency is expressed exclusively via products of powers of $\Omega_{1,2}$ which have been defined previously as:

$$\Omega_x = \tilde{b}_x \cos(\phi_s) + \tilde{c}_x \sin(\phi_s) \tag{2.47}$$

Thus, we found that the integral of Eq. 2.20 can be represented via:

$$\int_0^{2\pi} \hat{p} \cdot BRDF \ d\phi_s = \sum_{n=0}^{\infty} \sum_{k=0}^{n} \sin(\theta_s)^n \ \text{pseries}(k) \ \text{bseries}(n-k) \int_0^{2\pi} \Omega_1^k \ \Omega_2^{n-k} \ d\phi_s \tag{2.48}$$

where the remaining integrals left to solve are given by:

$$\int_0^{2\pi} \Omega_1^k \ \Omega_2^{n-k} \ d\phi_s = \int_0^{2\pi} \left[\tilde{b}_1 \cos(\phi_s) + \tilde{c}_1 \sin(\phi_s)\right]^k \left[\tilde{b}_2 \cos(\phi_s) + \tilde{c}_2 \sin(\phi_s)\right]^{n-k} d\phi_s \tag{2.49}$$

Providing a general solution for the above integral is rather tedious. However, in order to prove that the series-expansion coefficients of Eq. 2.20 exist in principle, it is sufficient to show that the integral vanishes if n is odd. The reason for this can directly be seen by looking at the summand of Eq. 2.48. Noticing that pseries(k) as well as bseries$(n-k)$ are already in the desired shape, namely they only contain powers of $\cos(\theta_s)$, we only have to ensure that we can express the multiplier $\sin(\theta_s)^n$ in terms of powers of $\cos(\theta_s)$ in order to be able to read out the f_n coefficients. This however is only possible if n is an even number, since only then we can use:

$$\sin(\theta_s)^{2n} = \left[1 - \cos(\theta_s)^2\right]^n \tag{2.50}$$

to express the whole summand in terms of powers of $\cos(\theta_s)$.

Thus, what is left to show is, that the following integral vanishes for odd n:

$$I = \int_0^{2\pi} [\tilde{b}_1 \cos(\phi_s) + \tilde{c}_1 \sin(\phi_s)]^k [\tilde{b}_2 \cos(\phi_s) + \tilde{c}_2 \sin(\phi_s)]^{n-k} d\phi_s \tag{2.51}$$

Now, if n is odd, we have:

- $k \ldots \text{odd} \quad \Rightarrow \quad n-k \ldots \text{even}$
- $k \ldots \text{even} \quad \Rightarrow \quad n-k \ldots \text{odd}$

Therefore, multiplying out the brackets, we end up with a sum containing only integrals of powers of trigonometric functions of the form:

- $\int_0^{2\pi} \sin(\phi_s)^i d\phi_s$ with i...odd
- $\int_0^{2\pi} \cos(\phi_s)^i d\phi_s$ with i...odd
- $\int_0^{2\pi} \sin(\phi_s)^i \cos(\phi_s)^j d\phi_s$ with $i + j$...odd

As shown in Appendix A.3.1, all those integrals can be shown to equal zero, which consequently completes the prove that the f_n-coefficients of any pair of functions that are expressible as power-series of a generalized scattering angle exist and can (in principle) be calculated.

2.4.2. An Algorithm for Coefficient Retrieval

In the preceding prove for the existence of the coefficients, we found that by expanding both $\hat{p}$ and the $BRDF$, we can express the integral Eq. 2.20 in terms of simple integrals of the form:

$$\int_0^{2\pi} \cos(\phi_s)^n d\phi_s \quad , \quad \int_0^{2\pi} \sin(\phi_s)^n d\phi_s \quad , \quad \int_0^{2\pi} \sin(\phi_s)^n \cos(\phi_s)^m d\phi_s$$

As shown in Appendix A.3.1, all those integrals can be evaluated analytically and the solutions are given by:

$$\int_0^{2\pi} \cos(\phi_s)^n d\phi = \int_0^{2\pi} \sin(\phi_s)^n d\phi = \begin{cases} \frac{2\pi}{2^n} \binom{n}{\frac{n}{2}} & \text{if n} \dots \text{ even} \\ 0 & \text{else} \end{cases} \tag{2.52}$$

$$\int_0^{2\pi} \cos(x)^n \sin(x)^m dx = \begin{cases} \frac{2\pi}{2^n 2^m} \sum_{k=0}^{n} \binom{n}{k} \binom{m}{\frac{n+m}{2} - k} (-1)^{m+k-\frac{n}{2}} & \text{if } n, m \dots \text{even} \\ 0 & \text{else} \end{cases} \tag{2.53}$$

The coefficients can now easily be extracted by performing the following steps (indicated in pseudo-code):

1) Expand the integrand of Eq.2.20 such that all ϕ-dependent terms are isolated.
   - `fPoly = EXPAND[ BRDF * p ]`
2) Use the above formulas to substitute the appearing integrals in the ϕ-averaged product. (One has to be careful in here since terms that are independent of ϕ have to be multiplied by $\int_0^{2\pi} d\phi = 2\pi$!)
   - `fPoly = 2π * fPoly`
   - `fPoly = REPLACE[ fPoly ,` $\cos(\phi)^n,\ \sin(\phi)^n \rightarrow \frac{Eq.2.52}{2\pi}$ $\cos(\phi)^n \sin(\phi)^m \rightarrow \frac{Eq.2.53}{2\pi}$ `]`
3) Since from the discussion in Sec.2.4.1 we know that only even powers of $\sin(\theta_s)^n$ will appear within the resulting series, express them in terms of powers of $\cos(\theta_s)$ and expand the resulting series such that all $\cos(\theta_s)^n$-terms are isolated.
   - `fPoly = REPLACE[ fPoly ,` $\sin(\theta_s)^n \rightarrow \left[1 - \cos(\theta_s)^2\right]^{n/2}$ `]`
4) Collect the coefficients for $\cos(\theta_s)^n$

3. Phase Functions

In the following, a list of possible scattering distributions is given along with their representation in terms of a series-expansion applicable for evaluating the f_n coefficients with an algorithm as suggested in Chapter 2.4.2.

Within the listing, the following notation is used:

$P_n(x)$	n^{th} Legendre Polynomial
$\Omega_i = (\theta_i \ , \ \phi_i) \quad \text{with} \quad \theta_0 := \pi - \theta_i \qquad \Big(d\Omega_i = \sin(\theta_i) d\theta_i d\phi_i\Big)$	Incidence Angles
$\Omega_s = (\theta_s \ , \ \phi_s) \qquad \Big(d\Omega_s = \sin(\theta_s) d\theta_s d\phi_s\Big)$	Emergent Angles
$\hat{i} \cdot \hat{s} = \cos(\Theta) = \cos(\theta_i)\cos(\theta_s) + \sin(\theta_i)\sin(\theta_s)\cos(\phi_i - \phi_s)$	Scattering Angle
$\hat{i}_{mirr} \cdot \hat{s} \ = cos(\Theta') = -\cos(\theta_i)\cos(\theta_s) + \sin(\theta_i)\sin(\theta_s)\cos(\phi_i - \phi_s)$	Reflection Angle

An illustration of the used angles is shown in the beginning of Section 2.4.1.
$\hat{i}_{mirr}$ hereby denotes the mirrored incident direction, i.e. $\hat{i}_{mirr}(\theta, \phi) = \hat{i}(\pi - \theta, \phi)$

3.1. Volume-Scattering Phase Functions

The volume-scattering phase functions describe the scattering characteristics of a constituent of the covering layer within all possible directions. It can be seen as the probability for scattering in a specific direction.

All phase-functions presented in the following are therefore normalized via:

$$\int_0^{2\pi} \int_0^{\pi} \hat{p}(\Theta) \sin(\theta_s) d\theta_s \, d\phi_s = 1 \tag{3.1}$$

This normalization coincides with the used form of the radiative transfer equation as given in Eq.2.1. Within other literature however, also an alternative normalization-convention, namely $\int_{4\pi} p \ d\Omega = 4\pi$ is common. To emphasize the use of Eq.3.1 as normalization-condition, a symbol with a hat, i.e. $\hat{p}$ is used within this text.

3.1.1. The Asymmetry Parameter *g*

An important quantity for classifying phase-functions is the so-called **asymmetry parameter** g which is defined as:

$$g = \langle \cos(\Theta) \rangle := \int_0^{2\pi} \int_0^{\pi} \cos(\Theta)\ \hat{p}\big(\cos(\Theta)\big)\ \sin(\theta_s)\ d\theta_s d\phi_s$$

It is used for characterizing the directionality of the phase-function, since:

$g = -1$: for entirely backward-scattering phase-functions

$g = \ \ 0$: for equally forward- and backward-scattering phase-functions

$g = \ \ 1$: for entirely forward-scattering phase-functions

For phase-functions that are **only dependent on the scattering angle** $\cos(\Theta)$, the asymmetry-parameter can be expressed very conveniently by noticing that we can (without loss of generality) arrange the coordinate-system such that $\theta_i = 0$:

$$\cos(\Theta)\big|_{\theta_i \to 0} = \big[\cos(\theta_i)\cos(\theta_s) + \sin(\theta_i)\sin(\theta_s)\cos(\phi_i - \phi_s)\big]\big|_{\theta_i \to 0} = \cos(\theta_s)$$

Therefore we find:

$$g = \int_0^{2\pi} \int_0^{\pi} \cos(\theta_s)\ \hat{p}\big(\cos(\theta_s)\big)\ \sin(\theta_s)\ d\theta_s d\phi_s \tag{3.2}$$

$$= 2\pi \int_0^{\pi} \cos(\theta_s)\hat{p}(\cos(\theta_s))\sin(\theta_s)d\theta_s = 2\pi \int_{-1}^{1} \mu_s\ \hat{p}(\mu_s)d\mu_s \tag{3.3}$$

Moreover, if the expansion of the phase-function in terms of Legendre-polynomials of the scattering angle $\cos(\Theta)$ is known, the asymmetry-parameter is directly related to the 1$^{\text{st}}$ expansion-coefficient of the Legendre-series as shown below:
Starting from Eq. 3.3, we have:

$$\hat{p}(\cos(\Theta)) := \sum_{n=0}^{\infty} \text{coef}(n) P_n(\cos(\Theta)) \qquad \Rightarrow$$

$$g = 2\pi \int_{-1}^{1} \mu_s\ \hat{p}(\mu_s)\ d\mu_s$$

$$= 2\pi \sum_{n=0}^{\infty} \text{coef}(n) \int_{-1}^{1} P_n(\mu_s)\ \mu_s\ d\mu_s = 2\pi \sum_{n=0}^{\infty} \text{coef}(n) \underbrace{\int_{-1}^{1} P_n(\mu)\ P_1(\mu)\ d\mu}_{\frac{2}{2n+1}\delta_{n,1}}$$

$$= 2\pi \sum_{n=0}^{\infty} \text{coef}(n) \frac{2}{2n+1} \delta_{n,1} = \frac{4\pi}{3}\ \text{coef}(1) \tag{3.4}$$

3.1.2. The Isotropic Phase Function:

If the media is assumed to scatter isotropically in all directions, we simply have:

$$\hat{p}(\Theta) = \frac{1}{4\pi} \qquad \Rightarrow \qquad g = 0$$

3.1.3. The Rayleigh Phase Function:

The Rayleigh phase-function is the scattering distribution that originates from the description of scattering by spheres that are small compared to the wavelength of the incident radiation. It is given by: [13]

$$\hat{p}(\Theta) = \frac{3}{16\pi}\left(1 + \cos(\Theta)^2\right)$$

Since it is symmetric with respect to scattering in forward- and backward direction, the asymmetry-factor is again equal to 0.

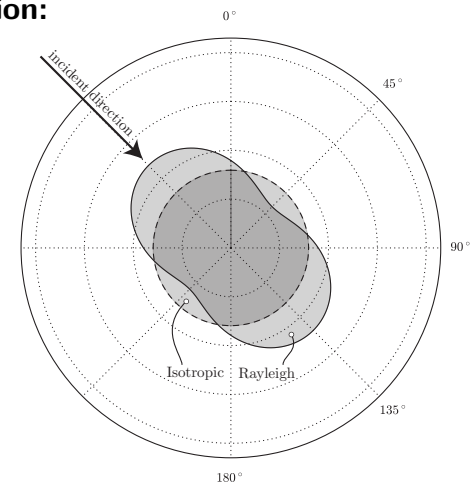

Figure 3.1.: Illustration of the Isotropic- and Rayleigh phase function

It's representation via Legendre-polynomials is furthermore directly given by:

$$\hat{p}(\Theta) = \frac{3}{16\pi}\left[\frac{4}{3}P_0(\cos(\Theta)) + \frac{2}{3}P_2(\cos(\Theta))\right]$$

3.1.4. The Forward-Scattering Phase Function

If the media is assumed to scatter entirely in the forward-direction ($g = 1$), the associated phase-function can be formulated via delta-functions, i.e.:[1]

$$\hat{p}(\Theta) = \frac{1}{\sin(\theta_s)}\delta(\theta_i - \theta_s)\delta(\phi_i - \phi_s) = \delta(\mu_i - \mu_s)\delta(\phi_i - \phi_s)$$

Since the integrals in Eq.2.13 and Eq.2.14 can directly be evaluated using the above phase-function, it's approximation in terms of Legendre-polynomials is omitted.

[1] The additional $\frac{1}{\sin(\theta)}$-factor appears due to the formulation of the delta-functions in a spherical coordinate system.

3.1.5. Henyey Greenstein Phase Function

A function that has been widely used as a single-parameter, analytic phase-function for the description of anisotropic volume-scattering effects is the is the so-called Henyey-Greenstein phase function [14], given by:

$$\begin{aligned}\hat{p}(t,\Theta) &= \frac{1}{4\pi}\frac{1-t^2}{(1+t^2-2t\cos(\Theta))^{3/2}} \\ &= \frac{1}{4\pi}\sum_{n=1}^{\infty} t^n(2n+1)P_n(\cos(\Theta))\end{aligned}$$

The parameter t hereby is equivalent to the asymmetry parameter g of the phase-function which can directly be seen by evaluating the first coefficient of the Legendre-expansion and comparing it with Eq. 3.4.

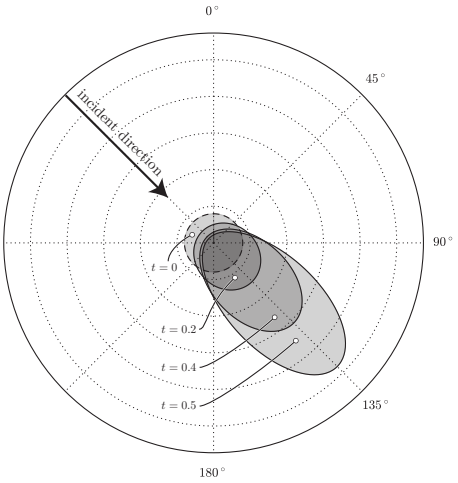

Figure 3.2.: Henyey-Greenstein function

For $t = 0$, the Henyey-Greenstein phase-function reduces to the Isotropic phase function. In order to be able to describe more complex scattering characteristics, a combination of two or more Henyey-Greenstein *"lobes"* can be used as proposed. See for example [15] where a so-called *"Two-term Henyey-Greenstein phase function"* is introduced in order to adequately describe the scattering-distribution of seawater.

3.1.6. Henyey Greenstein Rayleigh Phase Function

As shown by [16] the Rayleigh- and Henyey Greenstein phase function can be combined such that for $t = 0$ the distribution equals the Rayleigh-distribution, while for $t > 0$ the distribution becomes more and more forward-oriented. The asymmetry-parameter of this function is now no longer equal to the function-parameter, but related via:

$$g = \frac{3t(6t^2+5)}{40\pi(t^2+2)}$$

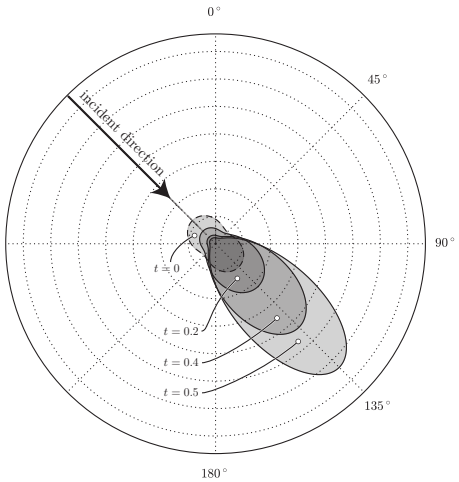

Figure 3.3.: HG-Rayleigh function

The Henyey-Greenstein Rayleigh function and it's expansion in terms of Legendre-polynomials is given by:

$$\hat{p}(t,\Theta) = \frac{8\pi}{2+t^2}\,\hat{p}_{\text{Rayleigh}} * \hat{p}_{\text{HG}} = \frac{3}{8\pi}\frac{1}{2+t^2}\frac{(1-t^2)\left(1+\cos(\Theta)^2\right)}{\left(1+t^2-2t\cos(\Theta)\right)^{3/2}}$$
$$= \sum_{n=0}^{\infty} p_n(t) P_n(\cos(\Theta))$$

with

$$p_n(t) = \frac{3}{8\pi}\frac{1}{2+t^2}\left[\frac{n(n-1)}{2n-1}t^{n-2} + \frac{(n+2)(n+1)}{2n+3}t^{n+2} + \frac{(n+1)^2}{2n+3}t^n + \frac{5n^2-1}{2n-1}t^n\right]$$

3.1.7. Gaussian Peak

The Gaussian Peak phase function has widely been used in modelling the scattering behaviour of vegetation for millimetre-waves [17, 18, 19]. It is given by:

$$\hat{p}(\Theta,\beta) = \frac{1}{4\pi}\left(\frac{2}{\beta}\right)^2 e^{-\frac{\Theta^2}{\beta^2}}$$
$$\approx \sum_{n=0}^{N} p_n(\beta) P_n(\cos(\Theta))$$

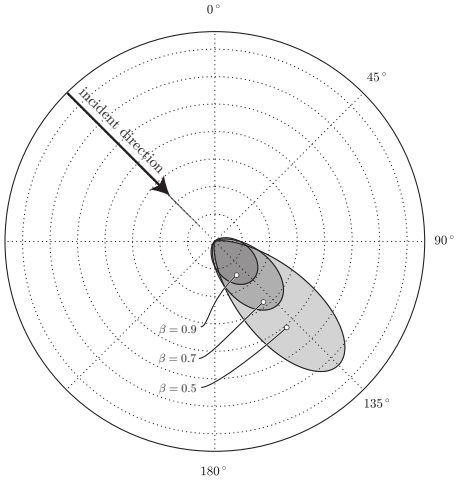

Figure 3.4.: Gaussian peak

Even though the Henyey-Greenstein- and related functions are much more suitable because they can directly be expressed via a Legendre-series, also the expansion-coefficients for the Gaussian peak phase-function can be evaluated analytically. They turn out to be given by:

$$p_n = \frac{2n+1}{2}\frac{1}{4\pi}\left(\frac{2}{\beta}\right)^2 \sum_{m=0}^{N} a_m\,\xi(m,n)$$

with

$$a_m = \frac{\beta\ e^{-\frac{m^2\beta^2}{4}}}{\sqrt{\pi}(1+\delta_{m,0})}\mathrm{Re}\left[\mathrm{erf}\left(\frac{\pi}{\beta}+\frac{im\beta}{2}\right)\right]$$

and

$$\xi(m,n) = \begin{cases} 2 & \text{if} \quad m=n=0 \\ -\frac{1}{4}\frac{m\ \Gamma\left(\frac{m+n}{2}\right)\Gamma\left(\frac{m-n-1}{2}\right)}{\Gamma\left(\frac{m-n+2}{2}\right)\Gamma\left(\frac{m+n+3}{2}\right)} & \text{if} \quad m+n\ldots\text{even} \\ 0 & \text{else} \end{cases}$$

Since the derivation of the above expansion is not straight forward, it is addressed briefly in Appendix A.3.2.

3.1.8. Gegenbauer Kernel Phase Function

The Gegenbauer-Kernel (GK) phase function proposed by Reynolds and McCormick [20] is a two-parameter phase function similar to the Henyey-Greenstein phase function mentioned above, but with an additional parameter $\alpha > -\frac{1}{2}$ that allows a wide variety of scattering distributions to be approximated. For $\alpha = 1/2$ the GK phase function reduces to the Henyey Greenstein phase function. In terms of application, it has for example been used to approximate the scattering behaviour of human blood at optical wavelengths [21].

$$\hat{p}(\Theta,\beta) = \frac{1}{\pi}\frac{\alpha g}{\left[(1+g)^{2\alpha}-(1-g)^{2\alpha}\right]}\frac{\left(1-g^2\right)^{2\alpha}}{\left[1+g^2-2g\cos(\Theta)\right]^{(\alpha+1)}} \tag{3.5}$$

$$= \frac{1}{\pi}\frac{\alpha g\left(1-g^2\right)^{\alpha}}{\left[(1+g)^{2\alpha}-(1-g)^{2\alpha}\right]}\sum_{n=0}^{\infty}\left(1+\frac{n}{\alpha}\right)g^n\ C_n^{(\alpha)}\left(\cos(\Theta)\right) \tag{3.6}$$

Where $C_n^{(\alpha)}(x)$ denote the Gegenbauer (or Ultraspherical)-polynomials [10].

3.2. Surface-BRDF's

The *Bidirectional Reflectance Distribution Function* which is used to describe the scattering properties of the soil-surface is defined via:

$$BRDF(\Omega_i \to \Omega_s) = \frac{\text{Scattered Intensity in direction } \Omega_s}{\text{Incident Power per unit illuminated area}} = \frac{dI_s(\Omega_s)}{I_i(\Omega_i)\cos(\theta_i)d\Omega_i} \tag{3.7}$$

In order to be physically consistent (and applicable to the method for evaluation of the interaction-term), a $BRDF$ has to obey the following constraints:

Reciprocity:
(Source and detector can be interchanged without altering the BRDF)

$$BRDF(\Omega_i \to \Omega_s) = BRDF(\Omega_s \to \Omega_i) \tag{3.8}$$

The validity of reciprocity for flat surfaces relates back to the validity of the reciprocity principle of electromagnetism. A detailed discussion can be found in [22].

For arbitrary structured surfaces this principle might in general be violated, but as has been shown by Snyder [23], under the assumption that the surface can be described as a collection of elements that itself obey reciprocity, the reciprocity of the structured surface is maintained. Moreover Leroy [24] showed that the measurement setup itself might induce non-reciprocal behaviour and presented a method on how to distinguish whether the assumption of reciprocity for a certain setup is reasonable or not. Throughout this text, the reciprocity condition is considered to be fulfilled.

Positivity:

$$BRDF(\Omega_i \to \Omega_s) \geq 0 \tag{3.9}$$

The necessity of a positive $BRDF$ is directly evident from it's definition and the fact that both intensity and power are positive quantities.

Energy Conservation:

$$\int_0^{2\pi}\int_0^{\frac{\pi}{2}} BRDF(\Omega_i \to \Omega_s)\cos(\theta)\sin(\theta)d\theta d\phi = R(\Omega_i) \leq 1 \tag{3.10}$$

$R(\Omega_i)$ hereby denotes the *Directional Hemispherical Reflectance* of the surface, i.e. the fraction of radiation that is scattered into the upper hemisphere from radiation impinging at a single incidence-angle.[2]

The above statement will in the following be derived briefly. A more general discussion can be found for example in [25].

[2] The fraction of radiation being absorbed by the surface is then given by $(1 - R(\Omega_i))$

Connection between Hemispherical Reflectance and the BRDF:

For the sake of compactness, the angular dependency of variables will be omitted in the following calculation. Furthermore we use the notation $d\Omega = \cos(\theta) d\theta d\phi$.

To consider only radiation impinging from a single direction, we define the incident intensity via:

$$I_i = \frac{I_0}{\sin(\theta_i)} \delta(\theta_i - \theta_0) \delta(\phi_i - \phi_0) \tag{3.11}$$

where I_0 is a constant and δ denotes the Dirac-delta function.

Denoting the incident/scattered power per unit illuminated area by Φ_i / Φ_s we know:

$$dI_s = BRDF \; d\Phi_i \qquad \text{with} \qquad d\Phi_i = I_i \cos(\theta_i) d\Omega_i \tag{3.12}$$

and similarly, for the scattered power per unit area we have:

$$d\Phi_s = I_s \cos(\theta_s) d\Omega_s \tag{3.13}$$

Finally, the *Directional Hemispherical Reflectance* is defined via:

$$R = \frac{\Phi_s}{\Phi_i} \tag{3.14}$$

where Φ_s denotes the scattered power per unit area into the upper hemisphere and Φ_i is the total incident power per unit area. Clearly we have $R \leq 1$ since the scattered power must be less or equal than the incident power.

Φ_i can now easily be calculated inserting the definition of I_i:

$$\Phi_i = \int_{2\pi} I_i \cos(\theta_i) d\Omega_i = I_0 \cos(\theta_0)$$

Using Eq. 3.11 and Eq. 3.12, the scattered power into the upper hemisphere is given by:

$$\Phi_s = \int_{2\pi} I_s \cos(\theta_s) d\Omega_s = \int_{2\pi} \int_{2\pi} BRDF \; I_i \cos(\theta_i) \cos(\theta_s) d\Omega_i d\Omega_s \tag{3.15}$$

$$= \int_{2\pi} BRDF \; I_0 \cos(\theta_0) \cos(\theta_s) d\Omega_s \tag{3.16}$$

Using the definition of hemispherical Reflectance we thus find:

$$\Phi_s = R \; \Phi_i \tag{3.17}$$

$$\int_{2\pi} BRDF \; \cancel{I_0 \; \cos(\theta_0)} \cos(\theta_s) d\Omega_s = R \; \cancel{I_0 \; \cos(\theta_0)}$$

$$\Rightarrow R = \int_{2\pi} BRDF \cos(\theta_s) d\Omega_s \qquad \blacksquare \tag{3.18}$$

When dealing with real surfaces, the associated BRDF has to account for numerous characteristics which can be summarized coarsely as:

- Geometric properties (Roughness, Topology)
- Dielectric Properties

In general those effects are presumably coupled in a complex way. Theoretical approaches for modelling the BRDF of a general rough surface usually assume certain statistical properties of the surface-roughness together with the knowledge of roughness-parameters such as the *correlation-length* λ and the *rms-height (root mean square-height)*. The most general approach utilizing this method is possibly the Integral Equation Model (IEM) [26] and it's numerous generalizations available within literature. While the IEM is capable of accurately simulating the BRDF of a surface with known λ and *rms-height*, relating those parameters to observable properties of natural surfaces can be a challenging task, since for example the 'roughness'-characteristics in the microwave-domain might be very different from the 'roughness'-characteristics as retrieved from optical observations.

In order to evaluate the first-order scattering contributions using the method of chapter 2.3, the BRDF is desirably given by an analytic function that can easily be expanded as power-series of the cosine of the scattering angle.

Since the BRDF-functions as provided by models such as the IEM usually have very complex angular dependencies, the following list provides possible analytic functions that can be used to approximate the BRDF in a suitable way.

3.2.1. Ideally Rough (*Lambertian*) Surface:

An ideally rough surface is a surface that appears equally bright in all directions.
Within the literature, such a surface is usually referred to as a *Lambertian surface*. The corresponding $BRDF$ consequently is a constant, i.e.:

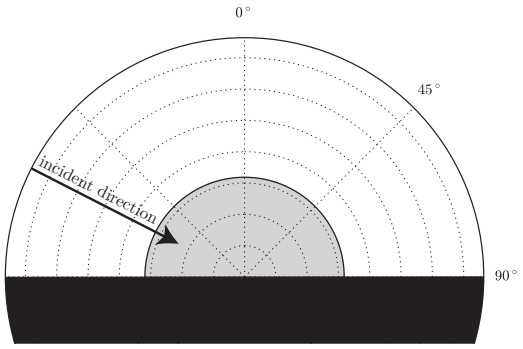

Figure 3.5.: Lambertian BRDF

$$BRDF(\Theta') = \frac{R_0}{\pi} \qquad \text{with} \qquad R_0 \in [0,1]$$

R_0 is hereby usually called the diffuse albedo, or diffuse reflection-coefficient.

3.2.2. Cosine Lobes (*Phong Model*)

One of the most easy models to mimic directional behaviour of a surface is the so-called cosine-lobe-(or Phong-)model which was first proposed by Phong as a shading-function for rendering of computer-graphics [27]. Hereby, the scattering behaviour of a surface is modelled as a peak in specular direction, described via powers of the cosine of the scattering-angle.

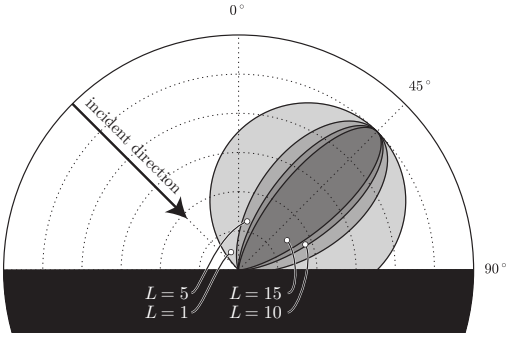

Figure 3.6.: Cosine lobes of power L

From [12] chapter (7.23) we find for the expansion in terms of Legendre-polynomials:

$$\begin{aligned} BRDF(\Theta', L) &= \mathrm{Max}[\cos(\Theta'), 0]^L \\ &= \sum_{n=0}^{\infty} \left[\frac{(2n+1)}{2^n} \frac{\Gamma(L+1)\,\Gamma\left(\frac{L-n+3}{2}\right)}{2\Gamma(L-n+2)\,\Gamma\left(\frac{L+n+3}{2}\right)} \right] P_n(\cos(\Theta')) \end{aligned}$$

For integer L this can be further simplified to:

$$\begin{aligned} BRDF(\Theta', L) &= \mathrm{Max}[\cos(\Theta'), 0]^L \\ &= \sqrt{\pi}\; L!\; 2^{-(L+2)} \sum_{n=0}^{\infty} \left[\frac{(1+2n)}{\Gamma\left(\frac{L-n+2}{2}\right)\Gamma\left(\frac{L+n+3}{2}\right)} \right] P_n(\cos(\Theta')) \end{aligned}$$

3.2.3. Generalized Cosine Lobes (*Lafortune Model*)

In order to have a more realistic approximation of the scattering-behaviour of natural surfaces, Lafortune [11] introduced a generalization of the cosine-lobe model, based on the introduction of a generalized scattering angle Θ_{laf}. Using this approach, it is possible to include non-linear behaviour of the BRDF while still using the simple representation of the BRDF as a cosine-lobe.

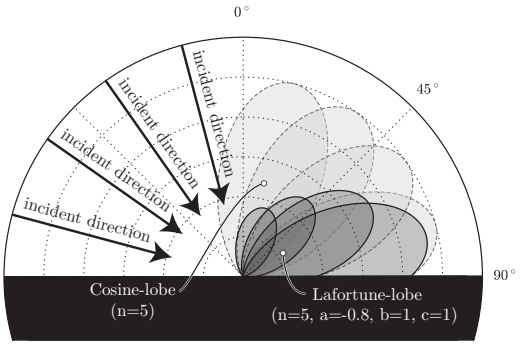

Figure 3.7.: Comparison Lafortune/Cosine-lobe

The generalized scattering angle that is used within the Lafortune-model has already been introduced in Chapter 2.4.1 and is given by:

$$\cos(\Theta_{laf}) = a\cos(\theta_i)\cos(\theta_s) + \sin(\theta_i)\sin(\theta_s)\left[b\cos(\phi_i)\cos(\phi_s) + c\sin(\phi_i)\sin(\phi_s)\right]$$

where a, b and c are constants.

The definition of the BRDF is then completely similar to that of the ordinary cosine-lobes, since the proposed method for the evaluation of the interaction-term works equally well when using a generalized scattering angle.

$$\begin{aligned} BRDF(\Theta_{laf}, L) &= \mathrm{Max}[\cos(\Theta_{laf}), 0]^L \\ &= \sum_{n=0}^{\infty} \left[\frac{(2n+1)}{2^n} \frac{\Gamma(L+1)\,\Gamma\left(\frac{L-n+3}{2}\right)}{2\Gamma(L-n+2)\,\Gamma\left(\frac{L+n+3}{2}\right)} \right] P_n(\cos(\Theta_{laf})) \end{aligned}$$

As an illustrative example of the possibilities of using such a generalization, Fig.3.7 shows a comparison between an ordinary cosine-lobe[3] and a Lafortune-lobe with (a=-0.8, b=1, c=-1). The effect of using such a modified scattering angle is, that the hemispherical reflectance associated with the BRDF increases as the scattering-angle increases. More details on the possibilities of the Lafortune-model and it's specification can be found in [11].

3.3. Further possibilities

While using the concept of a generalized cosine-lobe to approximate BRDF's already allows a wide range of modelling possibilities, it shall be noted in here that the concept of applying a generalized scattering angle is not restricted to cosine-lobes.

In fact, any of the functions introduced within this chapter can be defined with respect to a generalized scattering angle. As shown in Chapter 2.4.1, the presented method for evaluating the interaction-term remains applicable.

Furthermore, the use of linear-combinations of approximation functions together with the concept of generalized scattering angles allows consideration of a wide range of possible scattering behaviours.

To visualize the main idea behind this concept, Fig.3.3 shows 4 Henyey-Greenstein phase-functions ($\hat{p}_I - \hat{p}_{IV}$) (dashed lines) together with the combined phase-function ($\hat{p}_{comb}$) (solid line) resulting from a linear-combination of the form:

$$\hat{p}_{comb} = w_I * \hat{p}_I + w_{II} * \hat{p}_{II} + w_{III} * \hat{p}_{III} + w_{IV} * \hat{p}_{IV} \tag{3.19}$$

with equal weighting-factors $w_I = w_{II} = w_{III} = w_{IV} = 0.25$

[3] An ordinary cosine-lobe is equal to a Lafortune-lobe with a=b=c=1

The parameters of the 4 Henyey-Greenstein phase-functions are chosen as follows:

Ⓘ $t = 0.5$ $a = [-1., 1., 1.]$ (forward-peak)

Ⓘ$\!$Ⓘ $t = 0.5$ $a = [1., 1., 1.]$ (upward-specular-peak)

Ⓘ$\!$Ⓘ$\!$Ⓘ $t = -0.5$ $a = [-1., 1., 1.]$ (backward-peak)

Ⓘ$\!$Ⓥ $t = -0.5$ $a = [1., 1., 1.]$ (downward-specular-peak)

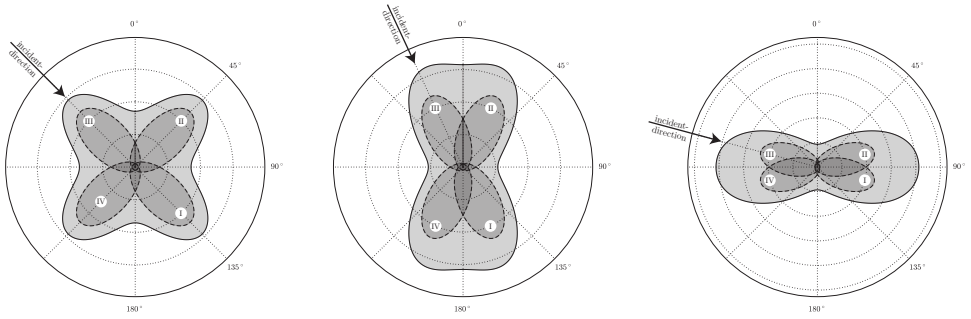

$\theta_0 = 45°$ $\theta_0 = 45°$ $\theta_0 = 45°$

Figure 3.8.: Linear combination of generalized Henyey-Greenstein phase-functions

As one can infer from the appearance of p_{II} and p_{III} in Fig.3.3, this concept can also be used to turn previously introduced volume-scattering phase-functions (like for example the Henyey-Greenstein phase-function) into possible approximation functions for BRDFs. This is indicated in the figure aside, showing a linear-combination of two Henyey-Greenstein phase-functions at $\theta_0 = (25, 64)[\text{deg}]$.

The used parameters are given by:

$$a_1 = [1, 1, 1] \qquad t_1 = 0.5$$
$$a_2 = [-1, 1, 1] \qquad t_2 = -0.3$$

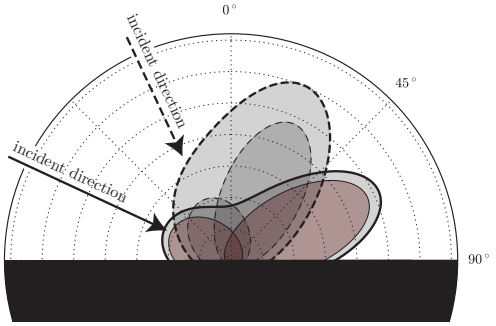

Figure 3.9.: Linear combination of BRDFs

4. Simulation results

The theoretical developments presented in the previous chapters are currently being implemented as a python-module that will be made public as soon as it is fully documented and made more user-friendly.[1] The python-module will allow evaluating the bistatic first-order radiative transfer solutions based on given input of approximate scattering distribution-functions for both the vegetative coverage and the underlying soil-surface.

All following plots are generated using the already existing code. The results are intended to show the capabilities of the model as well as some basic results on the behaviour of the scattered radiation to changes on the optical depth τ, the single scattering albedo ω and the choice of the distribution functions.

Since it is most common within satellite based remote sensing applications to express the backscattered radiation in terms of the so-called backscattering-coefficient σ_0, it's relation to the backscattered intensity I_f is briefly addressed in the following section.

4.1. Connection between I_s and σ_0

In [28] it is shown that the relation between the bistatic scattering coefficient σ_0 and the $BRDF$ of the observed scene is given by[2]

$$\sigma_0(\theta_0, \theta_s) = 4\pi \; BRDF(\theta_0, \theta_s) \; \cos(\theta_0) \; \cos(\theta_s) \tag{4.1}$$

For impinging radiation incoming from a single direction as defined in Eq.3.11, the scattered intensity I_s can be calculated via:

$$I_s(\theta_0, \theta_s) = \int_{2\pi} BRDF(\theta_i, \theta_s) I_i(\theta_0) \cos(\theta_i) d\Omega_i = I_0 \; BRDF(\theta_0, \theta_s) \; \cos(\theta_0)$$

Inserting the above result, we thus have:

$$\sigma_0(\theta_0, \theta_s) = 4\pi \left(\frac{I_s(\theta_0, \theta_s)}{I_0} \right) \cos(\theta_s) \tag{4.2}$$

[1] The source-code will be hosted at https://github.com/TUW-GEO/rt1

[2] For the sake of compactness, the azimuthal dependencies of σ_0 and the $BRDF$ have been suppressed.

4.2. Example specification

4.2.1. Surface parametrization

To be able to use a function as an approximation function for the BRDF, one has to take care on the associated hemispherical reflectance $R(\theta_0)$. To get an idea on the magnitude of $R(\theta_0)$, we can use the fact that the hemispherical reflectance can be related to the directional emissivity $\epsilon(\theta, \phi)$ of a soil surface via Kirchhoff's law [29]:

$$R(\theta) = 1 - \epsilon(\theta) \tag{4.3}$$

For horizontal polarized radiation in the microwave-range, directional emissivities are found in the range of $0.7 - 0.9$ and decrease with increasing incidence-angle [30].

To model such a behaviour within the presented example, the $BRDF$ is approximated using a generalized Henyey-Greenstein phase function with the parameters of the generalized scattering angle set to: $a = \text{diag}(-0.6, 1, 1)$. Furthermore, in order to gain comparable results, the functions are normalized with respect to the nadir hemispherical reflectance $R(0)$ (see Eq. 4.4), and multiplied by a normalization-factor of $N_R = 0.15$ to get the magnitude of the hemispherical reflectance in a reasonable range.

Since the general hemispherical reflectance $R(\theta_0)$ that is associated with the Henyey-Greenstein phase-function when being used as BRDF has a complicated dependency on the incidence-angle, the plot aside shows a numerical evaluation of $R(\theta_0)$ over the considered incidence-angle range.

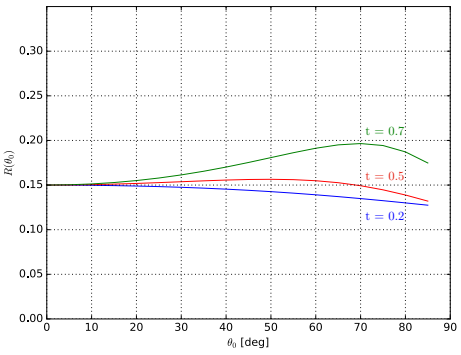

To illustrate the resulting function, Figure 4.1 shows polar-plots of the used BRDF for the considered asymmetry-parameters at incidence-angles $\theta_0 = (15, 35, 55, 75)$[deg].

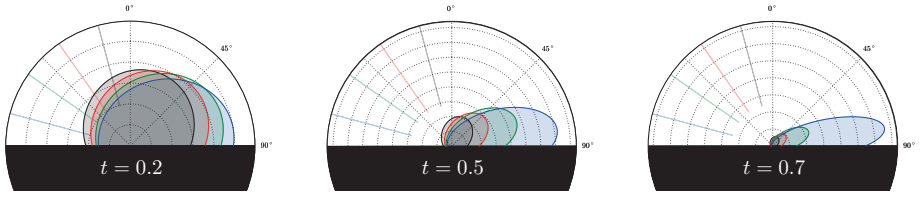

Figure 4.1.: Henyey Greenstein function used as BRDF approximation function

The nadir hemispherical reflectance associated with a Henyey-Greenstein phase-function can be evaluated analytically (see Appendix A.3.3) and is given by:
(a_1 denotes the first of the scattering-angle-parameters $a = \mathrm{diag}(a_1, a_2, a_3)$)

$$R(0) = \frac{(1-t^2)\left[1 + t(t+a_1) - \sqrt{\left(1+t^2\right)\left(1+2a_1t+t^2\right)}\right]}{2\ a_1^2\ t^2\sqrt{1+2a_1t+t^2}} \tag{4.4}$$

4.2.2. Covering layer parametrization

For the description of the scattering properties of the covering layer, three different choices of scattering-distribution functions are selected:

- Choice 1: Rayleigh Phase Function
- Choice 2: Isotropic Phase Function
- Choice 3: Henyey-Greenstein Rayleigh Phase Function
  - Asymmetry-parameters: $t = 0.2$ and $t = 0.4$

In order to fully parametrize the covering layer, we additionally need to specify the single scattering albedo ω and the optical depth τ.

Investigations of Kurum et.al [31] show that the single scattering albedo of forests can be as high as 0.6 at L-band. The optical depth can range from 0 for a bare surface to values higher than 1 for a densely forested region.

Within the presented example, the following values have been used:

$$\omega = 0.4 \qquad \text{and} \qquad \tau \in [0.01, 0.1, 0.3, 0.5, 0.7, 0.9]$$

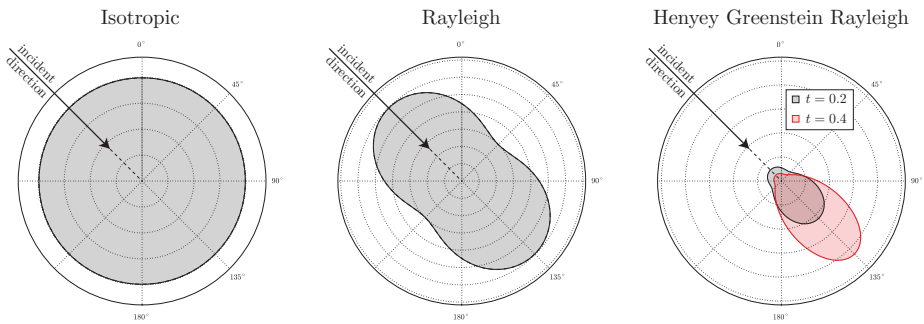

Figure 4.2.: Illustration of volume scattering phase functions

4.3. Example Results

4.3.1. Plot descriptions

Within the following sections, some results of the above specified example are shown. For clarity, the plots are grouped as indicated in the list below which provides an overview on the specifications of the plots.

- Bistatic scattering distributions
  - The plots show the bistatic scattering coefficient $\sigma_0(\theta, \phi)$ (as defined in Eq. 4.2) in linear scale for $\theta_s \in (0, \pi/2)$, $\phi_s \in (0, \pi)$ at two different incidence-angles $\theta_i = 15$ and 55 degrees.
  - The surface anisotropy parameter is set to 0.5 for all plots
  - The optical depth τ is set to $\tau = 0.7$ for all plots
  - The aim of the visualizations is to provide a qualitative visual impression of the resulting magnitudes of the individual contributions for bistatic measurement configurations.
- Tau variations
  - Plots show the monostatic (i.e. $\theta_0 = \theta_s$, $\phi_s = \phi_i + \pi$) backscattering coefficient σ_0 both with and without the interaction-term in dB for $\theta_0 \in (0, \pi/2)$
  - Each plot shows the variations of σ_0 with respect to changes in the optical depth *tau* for the values $\tau \in [0.01, 0.1, 0.3, 0.5, 0.7, 0.9]$
  - The plots reveal the impact of the optical depth and the surface-anisotropy parameter on the so-called cross-over angle, which is defined as the incidence-angle at which the σ_0 curves of a developing (low τ) and full grown vegetation canopy (high τ) cross over [32].
- Contributions
  - Plots show the monostatic (i.e. $\theta_0 = \theta_s$, $\phi_s = \phi_i + \pi$) backscattering coefficient contributions in dB as well as its fractional contributions to the total signal for $\theta_0 \in (0, \pi/2)$
  - The parametrization is identical to the *"tau-variation"* plots
  - The plots are intended to reveal the composition of the total backscattering coefficient that remains hidden in the *"tau-variation"* plots.

4.3.2. Bistatic scattering distributions

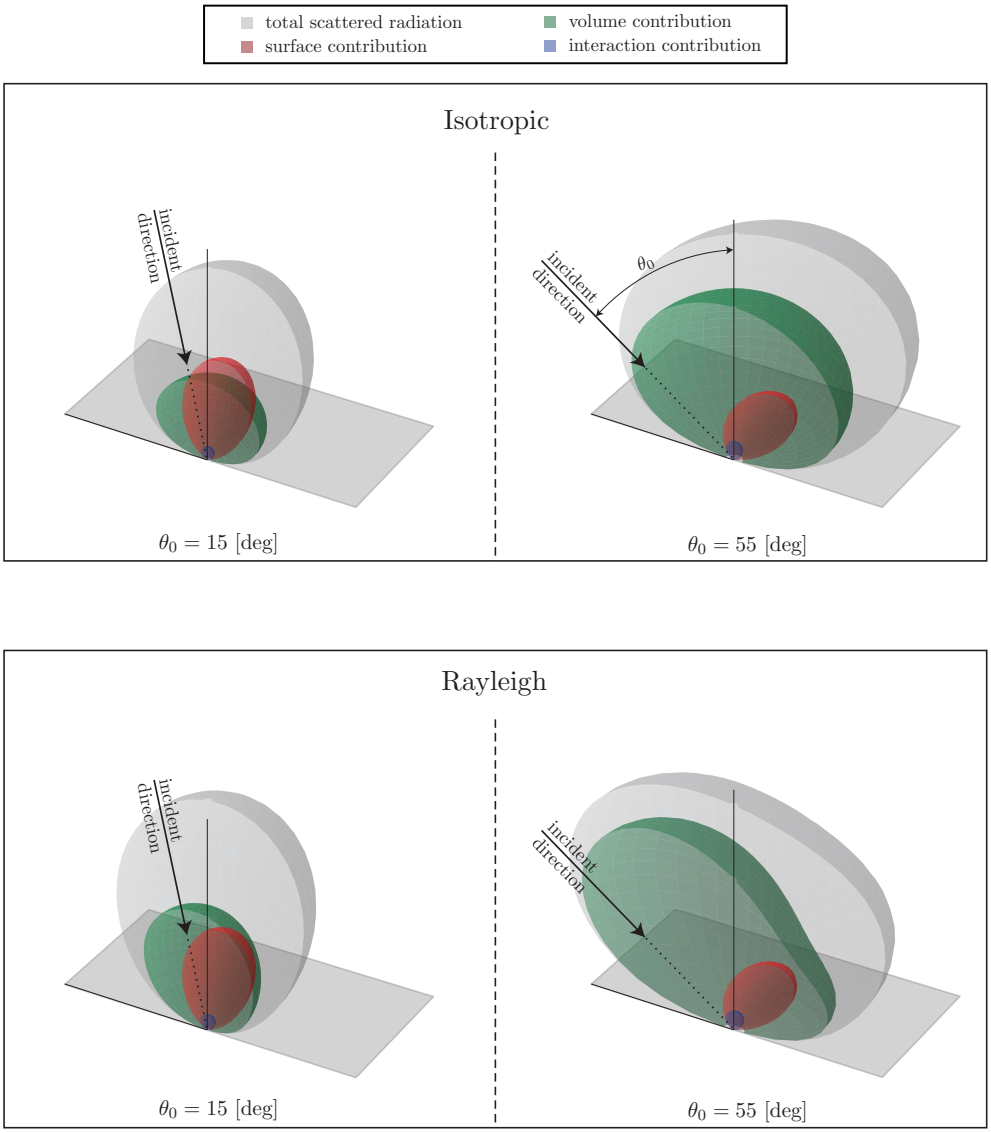

Figure 4.3.: Illustration of the bistatic scattering coefficient $\sigma_0(\theta, \phi) = 4\pi \cos(\theta) \frac{I(\theta,\phi)}{I_{inc}}$

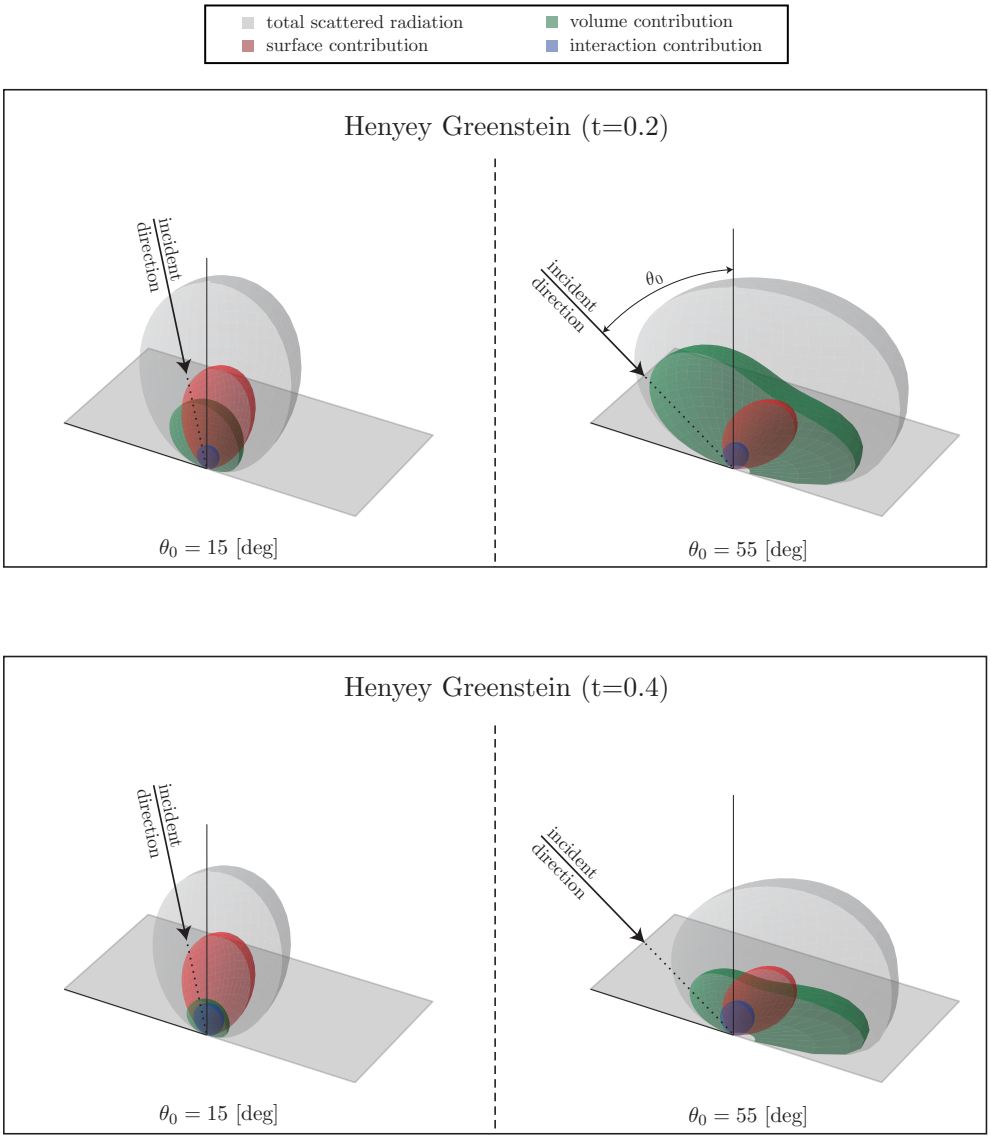

Figure 4.4.: Illustration of the bistatic scattering coefficient $\sigma_0(\theta, \phi) = 4\pi \cos(\theta) \frac{I(\theta,\phi)}{I_{inc}}$

4.3.3. Tau variations (Isotropic)

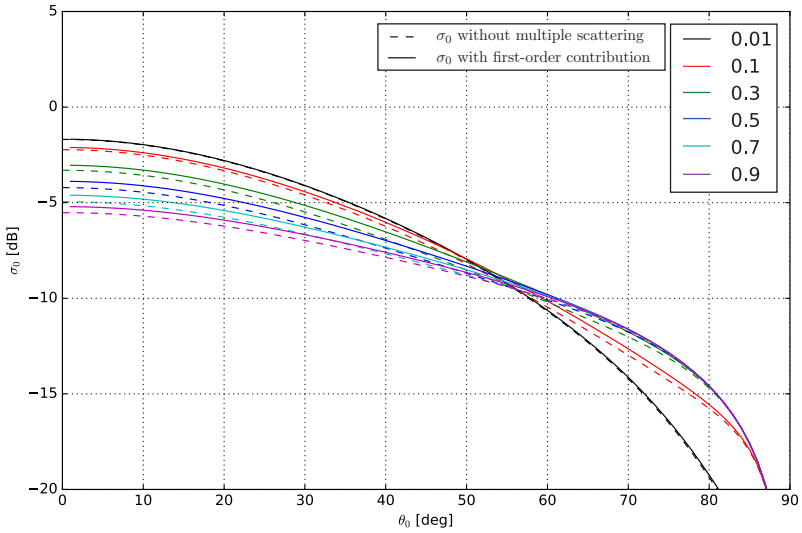

Figure 4.5.: Surface asymmetry-parameter = 0.2

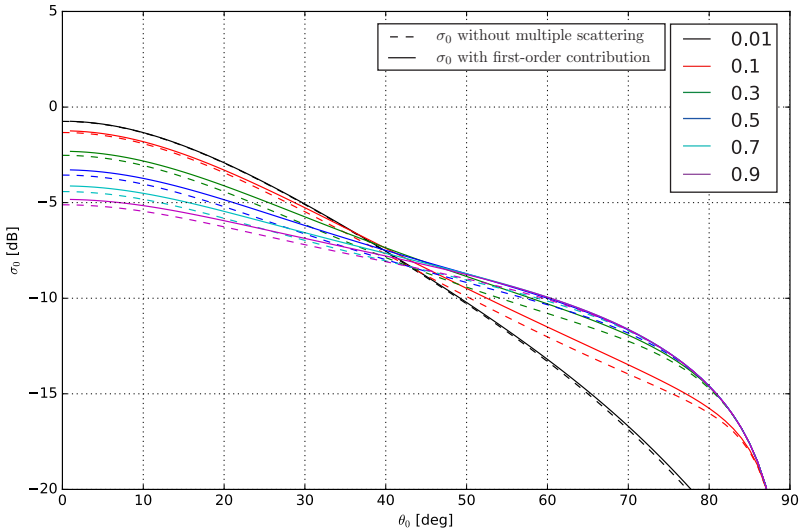

Figure 4.6.: Surface asymmetry-parameter = 0.5

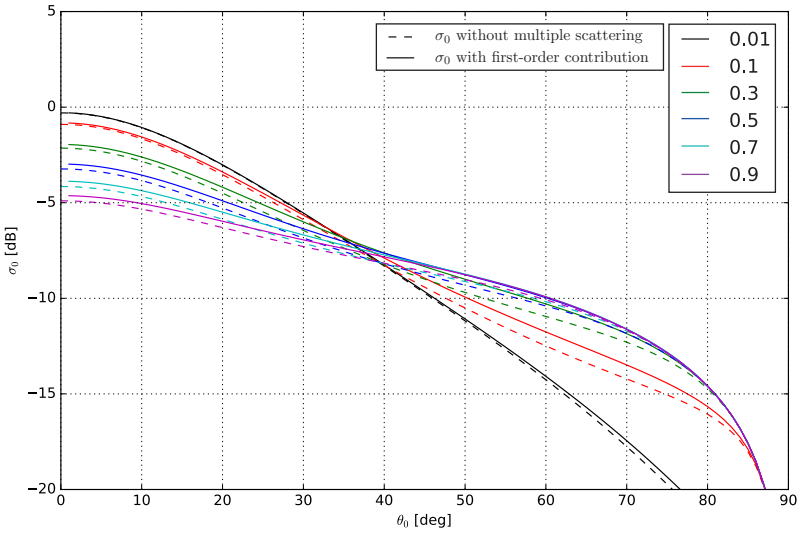

Figure 4.7.: Surface asymmetry-parameter = 0.7

4.3.4. Tau variations (Rayleigh)

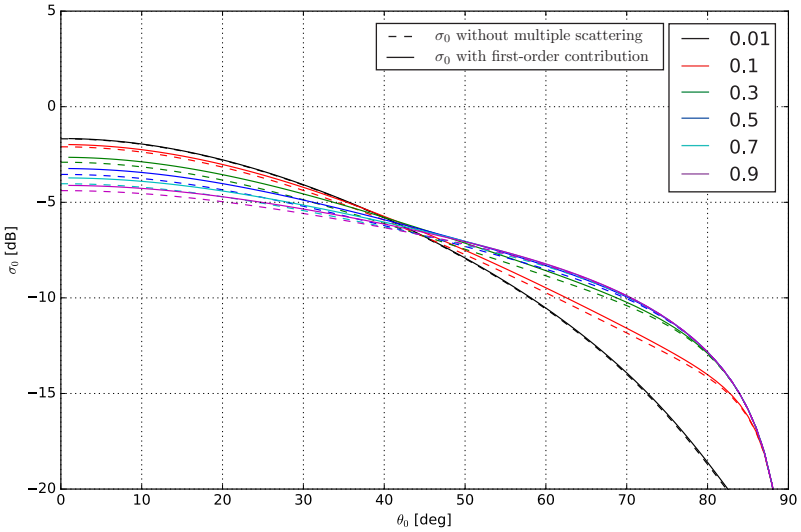

Figure 4.8.: Surface asymmetry-parameter = 0.2

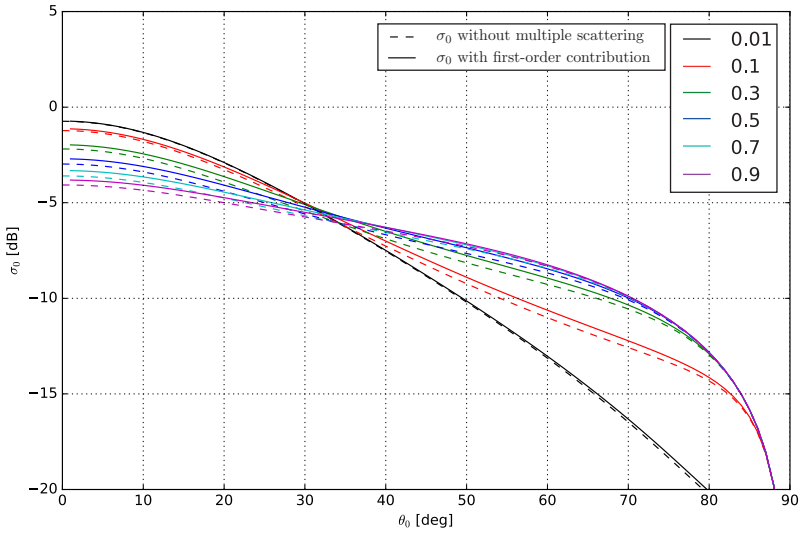

Figure 4.9.: Surface asymmetry-parameter = 0.5

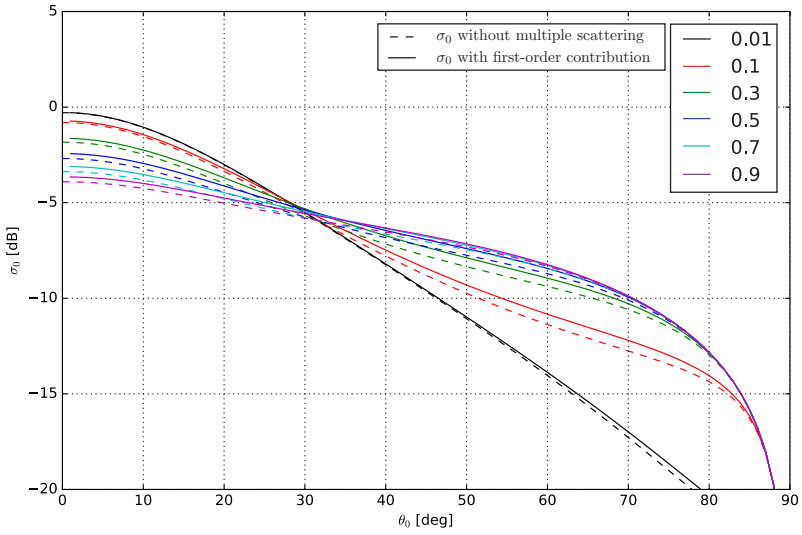

Figure 4.10.: Surface asymmetry-parameter = 0.7

4.3.5. Tau variations (Henyey Greenstein $t = 0.2$)

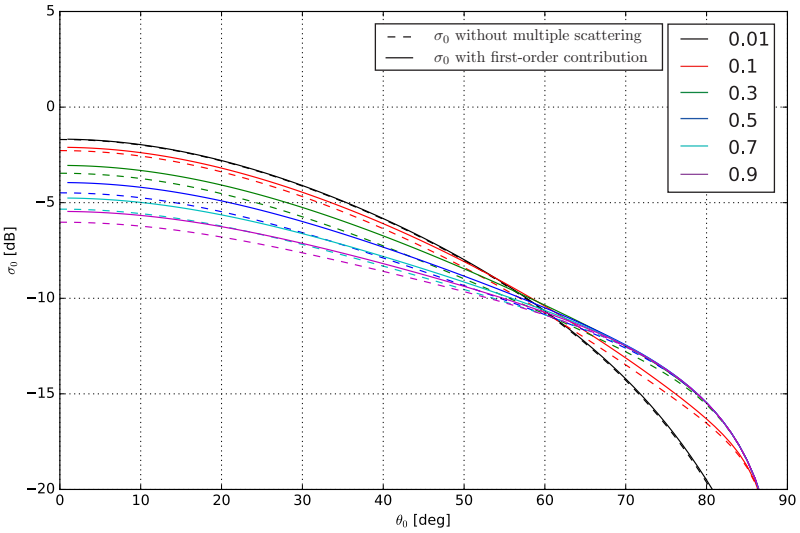

Figure 4.11.: Surface asymmetry-parameter = 0.2

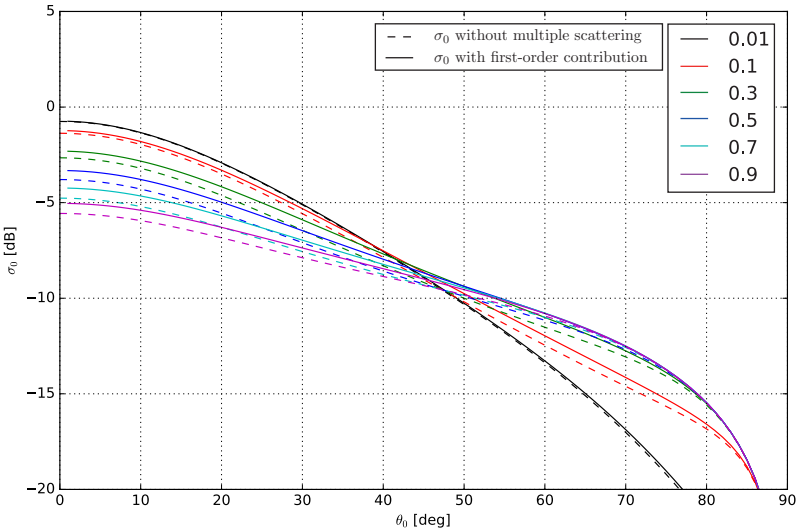

Figure 4.12.: Surface asymmetry-parameter = 0.5

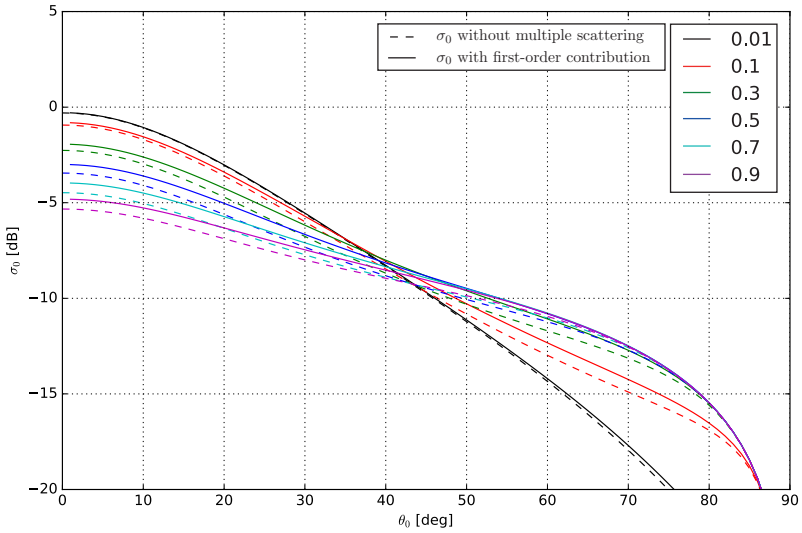

Figure 4.13.: Surface asymmetry-parameter = 0.7

4.3.6. Tau variations (Henyey Greenstein $t = 0.4$)

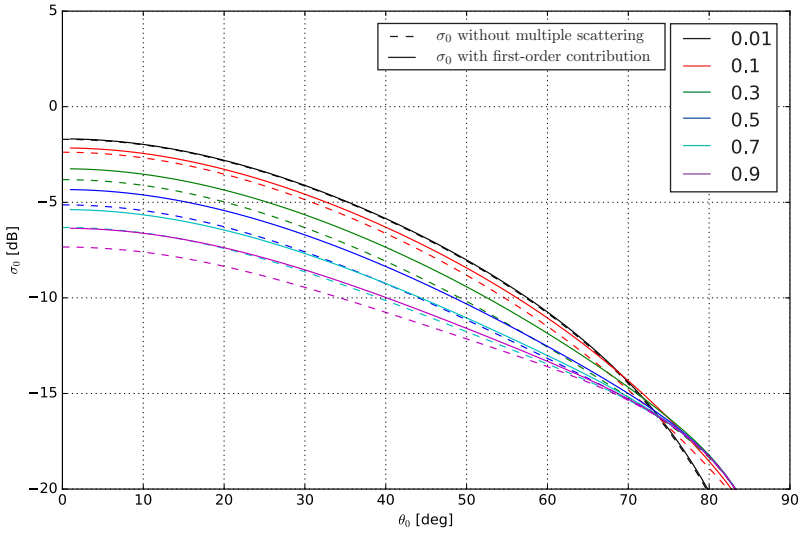

Figure 4.14.: Surface asymmetry-parameter = 0.2

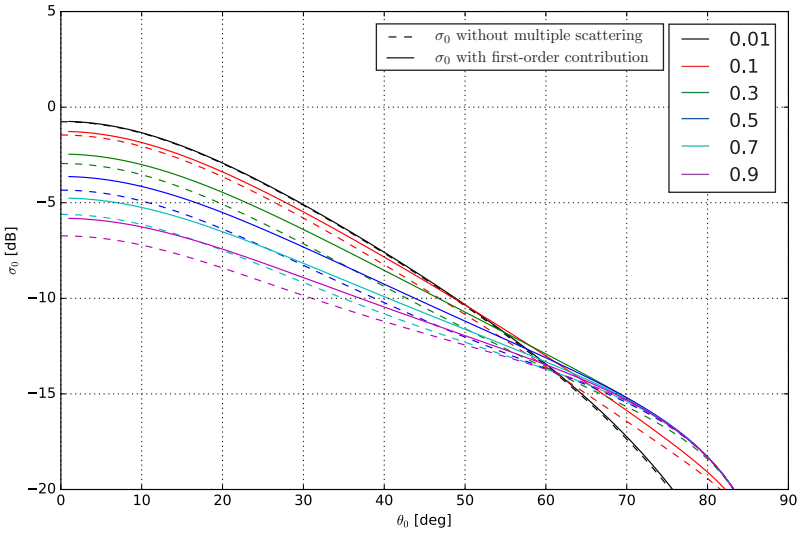

Figure 4.15.: Surface asymmetry-parameter = 0.5

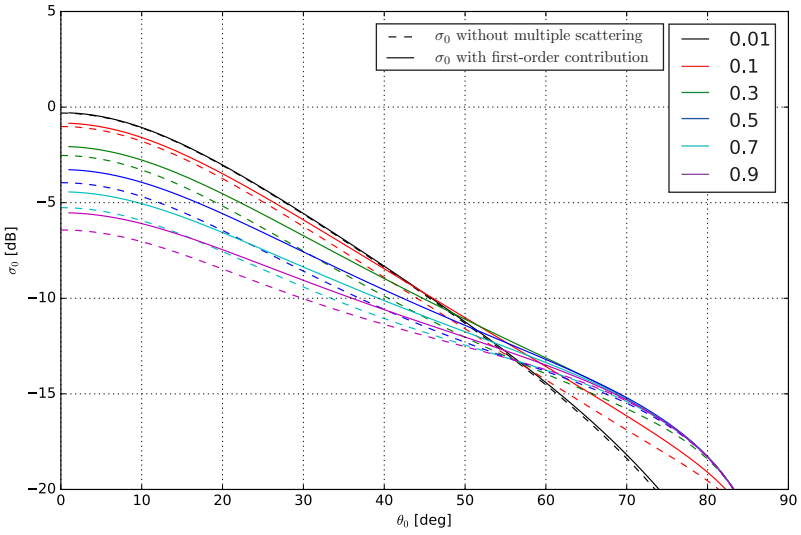

Figure 4.16.: Surface asymmetry-parameter = 0.7

4.3.7. Contributions (Isotropic)

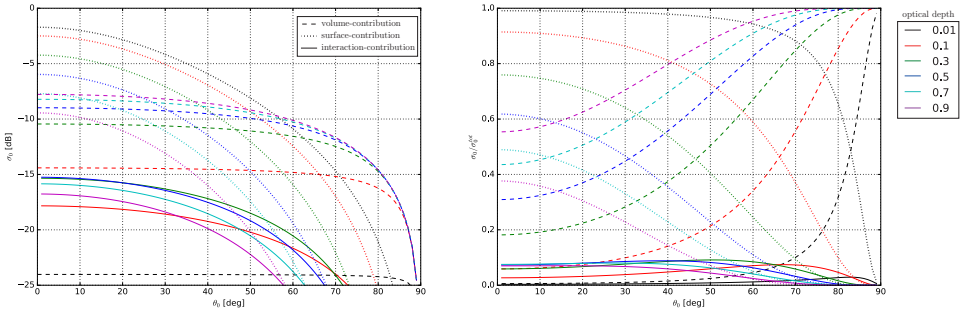

Figure 4.17.: Surface asymmetry-parameter = 0.2

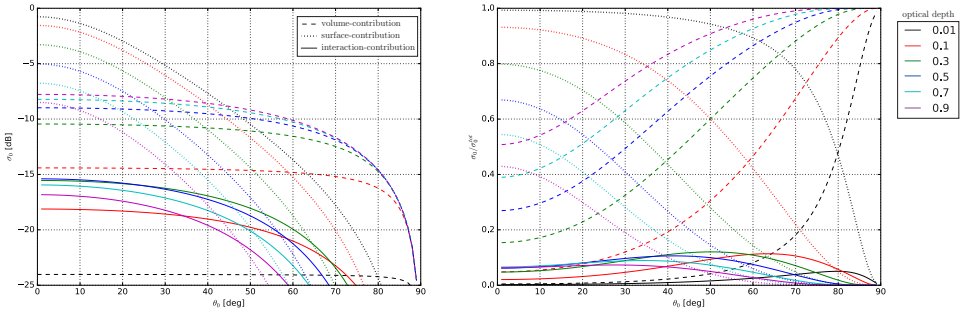

Figure 4.18.: Surface asymmetry-parameter = 0.5

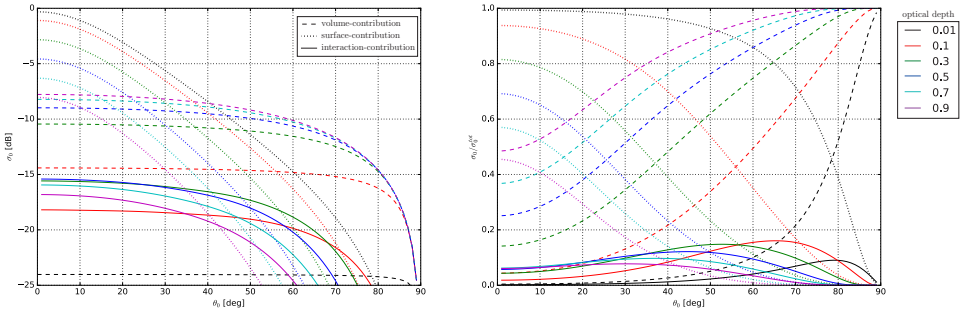

Figure 4.19.: Surface asymmetry-parameter = 0.7

4.3.8. Contributions (Rayleigh)

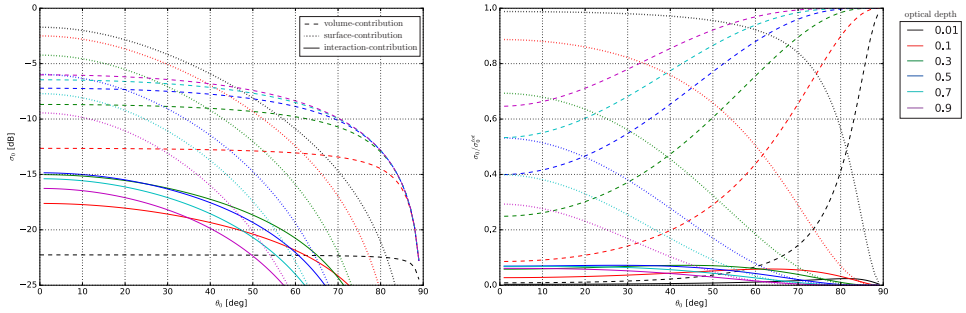

Figure 4.20.: Surface asymmetry-parameter = 0.2

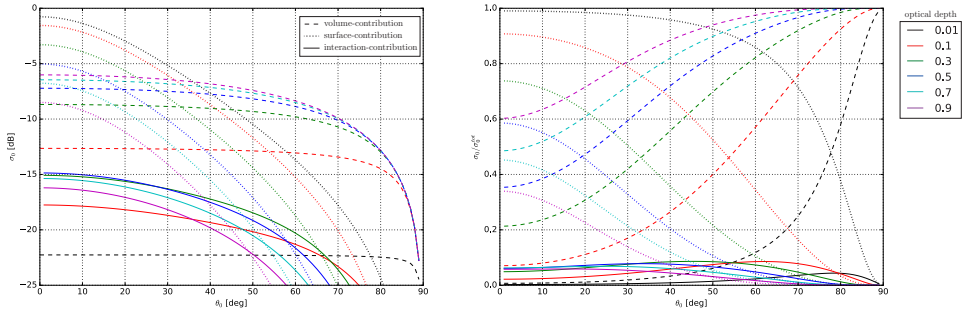

Figure 4.21.: Surface asymmetry-parameter = 0.5

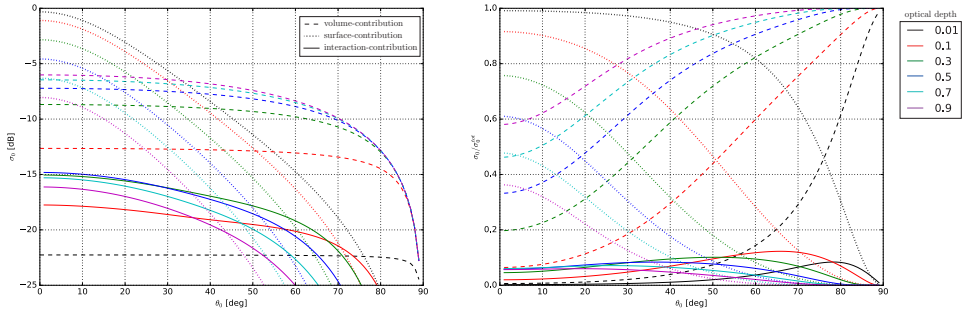

Figure 4.22.: Surface asymmetry-parameter = 0.7

4.3.9. Contributions (Henyey Greenstein $t = 0.2$)

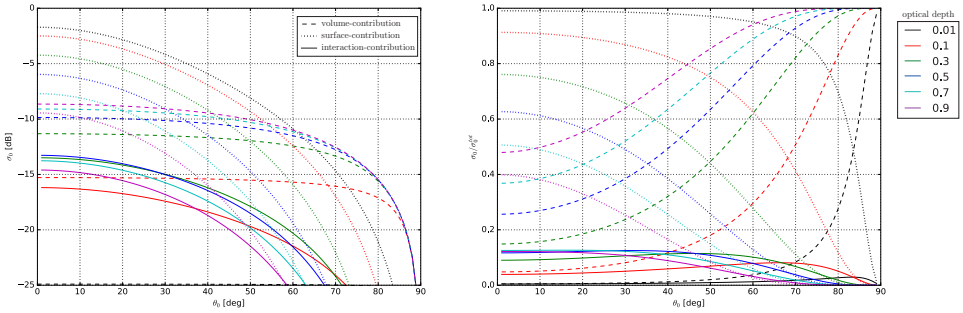

Figure 4.23.: Surface asymmetry-parameter = 0.2

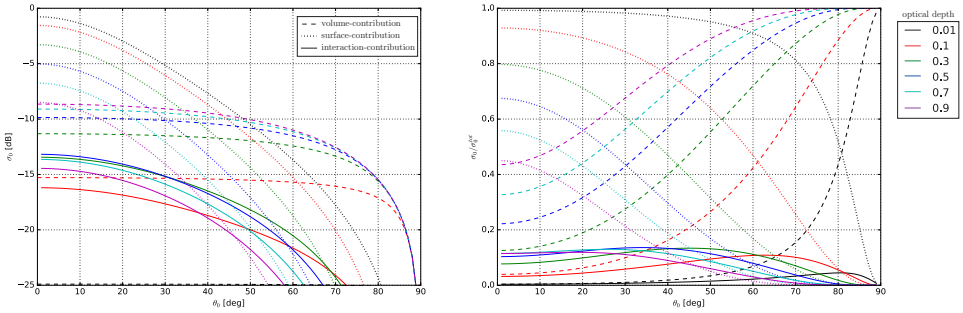

Figure 4.24.: Surface asymmetry-parameter = 0.5

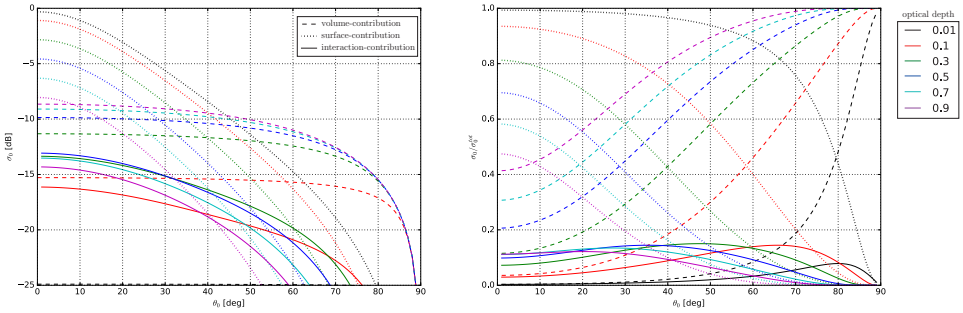

Figure 4.25.: Surface asymmetry-parameter = 0.7

4.3.10. Contributions (Henyey Greenstein $t = 0.4$)

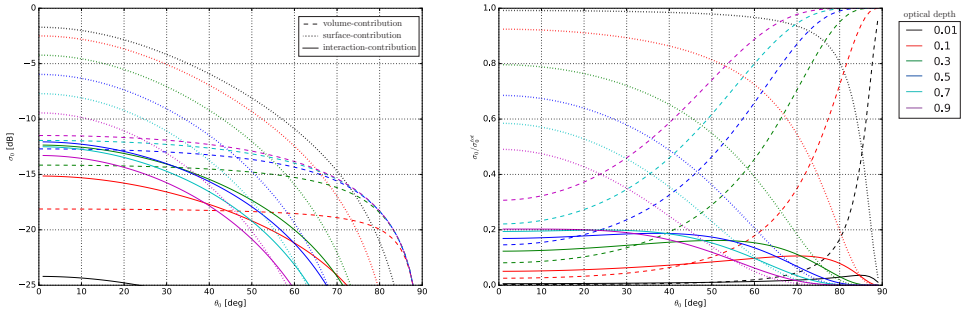

Figure 4.26.: Surface asymmetry-parameter = 0.2

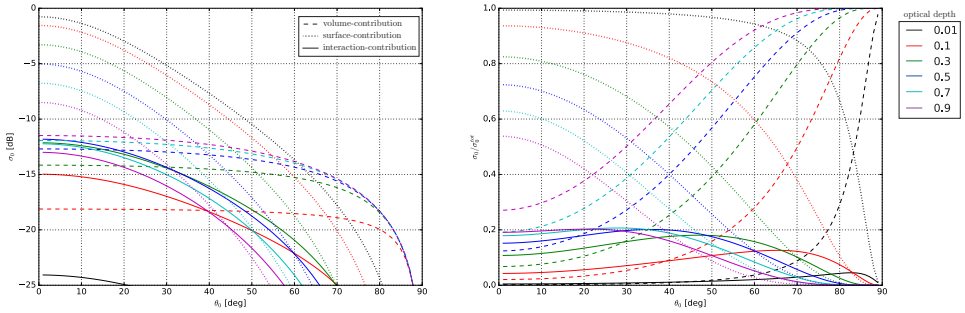

Figure 4.27.: Surface asymmetry-parameter = 0.5

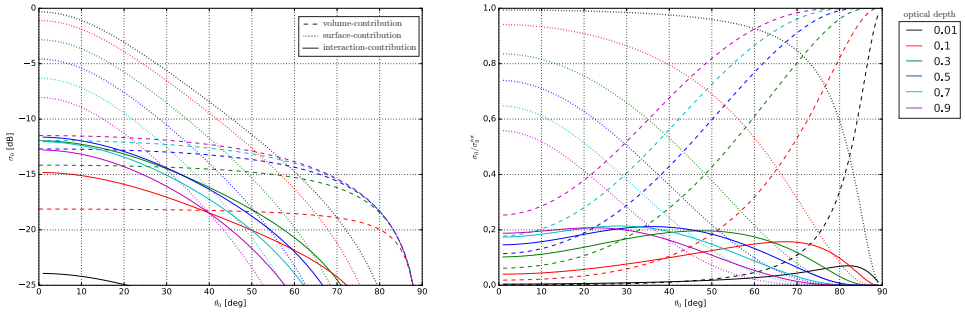

Figure 4.28.: Surface asymmetry-parameter = 0.7

A. Appendix

A.1. Used symbols and definitions

Symbol	Unit	Definition	Reference
r	$[m]$	Vertical distance within the covering layer	Fig.2.3
d	$[m]$	Total height of the covering layer	Fig.2.3
Ω	–	Placeholder for function-arguments (θ, ϕ) $f(\Omega) = f(\theta, \phi)$	-
θ_i, ϕ_i θ_{ex}, ϕ_{ex}	[deg]	Polar- and azimuth angle of incident (i)- and exiting (ex)-radiation in a right-handed spherical coordinate system	Fig.2.3
θ_0	[deg]	Zenith-angle of the incident radiation $\theta_0 = \pi - \theta_i$	Fig.2.3
μ_x	[1]	Cosine of the corresponding angle $\mu_x = \cos(\theta_x)$	-
$d\Omega$	$[sr]$	Differential solid angle $d\Omega = \sin(\theta)\ d\theta\ d\phi$	-
κ_s	$[m^{-1}]$	Scattering coefficient = Scattering cross section per unit volume	[33]
κ_a	$[m^{-1}]$	Absorption coefficient = Absorption cross section per unit volume	[33]
κ_{ex}	$[m^{-1}]$	Extinction coefficient = Extinction cross section per unit volume $\kappa_{ex} = \kappa_s + \kappa_a$	[33]
τ	[1]	Optical depth $\tau = \kappa_{ex}\ d$	Eq.2.10
ω	[1]	Single scattering albedo $\omega = \frac{\kappa_s}{\kappa_{ex}} = \frac{\kappa_s}{\kappa_s + \kappa_a}$	-

Symbol	Unit	Definition	Reference
I_f	$\left[\frac{W}{m^2\ sr\ Hz}\right]$	Specific Intensity $I_f = \frac{dP}{\cos(\theta)\ dA_{ill}\ d\Omega\ df}$ dP ... Power flowing through the illuminated area dA_{ill} df ... considered frequency-interval $\cos(\theta)$ ... cosine of the incidence-angle θ	[33]
I^+	$\left[\frac{W}{m^2\ sr\ Hz}\right]$	Upwelling specific intensity	Fig.2.4
I^-	$\left[\frac{W}{m^2\ sr\ Hz}\right]$	Downwelling specific intensity	Fig.2.4
$\sigma_0()$	[1]	Bistatic scattering coefficient $\sigma_0(\theta_0, \theta_s) = 4\pi \left(\frac{I_s(\theta_0,\theta_s)}{I_0}\right) \cos(\theta_s)$	Sec.4.1
$BRDF()$	$\left[sr^{-1}\right]$	Bidirectional reflectance distribution function $BRDF(\mu_i \to \mu_{ex}) := f_r(\theta_i, \phi_i, \theta_{ex}, \phi_{ex})$ with $\mu_i = \cos(\theta_i)$ and $\mu_{ex} = \cos(\theta_{ex})$ $f_r(\theta_i, \phi_i, \theta_{ex}, \phi_{ex}) = \frac{dI_{ex}(\theta_{ex},\phi_{ex})}{I_i(\theta_i,\phi_i)\ \cos(\theta_i)\ d\Omega_i}$	Sec.3.2 [25]
R()	[1]	Directional hemispherical reflectance $R(\theta_i, \phi_i) = \int_0^{2\pi} \int_0^{\pi/2} BRDF(\theta_i, \phi_i, \theta_s, \phi_s) \cos(\theta_s) \sin(\theta_s) \theta_s, \phi_s) d\theta_s d\phi_s$ In the nomenclature of [25] we have: $R(\theta_i, \phi_i) = \rho(\theta_i, \phi_i, 2\pi)$	Sec.3.2 [25]
g	[1]	Asymmetry parameter	Sec.3.1.1
$\hat{p}()$	$\left[sr^{-1}\right]$	Scattering phase function = Normalized differential scattering cross section $\hat{p}(\Omega_i \to \Omega_{ex}) = \hat{p}(\theta_i, \phi_i, \theta_{ex}, \phi_{ex})$ The normalization of the scattering phase function within this text differs from [33], i.e. we use: $\int_{4\pi}\ \hat{p}\ d\Omega = 1$	Sec.3.1 [33]
$Ei()$	[1]	Exponential integral function $Ei(x) := \int_{-\infty}^{x} \frac{e^t}{t} dt$ for $x > 0$	Sec.A.2.2 [10]
$E_n()$	[1]	Generalized exponential integral function $E_n(x) := \int_1^{\infty} \frac{e^{-xt}}{t^n} dt$ for $x > 0$	Eq.2.27 [10]

A.2. Mathematical Methods

A.2.1. Cauchy Principal Value:

In the following we will not go into details on the definition and justification of the Cauchy Principal Value, but only state it's main properties and relations needed to follow the presented solution-approaches. (for more detailed information see Chapter 11.7, Page 512 of [12]).

The reason for introducing the notion of the *Cauchy Principal Value* is, that we have to solve a definite integral from a to b where the integrand $f(x)$ encounters a first-order pole at $f(c)$ with $c \in (a, b)$. Since integrating a such a function will certainly lead to a diverging outcome, a meaningful value can only be assigned to such an integral by evaluating it's *Cauchy Principal Value*. The basic idea behind this procedure is, to split the integral at the location of the pole and write:

$$\int_a^b f(x)dx = \lim_{\epsilon \to 0} \int_a^{c-\epsilon} f(x)dx + \lim_{\epsilon \to 0} \int_{c+\epsilon}^b f(x)dx$$

The two appearing limits on the right side will again both diverge. However in some cases the limits diverge similarly but with opposite signs, and by performing both limits simultaneously, the divergences cancel each other and a solution can be obtained. Since a proper solution to the integral would require the individual limits to be convergent, the solution obtained by performing the limits simultaneously is called the *Cauchy Principal Value* of the integral.

The definition of the *Cauchy Principal Value* as taken from Page 6 of the NIST Handbook of Mathematical Functions [10] is therefore given by:

Let $c \in (a, b)$ and assume that $\int_a^{c-\epsilon} f(x)dx$ and $\int_{c+\epsilon}^b f(x)dx$ exist when $0 < \epsilon < min(c - a, b - c)$, but not necessarily when $\epsilon = 0$.

Then we define the *Cauchy Principal Value* of the integral $\int_a^b f(x)dx$ via:

$$⨍_a^b f(x)dx = \lim_{\epsilon \to 0^+} \left(\int_a^{c-\epsilon} f(x)dx + \int_{c+\epsilon}^b f(x)dx \right)$$

A.2.2. Exponential Integral Function $Ei(x)$

The *Exponential Integral Function* is defined as follows:[1]

$$Ei(x) := \fint_{-\infty}^{x} \frac{e^t}{t} dt \qquad \text{for} \quad x > 0 \tag{A.1}$$

A representation of the Exponential Integral Function with an arbitrary argument is then given by:

$$Ei\left(f(x)\right) = \fint_{-\infty}^{f(x)} \frac{e^t}{t} dt = \left| \begin{array}{l} t = f(u) \\ dt = f'(u)du \end{array} \right. = \fint_{-\infty}^{x} \frac{f'(u)}{f(u)} e^{f(u)} du \tag{A.2}$$

Since in the calculations we encounter integrals with limits $(0, 1)$, they can be expressed in terms of the Exponential Integral via:

$$\fint_{0}^{1} \frac{e^{-\frac{\tau}{\mu}}}{\mu} d\mu = \left| \begin{array}{l} u = -\frac{\tau}{\mu} \\ d\mu = \frac{\tau}{u^2} du \end{array} \right. = -\fint_{-\infty}^{-\tau} \frac{e^u}{u} du = -Ei(-\tau) \tag{A.3}$$

Furthermore in the general case we have:

$$\fint_{0}^{1} e^{f(x)} \frac{f'(x)}{f(x)} dx = \left| \begin{array}{l} u = f(x) \\ dx = \frac{1}{f'(x)} du \end{array} \right. = \fint_{f(0)}^{f(1)} \frac{e^u}{u} du = Ei(f(1)) \quad \text{if} \quad \begin{array}{l} \lim_{x \to 0} f(x) = -\infty \\ \lim_{x \to 1} f(1) \in \mathbb{R} \end{array} \tag{A.4}$$

[1] Notice that since the integrand encounters a singularity at $x = 0$, the value of the integral is given by means of its *Cauchy Principal Value*

A.3. Auxiliary Calculations

A.3.1. Solutions for Chapter 2.4.1 and 2.4.2

In the following it will be shown that:

$$\int_0^{2\pi} \cos(x)^n dx = \begin{cases} \frac{2\pi}{2^n}\binom{n}{n/2} & \text{if n} \dots \text{even} \\ 0 & \text{if n} \dots \text{odd} \end{cases} \tag{A.5}$$

In order to solve the integral we use the complex representation of $\cos(x)$. Therefore we find for the integrand:

$$\cos(x)^n = \frac{1}{2^n}\left(e^{ix} + e^{-ix}\right)^n = \frac{1}{2^n}\sum_{k=0}^{n}\binom{n}{k} e^{ikx} e^{i(n-k)x} = \frac{1}{2^n}\sum_{k=0}^{n}\binom{n}{k} e^{i(2k-n)x}$$

Inserting the representation we are thus left with:

$$\begin{aligned} \int_0^{2\pi} \cos(x)^n dx &= \frac{1}{2^n}\sum_{k=0}^{n}\binom{n}{k}\int_0^{2\pi} e^{i(2k-n)x} dx \\ &= \frac{1}{2^n}\sum_{k=0}^{n}\binom{n}{k}\left[\frac{e^{i(2k-n)x}}{i(2k-n)}\right]\Bigg|_{x=0}^{2\pi} \\ &= \frac{1}{2^n}\sum_{k=0}^{n}\binom{n}{k}\left[\frac{e^{i2\pi(2k-n)}-1}{i(2k-n)}\right] \end{aligned} \tag{A.6}$$

Since we know that:

$$e^{i2\pi n} = \cos(2\pi n) + i\sin(2\pi n) = 1 \qquad \forall n \in \mathbb{N} \tag{A.7}$$

the numerator of the summand in Eq. A.6 is zero. However, if $2k - n = 0$ also the denominator vanishes and we are left with an indeterminate form which we have to evaluate separately. Since the indeterminate form is $\frac{0}{0}$, we can use l'Hôpital's rule to find the correct value, i.e.:

$$\lim_{N\to 0}\left[\frac{e^{i2\pi N}-1}{i\ N}\right] = \lim_{N\to 0}\left[\frac{2\pi\ i\ e^{i2\pi N}}{i}\right] = 2\pi \tag{A.8}$$

Therefore we find for the summand:

$$\left[\frac{e^{i2\pi(2k-n)}-1}{i(2k-n)}\right] = \begin{cases} 2\pi & \text{for} \quad 2k = n \\ 0 & \text{else} \end{cases} \tag{A.9}$$

Since the condition $2k = n$ can only be fulfilled if n is an even number, the above statement already proves that the integral vanishes if n is odd. Inserting it in the

sum, only a single term, namely $k = \frac{n}{2}$ remains, and thus the solution is given by:

$$\int_0^{2\pi} \cos(x)^n dx = \begin{cases} \frac{2\pi}{2^n} \binom{n}{n/2} & \text{if n} \dots \text{even} \\ 0 & \text{else} \end{cases} \quad \blacksquare \tag{A.10}$$

The same trick can similarly be used to show that the above solution is also valid for $\sin(x)^n$, i.e.:

$$\int_0^{2\pi} \sin(x)^n dx == \begin{cases} \frac{2\pi}{2^n} \binom{n}{n/2} & \text{if n} \dots \text{even} \\ 0 & \text{else} \end{cases} \tag{A.11}$$

Here we use the completely similar representation:

$$\sin(x)^n = \frac{1}{(2i)^n}(e^{ix} - e^{-ix})^n = \frac{1}{(2i)^n} \sum_{k=0}^{n} \binom{n}{k} (-1)^{n-k}\ e^{i(2k-n)x} \tag{A.12}$$

Consequently we find for the integral:

$$\begin{aligned} \int_0^{2\pi} \sin(x)^n dx &= \frac{1}{(2i)^n} \sum_{k=0}^{n} \binom{n}{k} (-1)^{n-k}\ \frac{e^{i(2k-n)2\pi} - 1}{i(2k-n)} \\ &= \begin{cases} \frac{(-1)^{\frac{n}{2}}}{i^n} \frac{2\pi}{2^n} \binom{n}{n/2} & \text{if n} \dots \text{even} \\ 0 & \text{else} \end{cases} \\ &= \begin{cases} \frac{2\pi}{2^n} \binom{n}{n/2} & \text{if n} \dots \text{even} \\ 0 & \text{else} \end{cases} \quad \blacksquare \end{aligned} \tag{A.13}$$

where the last equality follows directly from the fact that n is an even number.

Finally, we have to show that:

$$\int_0^{2\pi} \sin(x)^n \cos(x)^m dx = \begin{cases} \frac{2\pi}{2^n 2^m} \sum_{k=0}^{n} \binom{n}{k} \binom{m}{\frac{n+m}{2} - k} (-1)^{m+k-\frac{n}{2}} & \text{if } n \text{ and } m \dots \text{even} \\ 0 & \text{else} \end{cases} \tag{A.14}$$

Again, the prove follows the same concept as before. Thus, after expressing the sine's and cosine's in terms of complex exponentials, applying the binomial theorem and integrating the resulting exponential function, we are left with:

$$\int_0^{2\pi} \cos(x)^n \sin(x)^m dx = \frac{1}{2^n 2^m \; i^m} \sum_{k=0}^{n} \sum_{j=0}^{m} \binom{n}{k} \binom{m}{j} (-1)^{m-j} \; \frac{e^{2\pi \; i \; (2k+2j-n-m)} - 1}{2k+2j-n-m} \tag{A.15}$$

from the above representation we can again directly see that the summand is only nonzero if $2k+2j-n-m=0$. Therefore we can conclude that $m+n$ must be an even number. Furthermore the multiplier $\frac{1}{i^m}$ indicates that the solution of the integral is complex for $m \ldots$ odd which of course cannot be true since we are integrating the product of two real-valued (non-singular) functions from 0 to 2π. Therefore we can conclude (without further investigation) that m itself (and consequently n itself) must actually be an even number.

With this insight, all that's left to do is finding the root of the denominator which is given by $j = \frac{n+m}{2} - k$ and using the insight from before that:

$$\frac{e^{2\pi \; i \; N} - 1}{N} = \begin{cases} 2\pi & \text{for} \quad N = 0 \\ 0 & \text{else} \end{cases} \tag{A.16}$$

Inserting the above finding (i.e. evaluating the j-sum) we therefore find:

$$\int_0^{2\pi} \cos(x)^n \sin(x)^m dx = \begin{cases} \frac{2\pi}{2^n 2^m} \sum_{k=0}^{n} \binom{n}{k} \binom{m}{\frac{n+m}{2} - k} (-1)^{m+k-\frac{n}{2}} & \text{if } n \text{ and } m \ldots \text{even} \\ 0 & \text{else} \end{cases} \tag{A.17}$$

■

A.3.2. Legendre-expansion of the Gaussian Peak

In the following the main steps for the calculation of the Legendre-expansion coefficients for the Gaussian peak phase function are presented.

Thus, in the following we are interested in evaluating:

$$\hat{p}(\Theta) = \frac{1}{4\pi} \left(\frac{2}{\beta} \right)^2 e^{-\frac{\Theta^2}{\beta^2}} \approx \sum_{n=0}^{N} p_n P_n[\cos(\Theta)] \tag{A.18}$$

From the general form of a Legendre-expansion, we know:

$$\begin{aligned} p_n &= \frac{2n+1}{2}\int_0^\pi \hat{p}(\Theta)P_n[\cos(\Theta)]\sin(\Theta)d\Theta \\ &= \frac{2n+1}{2}\frac{1}{4\pi}\left(\frac{2}{\beta}\right)^2\int_0^\pi e^{-\frac{\Theta^2}{\beta^2}}P_n[\cos(\Theta)]\sin(\Theta)d\Theta \end{aligned} \tag{A.19}$$

In order to be able to find an analytic solution to this integral, we notice that the Gaussian peak phase function is an even function. Since we are only interested in the values of the phase-function in the interval $\Theta \in (0,\pi)$, we can evaluate the Fourier-expansion of it's periodic continuation, and the resulting expansion will only contain *cosine*-terms, i.e. we can write:

$$e^{-\frac{\Theta^2}{\beta^2}} \hat{=} \sum_{m=0}^{\infty} a_m \cos(m\Theta) \qquad \text{for} \qquad \Theta \in (0,\pi) \tag{A.20}$$

where the expansion-coefficients are given by:

$$a_m = \frac{2}{(1+\delta_{n,0})\pi}\int_0^\pi e^{-\frac{\Theta^2}{\beta^2}}\cos(m\Theta)d\Theta \tag{A.21}$$

In order to solve the above integral we will transform it such that it can be recognized as a shifted Error-function $\mathrm{erf}(x)$ which is defined via:

$$\mathrm{erf}(x) = \frac{2}{\sqrt{\pi}}\int_0^x e^{-t^2}dt \tag{A.22}$$

Thus, using the representation of the cosine in terms of complex exponential functions we find: [2]

$$2\int_0^\pi e^{-\frac{\Theta^2}{\beta^2}}\cos(m\Theta)d\Theta = e^{-\frac{m^2\beta^2}{4}}\int_0^\pi \left[e^{-\left(\frac{\Theta}{\beta}-\frac{im\beta}{2}\right)^2} + e^{-\left(\frac{\Theta}{\beta}+\frac{im\beta}{2}\right)^2}\right]d\Theta \tag{A.23}$$

$$\begin{aligned} \Rightarrow \qquad & \left\{u = \frac{\Theta}{\beta} - \frac{im\beta}{2} \qquad v = \frac{\Theta}{\beta} + \frac{im\beta}{2}\right\} \qquad \Rightarrow \\ & = e^{-\frac{m^2\beta^2}{4}}\left[\int_{u_0}^{u_1} e^{-u^2}\ \beta\ du + \int_{v_0}^{v_1} e^{-v^2}\ \beta\ dv\right] \\ & = \frac{\sqrt{\pi}}{2}\ \beta\ e^{-\frac{m^2\beta^2}{4}}\left[\mathrm{erf}\left(\frac{\pi}{\beta}-\frac{im\beta}{2}\right) + \mathrm{erf}\left(\frac{\pi}{\beta}+\frac{im\beta}{2}\right)\right] \\ & = \sqrt{\pi}\ \beta\ e^{-\frac{m^2\beta^2}{4}}\mathrm{Re}\left[\mathrm{erf}\left(\frac{\pi}{\beta}+\frac{im\beta}{2}\right)\right] \end{aligned}$$

[2] A derivation of the identity used for the last equality can be found in [34], i.e.:
$\mathrm{Re}\left[\mathrm{erf}(a+ib)\right] = \frac{\mathrm{erf}(a+ib)+\mathrm{erf}(a-ib)}{2}$

and therefore, the Fourier-coefficients are given by:

$$a_m = \frac{\beta\ e^{-\frac{m^2\beta^2}{4}}}{\sqrt{\pi}(1+\delta_{n,0})}\mathrm{Re}\left[\mathrm{erf}\left(\frac{\pi}{\beta}+\frac{im\beta}{2}\right)\right] \tag{A.24}$$

Now that the Fourier-coefficients are found, we can go on evaluating the coefficients of the Legendre-expansion by inserting the expansion in Eq. A.19:

$$\begin{aligned} p_n &= \frac{2n+1}{2}\frac{1}{4\pi}\left(\frac{2}{\beta}\right)^2 \int_0^\pi e^{-\frac{\Theta^2}{\beta^2}} P_n[\cos(\Theta)]\sin(\Theta)d\Theta \\ &= \frac{2n+1}{2}\frac{1}{4\pi}\left(\frac{2}{\beta}\right)^2 \sum_{m=0}^{\infty} a_m \int_0^\pi \cos(m\ \Theta) P_n[\cos(\Theta)]\sin(\Theta)d\Theta \\ &= \frac{2n+1}{2}\frac{1}{4\pi}\left(\frac{2}{\beta}\right)^2 \sum_{m=0}^{\infty} a_m \int_{-1}^1 T_m(x)P_n(x)dx \end{aligned} \tag{A.25}$$

where $T_m(x)$ denote the Chebyshev-polynomials (and the substitution $x = \cos(\Theta)$ has been applied). Since the Chebyshev-polynomials $T_n(x)$ as well as the Legendre-polynomials $P_n(x)$ are polynomial of order n, and the above integral basically represents the Legendre-expansion coefficients of the Chebyshev-polynomials, the integral must vanish vor all $n > m$ due to the orthogonality-property of the Legendre-polynomials. Therefore the upper boundary of the sum actually only extends till the number of coefficients included in the Legendre-expansion (N), and we have:

$$p_n = \frac{2n+1}{2}\frac{1}{4\pi}\left(\frac{2}{\beta}\right)^2 \sum_{m=0}^{N} a_m \int_{-1}^1 T_m(x)P_n(x)dx \tag{A.26}$$

The remaining integral can once again be evaluated analytically (the major steps of the derivation can be found here: [35]) and is given by:

$$\xi(m,n) := \int_{-1}^1 T_m(x)P_n(x)dx = \begin{cases} 2 & \text{if} \quad m=n=0 \\ -\frac{1}{4}\frac{m\ \Gamma\left(\frac{m+n}{2}\right)\Gamma\left(\frac{m-n-1}{2}\right)}{\Gamma\left(\frac{m-n+2}{2}\right)\Gamma\left(\frac{m+n+3}{2}\right)} & \text{if} \quad m+n\ldots\text{even} \\ 0 & \text{else} \end{cases} \tag{A.27}$$

Using this result, the Legendre-expansion coefficients are finally found as:

$$p_n = \frac{2n+1}{2}\frac{1}{4\pi}\left(\frac{2}{\beta}\right)^2 \sum_{m=0}^{N} a_m\ \xi(m,n) \tag{A.28}$$

■

A.3.3. Nadir hemispherical reflectance of Henyey-Greenstein Function

Since we are interested in the nadir (i.e. $\theta_s = 0$) hemispherical reflectance, the generalized scattering angle is drastically simplified and reduces to:

$$\cos(\Theta) := a\cos(\theta_i)\cos(\theta_s) + \sin(\theta_i)\sin(\theta_s)\left[b\cos(\phi_i)\cos(\phi_s) + c\sin(\phi_i)\sin(\phi_s)\right]$$

$$\Rightarrow \qquad \cos(\Theta)\Big|_{\theta_s=0} = a\cos(\theta_i) \tag{A.29}$$

Therefore, the Henyey-Greenstein function at $\theta_s = 0$ is given by:

$$HG = \frac{1}{4\pi}\frac{1-t^2}{\left[1+t^2-2ta\cos(\theta_i)\right]^{3/2}} = \frac{1}{4\pi}\frac{1-t^2}{\left[1+t^2+2ta\cos(\theta_0)\right]^{3/2}} \tag{A.30}$$

Consequently, using Eq.3.10, the associated hemispherical reflectance at $\theta_s = 0$ is given by:

$$R(0) = \frac{1}{4\pi}\int_0^{2\pi}\int_0^{\pi/2}\frac{1-t^2}{1+t^2+2ta\cos(\theta)}\cos(\theta)\sin(\theta)d\theta d\phi \tag{A.31}$$

Evaluating the ϕ-integral and substituting $\mu = \cos(\theta)$, the Integral reduces to:

$$R(0) = \frac{1}{2}\int_0^1 \frac{(1-t^2)\mu}{1+t^2+2ta\ \mu}d\mu \tag{A.32}$$

With the substitution $u = 1+t^2+2at\mu$, the integral directly reduces to a sum of elementary integrals, i.e.:

$$\begin{aligned}
R(0) &= \frac{(1-t^2)}{8a^2t^2}\int_{1+t^2}^{1+t^2+2at}\left[u^{-\frac{1}{2}} - (1+t^2)\ u^{-\frac{3}{2}}\right] \\
&= \frac{(1-t^2)}{8a^2t^2}\left[2\sqrt{u} + 2\frac{(1+t^2)}{\sqrt{u}}\right]\Bigg|_{1+t^2}^{1+t^2+2at} \\
&= \frac{(1-t^2)}{4a^2t^2}\left[\frac{(1+t^2)+u}{\sqrt{u}}\right]\Bigg|_{1+t^2}^{1+t^2+2at} = \frac{(1-t^2)}{4a^2t^2}\left[\frac{2+2t^2+2at}{\sqrt{1+t^2+2at}} - \frac{2+2t^2}{\sqrt{1+t^2}}\right] \\
&= \frac{(1-t^2)}{2a^2t^2}\left[\frac{(1+t^2+at)\sqrt{1+t^2} - (1+t^2)\sqrt{1+t^2+2at}}{\sqrt{1+t^2+2at}\sqrt{1+t^2}}\right] \\
&= \frac{(1-t^2)}{2a^2t^2}\left[\frac{(1+t^2+at)\cancel{(1+t^2)} - \cancel{(1+t^2)}\sqrt{(1+t^2+2at)(1+t^2)}}{\sqrt{1+t^2+2at}\cancel{(1+t^2)}}\right] \\
&= \frac{(1-t^2)}{2a^2t^2}\left[\frac{(1+t^2+at) - \sqrt{(1+t^2+2at)(1+t^2)}}{\sqrt{1+t^2+2at}}\right]
\end{aligned} \tag{A.33}$$

■

B. Published Paper

Research Article Vol. 55, No. 20 / July 10 2016 / Applied Optics 5379

applied optics

Analytical solution for first-order scattering in bistatic radiative transfer interaction problems of layered media

RAPHAEL QUAST* AND WOLFGANG WAGNER

Department of Geodesy and Geo-Information, Vienna University of Technology, Vienna, Austria
**Corresponding author: raphael.quast@geo.tuwien.ac.at*

Received 11 March 2016; revised 31 May 2016; accepted 6 June 2016; posted 6 June 2016 (Doc. ID 260548); published 7 July 2016

An approximate solution to the *radiative transfer equation* for bistatic scattering from a rough surface covered by a tenuous distribution of particulate (scattering and absorbing) media is derived by means of a series expansion in the scattering coefficient κ_s of the covering layer up to the first order. The formulation of the successive orders of a scattering series is reviewed, and an analytic solution to the first-order interaction contribution is given by means of a series expansion of the azimuthally averaged product of the *bidirectional reflectance distribution function* of the surface and the *scattering phase function* of the covering layer.

OCIS codes: (290.0290) Scattering; (290.5880) Scattering, rough surfaces; (000.3860) Mathematical methods in physics; (280.5600) Radar; (290.7050) Turbid media; (010.5620) Radiative transfer.

http://dx.doi.org/10.1364/AO.55.005379

1. INTRODUCTION

The formulation of an approximate analytic radiative-transfer model to calculate the radiation scattered by a rough surface covered by a tenuous distribution of particulate media (also referred to as *"turbid media"*) as illustrated in Fig. 1 is discussed. Our motivation for investigating the possibility for deriving an analytical solution for first-order interaction problems stems from studies in the field of satellite-based microwave remote sensing. The effects induced by a vegetative coverage of a soil surface on the backscatter in the microwave domain are commonly treated via a zero-order approximation of the solution to the radiative transfer equation (RTE) [1–5]. However, first- and higher-order interaction contributions are either added via empirically driven correction terms or assumed to be negligible to omit the high computational effort and furthermore to circumvent the problem of under-determination since the required bistatic scattering properties of the vegetative coverage and the soil surface are generally rarely known. In the following, it is shown that, by using approximate analytic functions to represent the bistatic scattering properties, an approximation of the first-order contributions can be gained with reasonable computational effort, providing a consistent estimate of necessary corrections (applied to microwave backscatter observations) in the retrieval of soil and vegetation characteristics. For the sake of generality, the scattering distributions of the surface and the covering layer are defined as general functions.

To clarify the appearing equations, the representation of the solution to the RTE in terms of a series expansion in the scattering coefficient κ_s of the covering layer (following Fung [6] and Ulaby *et al.* [7]), based on the assumption that the covering layer can be considered as a weakly scattering medium, is reviewed. The zero-order approximation to this expansion is the widely known $\omega - \tau$ (or *water-cloud*) model as used in the remote sensing community [8]. In Section 3, the general solution to the first-order interaction contribution is presented in detail. Since the solution is based on an expansion of the azimuthally averaged product of the *bidirectional reflectance distribution function* (BRDF) and the *scattering-phase function* $\hat{p}$ of the covering layer, the existence of those expansion coefficients is briefly discussed in Section 4.

2. SUCCESSIVE ORDERS OF SCATTERING APPROXIMATION TO THE RTE

A. Separation of the RTE

The well-known RTE [9], governing the alteration of a beam of *specific intensity* $I_f(r, \Omega)$ propagating within a scattering and absorbing media described via:

- an *extinction coefficient* κ_{ex}
- a scattering coefficient κ_s along with
- a scattering phase function $\hat{p}(\Omega_i \rightarrow \Omega_i)$ describing the directionality of the scattered radiation,

1559-128X/16/205379-08 Journal © 2016 Optical Society of America

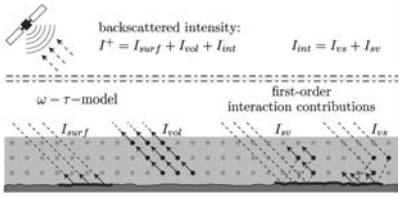

Fig. 1. Schematic illustration of the model geometry and the individual contributions considered in the calculated intensity.

is given by (neglecting the emission contributions)

$$\cos(\theta)\frac{\partial I_f(r,\Omega)}{\partial r} = -\kappa_{ex} I_f(r,\Omega) + \kappa_s \iint_{\Omega'=4\pi} I_f(r,\Omega')\hat{p}(\Omega' \to \Omega)\mathrm{d}\Omega', \quad (1)$$

where $\hat{p}(\Omega_i \to \Omega_s)$ has to obey the normalization condition

$$\int_0^{2\pi}\int_0^{\pi} \hat{p}(\Omega_i \to \Omega')\sin(\theta')\mathrm{d}\theta'\mathrm{d}\phi' = 1. \quad (2)$$

$\Omega = (\theta, \phi)$ hereby denotes the pair of polar and azimuthal angles, and $d\Omega = \sin(\theta)d\theta d\phi$ denotes the differential solid angle.

In order to increase the readability, the radial and azimuthal dependency will be suppressed in the following as long as their appearance is clearly deducible.

Noting that the integral appearing in Eq. (1) can be written (without loss of generality) as

$$\begin{aligned}\int_{\theta'=0}^{\pi} & I_f(\theta')\hat{p}(\theta' \to \theta)\sin(\theta')\mathrm{d}\theta' \\ &= \int_{\theta'=0}^{\pi/2} [I_f(\theta')\hat{p}(\theta' \to \theta)\sin(\theta') \\ &\quad + I_f(\pi - \theta')\hat{p}(\pi - \theta' \to \theta)\sin(\theta')]\mathrm{d}\theta', \end{aligned} \quad (3)$$

one can perform a separation of the RTE into a set of two coupled equations by splitting the *specific intensity* into an upwelling and downwelling part and introducing the upwelling and downwelling angle as illustrated in Fig. 2

upwelling gradiation: If $\theta \in [0, \pi/2]$

$$\theta_u := \theta \quad \text{and} \quad I^+(\theta_u) := I_f(\theta_u), \quad (4)$$

downwelling radiation: If $\theta \in [\pi/2, \pi]$

$$\theta_d := \pi - \theta \quad \text{and} \quad I^-(\theta_d) := I_f(\pi - \theta_d). \quad (5)$$

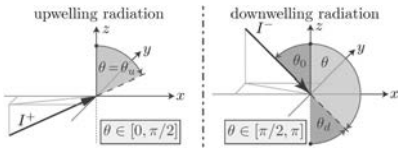

Fig. 2. Angles introduced in the separation of the RTE.

Writing Eq. (1) separately for $\theta \in [0, \pi/2]$ and $\theta \in [\pi/2, \pi]$, inserting the integral representation Eq. (3), and introducing the new angles as defined in Eqs. (4) and (5) as well as the specific notation for upwelling and downwelling radiation, one finds the following separation of the RTE (with the shorthand notation $\mu = \cos(\theta)$):

$$\boldsymbol{\theta \in [0, \pi/2]}: \quad \mu_u \frac{\partial I^+(\mu_u)}{\partial r} + \kappa_{ex} I^+(\mu_u) = F^+(\mu_u), \quad (6)$$

$$\boldsymbol{\theta \in [\pi/2, \pi]}: \quad -\mu_d \frac{\partial I^-(\mu_d)}{\partial r} + \kappa_{ex} I^-(\mu_d) = F^-(\mu_d), \quad (7)$$

where the *source functions* $F^{\pm}(\mu)$ are given by

$$\begin{aligned} F^{\pm}(\mu) = \kappa_s \int_0^{2\pi}\int_0^1 & [I^+(\mu')\hat{p}(\mu' \to \pm\mu) \\ & + I^-(\mu')\hat{p}(-\mu' \to \pm\mu)]\mathrm{d}\mu'\mathrm{d}\phi'. \end{aligned} \quad (8)$$

This set of coupled integro-differential equations can now be used as a starting point for calculating the backscattered radiation from a uniformly illuminated rough surface covered by a layer of scattering and absorbing material.

B. Problem Geometry and Boundary Conditions

In the following subsection, the problem geometry and boundary conditions are specified. As illustrated in Fig. 3, we consider a rough surface separating a homogeneous ground layer from a volume layer of depth d containing a scattering and absorbing media.

The top of the volume layer is assumed to be uniformly illuminated with an incident intensity I_{inc} incoming from a single incidence direction $\Omega_i = (\theta_i, \phi_i)$. Thus, the boundary condition at $z = 0$ can be written as

$$I^-(z = 0, \mu_d) = I_{\mathrm{inc}}\delta(\mu_d - \mu_0)\delta(\phi_d - \phi_i), \quad (9)$$

where $\delta(x - x_0)$ denotes the Dirac-delta function.

The scattering properties of the surface are described by means of BRDF$(\Omega_i \to \Omega_s)$, relating the downwelling intensity incident on the ground surface to the upwelling intensity emerging from the ground surface, i.e.,

$$\begin{aligned} I^+(z = -d, \mu_u) = \int_0^{2\pi}\int_0^1 & I^-(z = -d, \mu') \\ & \times \mathrm{BRDF}(-\mu' \to \mu_u)\mu'\mathrm{d}\mu'\mathrm{d}\phi. \end{aligned} \quad (10)$$

For physical consistency, the BRDF has to be normalized via

$$\begin{aligned} \int_0^{2\pi}\int_0^{\pi/2} & \mathrm{BRDF}(\theta_i \to \theta')\cos(\theta') \\ & \times \sin(\theta')\mathrm{d}\theta'\mathrm{d}\phi' = \rho(\theta_i, \phi_i) \le 1, \end{aligned} \quad (11)$$

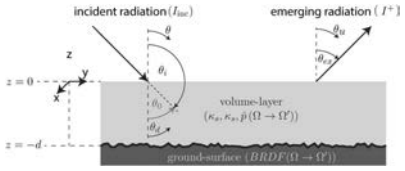

Fig. 3. Illustration of the problem geometry.

where $\rho(\theta_i, \phi_i)$ is the *directional-hemispherical reflectance* [10], describing the fraction of radiation being re-scattered into the upper hemisphere.

Furthermore, in the following, both the *volume scattering phase function* and the *BRDF* are assumed to obey **reciprocity**:

$$\mathrm{BRDF}(\theta_i \to \theta_s) = \mathrm{BRDF}(\theta_s \to \theta_i), \tag{12}$$

$$\hat{p}(\theta_i \to \theta_s) = \hat{p}(\theta_s \to \theta_i). \tag{13}$$

C. Formulation of the Scattering Series

Since Eqs. (6) and (7) still contain the unknown source terms $F^{\pm}(\mu)$, which contain integrals of the desired upwelling and downwelling intensities $I^{\pm}(\mu)$, solving this set of equations directly is generally not possible. Therefore, we restrict the following discussion to a **weakly scattering volume layer** ($\kappa_s \ll \mathbf{1}$), and assume contributions of $\mathcal{O}(\kappa_s^2)$ to be negligible. Thus, we seek an expansion of the solution in terms of a power series in κ_s.

In order to generate such a series, we will first generate a *formal solution* by considering the source terms $F^{\pm}(\mu)$ to be known functions. Doing so, one can directly solve Eqs. (6) and (7) by using the method of variation of constants, which leads to the following formal solutions for upwelling and downwelling radiation:

$$I^{+}(z,\mu_u) = I^{+}(-d,\mu_u)\exp\left[-\frac{\kappa_{ex}}{\mu_u}(z+d)\right] + \int_{-d}^{z}\frac{1}{\mu_u}\exp\left[-\frac{\kappa_{ex}}{\mu_u}(z-z')\right]F^{+}(z',\mu_u)\mathrm{d}z', \tag{14}$$

$$I^{-}(z,\mu_d) = I^{-}(0,\mu_d)\exp\left[\frac{\kappa_{ex}}{\mu_d}z\right] + \int_{z}^{0}\frac{1}{\mu_d}\exp\left[\frac{\kappa_{ex}}{\mu_d}(z-z')\right]F^{-}(z',\mu_d)\mathrm{d}z'. \tag{15}$$

Inserting the boundary conditions Eqs. (9) and (10) for the appearing boundary terms $I^{+}(-d,\mu_u)$ and $I^{-}(0,\mu_d)$, a first-order expansion of the solution for the upwelling radiation $I^{+}(\mu_u)$ in terms of κ_s can be found by successively inserting the gained solutions in the source terms Eq. (8) and neglecting all terms of $\mathcal{O}(\kappa_s^2)$ or higher. Performing the calculation, one arrives at the following representation for the upwelling radiation:

$$I^{+}(z,\mu_u) = I^{+}_{\mathrm{surf}} + \underbrace{(I^{+}_{\mathrm{vol}} + I^{+}_{\mathrm{int}} + I^{+}_{\mathrm{svs}})}_{\text{terms proportional to }\kappa_s} + \mathcal{O}(\kappa_s^2). \tag{16}$$

Assuming the interaction coefficients of the volume layer (κ_s, κ_{ex}) to be uniform within the volume layer, the first-order contributions to the upwelling radiation at the top of the layer (i.e., $z = 0$) in direction $\Omega_{ex} = (\mu_{ex}, \phi_{ex})$ are found to be given by the surface contribution

$$I^{+}_{\mathrm{surf}}(\mu_0,\mu_{ex}) = I_{\mathrm{inc}}\exp\left[-\frac{\tau}{\mu_0}-\frac{\tau}{\mu_{ex}}\right]\mu_0\mathrm{BRDF}(-\mu_0\to\mu_{ex}), \tag{17}$$

the volume contribution

$$I^{+}_{\mathrm{vol}}(\mu_0,\mu_{ex}) = \frac{I_{\mathrm{inc}}\omega\mu_0}{\mu_0+\mu_{ex}}\left(1-\exp\left[-\frac{\tau}{\mu_0}-\frac{\tau}{\mu_{ex}}\right]\right)\hat{p}(-\mu_0\to\mu_{ex}), \tag{18}$$

and the first-order interaction contribution

$$I^{+}_{\mathrm{int}}(\mu_0,\mu_{ex}) = I_{\mathrm{inc}}\mu_0\omega\left\{\exp\left[-\frac{\tau}{\mu_{ex}}\right]F_{\mathrm{int}}(\mu_0,\mu_{ex}) + \exp\left[-\frac{\tau}{\mu_0}\right]F_{\mathrm{int}}(\mu_{ex},\mu_0)\right\}, \tag{19}$$

where the remaining interaction integral F_{int} is given by

$$F_{\mathrm{int}}(\mu_0,\mu_{ex}) = \int_0^{2\pi}\int_0^1 \frac{\mu'}{\mu_0-\mu'}\left(\exp\left[-\frac{\tau}{\mu_0}\right]-\exp\left[-\frac{\tau}{\mu'}\right]\right) \times \hat{p}(\mu_0\to\mu')\mathrm{BRDF}(-\mu'\to\mu_{ex})\mathrm{d}\mu'\mathrm{d}\phi', \tag{20}$$

and the following quantities have been introduced:

$$\text{Single Scattering Albedo: } \omega = \frac{\kappa_s}{\kappa_{ex}}, \tag{21}$$

$$\text{Optical Depth: } \tau = \kappa_{ex} d. \tag{22}$$

The third first-order contribution appearing in Eq. (16) denoted by I_{svs} would describe radiation that has been scattered once by the volume layer and twice by the surface. Even though this contribution is also directly proportional to κ_s, its contribution will not be considered in the following since it is a second-order surface scattering contribution. Validation of the negligibility of this contribution has to be done with respect to the considered problem specifications using, e.g., numerical simulations. (For microwave scattering from forest canopies, this can be seen, for example, from the simulations in [11].)

3. GENERAL ANALYTIC SOLUTION TO THE FIRST-ORDER INTERACTION CONTRIBUTION

In the following, it will be shown that an analytic solution to the remaining integral of the interaction contribution can be found by assuming that the following series expansion of the ϕ-averaged product of the BRDF and the *volume scattering phase function* $\hat{p}$ exists and that the functions f_n of this expansion are known

$$\int_0^{2\pi}\hat{p}(\mu_0\to\mu_s)\mathrm{BRDF}(-\mu_s\to\mu_{ex})\mathrm{d}\phi_s = \sum_{n=0}^{\infty} f_n(\mu_0,\mu_{ex})\mu_s^n. \tag{23}$$

Inserting the expansion of Eq. (23) in Eq. (20), the integral simplifies to

$$F_{\mathrm{int}}(\mu_0,\mu_{ex}) = \sum_{n=0}^{\infty} f_n(\mu_0,\mu_{ex})[\exp(-\tau/\mu_0)A(n+1) - B(n+1)], \tag{24}$$

where the remaining integrals $A(N)$ and $B(N)$ are given by

$$A(N) = \int_0^1 \frac{(\mu')^N}{\mu_0-\mu'}\mathrm{d}\mu', \tag{25}$$

$$B(N) = \int_0^1 \frac{(\mu')^N}{\mu_0-\mu'}\exp(-\tau/\mu')\mathrm{d}\mu'. \tag{26}$$

Since both integrals encounter a singularity at $\mu' = \mu_0$, which is certainly located on the integration path since $\mu_0 \in (0, 1)$, a meaningful solution will be obtained in the following by means of the *Cauchy principal value*.

For a function $f(x)$ encountering a singularity at $x_0 \in (a, b)$, the *Cauchy principal value* is defined by [12]

$$\mathcal{P}\int_a^b f(x)\mathrm{d}x = \lim_{\epsilon\to 0}\left(\int_a^{x_0-\epsilon} f(x)\mathrm{d}x + \int_{x_0+\epsilon}^b f(x)\mathrm{d}x\right). \tag{27}$$

In order to find a solution to the integrals Eqs. (25) and (26), we notice that we can expand the term $(\mu')^N/(\mu_0 - \mu')$ appearing in the integrands as

$$\frac{(\mu')^N}{\mu_0 - \mu'} = \frac{\mu_0^N}{\mu_0 - \mu'} - \sum_{k=1}^{N} \mu_0^{N-k}(\mu')^{k-1}. \tag{28}$$

Inserting this expansion in Eqs. (25) and (26) leads to

$$A(N) = \int_0^1 \frac{\mu_0^N}{\mu_0 - \mu'}\mathrm{d}\mu' - \sum_{k=1}^{N}\int_0^1 \mu_0^{N-k}(\mu')^{k-1}\mathrm{d}\mu', \tag{29}$$

$$B(N) = \int_0^1 \frac{\mu_0^N}{\mu_0 - \mu'}\exp(-\tau/\mu')\mathrm{d}\mu' - \sum_{k=1}^{N}\int_0^1 \mu_0^{N-k}(\mu')^{k-1}\exp(-\tau/\mu')\mathrm{d}\mu'. \tag{30}$$

As shown in Appendix A.1, the *Cauchy principal values* of the remaining integrals are found to be given by

$$\mathcal{P}\int_0^1 \frac{\mu_0^N}{\mu_0 - \mu'}\mathrm{d}\mu' = \mu_0^N \ln\left(\frac{\mu_0}{1-\mu_0}\right), \tag{31}$$

$$\int_0^1 \mu_0^{N-k}(\mu')^{k-1}\mathrm{d}\mu' = \frac{\mu_0^{N-k}}{k}, \tag{32}$$

$$\mathcal{P}\int_0^1 \frac{\mu_0^N}{\mu_0 - \mu'}\exp(-\tau/\mu')\mathrm{d}\mu' = \mu_0^N[Ei(-\tau) - \exp(-\tau/\mu_0) \times Ei(\tau/\mu_0 - \tau)], \tag{33}$$

$$\mathcal{P}\int_0^1 \mu_0^{N-k}(\mu')^{k-1}\exp(-\tau/\mu')\mathrm{d}\mu' = \mu_0^{N-k}E_{k+1}(\tau), \tag{34}$$

where $Ei(x)$ denotes the exponential integral function, and $E_n(x)$ denotes the generalized exponential integral.

Inserting Eqs. (31)–(34) in Eqs. (29) and (30), analytic solutions for the integrals $A(N)$ and $B(N)$ are given by

$$A(N) = \mu_0^N\left[\ln\left(\frac{\mu_0}{1-\mu_0}\right) - \sum_{k=1}^{N}\frac{\mu_0^k}{k}\right], \tag{35}$$

$$B(N) = \mu_0^N\left[Ei(-\tau) - \exp(-\tau/\mu_0)Ei(\tau/\mu_0 - \tau) - \sum_{k=1}^{N}\frac{E_{k+1}(\tau)}{\mu_0^k}\right]. \tag{36}$$

Finally, inserting Eqs. (35) and (36) in Eq. (24), an analytic representation of the interaction integral can be given by

$$F_{\mathrm{int}}(\mu_0, \mu_{\mathrm{ex}}) = \sum_{n=0}^{\infty} f_n(\mu_0, \mu_{\mathrm{ex}})\mu_0^{n+1}\left\{\exp(-\tau/\mu_0)\ln\left(\frac{\mu_0}{1-\mu_0}\right) - Ei(-\tau) + \exp(-\tau/\mu_0)Ei(\tau/\mu_0 - \tau) + \sum_{k=1}^{n+1}\mu_0^{-k}\left(E_{k+1}(\tau) - \frac{\exp(-\tau/\mu_0)}{k}\right)\right\}. \tag{37}$$

4. ON THE EXISTENCE OF THE EXPANSION COEFFICIENTS

The existence of the f_n coefficients Eq. (23) as needed to compute Eq. (37) is in general not assured. If, however, the phase function $\hat{p}$ and the BRDF can be expressed in terms of a power series of a generalized scalar product $(\hat{i}^T\mathbf{M}_j \cdot \hat{s})$ between an incoming $(\hat{i})$ and an outgoing $(\hat{s})$ vector as stated below, it will be shown in the following that the coefficients can (in principle) always be computed ($\hat{i}^T$ denotes the transpose of the vector $\hat{i}$).

Using spherical coordinates, we have

$$\hat{i} = \begin{pmatrix}\sin(\theta_i)\cos(\phi_i)\\ \sin(\theta_i)\sin(\phi_i)\\ \cos(\theta_i)\end{pmatrix} \qquad \hat{s} = \begin{pmatrix}\sin(\theta_s)\cos(\phi_s)\\ \sin(\theta_s)\sin(\phi_s)\\ \cos(\theta_s)\end{pmatrix}, \tag{38}$$

$$\cos(\tilde{\Theta}_i) = \hat{i}^T\mathbf{M}_i \cdot \hat{s} \quad \text{with} \quad \mathbf{M}_j = \begin{pmatrix} a_i & 0 & 0\\ 0 & b_i & 0\\ 0 & 0 & c_i\end{pmatrix}, \tag{39}$$

and, therefore,

$$\cos(\tilde{\Theta}_i) = \hat{i}^T\mathbf{M}_i \cdot \hat{s} = a_i\cos(\theta_i)\cos(\theta_s) + \sin(\theta_i)\sin(\theta_s)[b_i\cos(\phi_i)\cos(\phi_s) + c_i\sin(\phi_i)\sin(\phi_s)]. \tag{40}$$

The diagonal elements (a_i, b_i, c_i) of the weighting matrix $\mathbf{M_i}$ are hereby seen as fitting parameters that allow consideration of off-specular and anisotropic effects as proposed in [13].

Assuming that both $\hat{p}$ and the BRDF can be represented as a power series in a generalized scattering angle $\cos(\tilde{\Theta}_i)^n$, we have

$$\hat{p} \sim \sum_{n=0}^{\infty} p_n\cos(\tilde{\Theta}_1)^n \qquad \mathrm{BRDF} \sim \sum_{n=0}^{\infty} b_n\cos(\tilde{\Theta}_2)^n. \tag{41}$$

Expanding $\cos(\tilde{\Theta}_i)^n$ in the above representations, the series can be written as (with $\tilde{b}_i = b_i\cos(\phi_i)$ and $\tilde{c}_i = c_i\sin(\phi_i)$)

$$\hat{p} \sim \sum_{n=0}^{\infty}\{\alpha_n + \beta_n[\tilde{b}_1\cos(\phi_s) + \tilde{c}_1\sin(\phi_s)]^n\}, \tag{42}$$

$$\mathrm{BRDF} \sim \sum_{n=0}^{\infty}\{\gamma_n + \eta_n[\tilde{b}_2\cos(\phi_s) + \tilde{c}_2\sin(\phi_s)]^n\}, \tag{43}$$

where the coefficients $\alpha_n, \beta_n, \gamma_n$, and η_n can furthermore be represented as a series of the form

$$\alpha_n = \sum_i [\alpha_n]_i\cos(\theta_s)^i \qquad \beta_n = \sin(\theta_s)^n\sum_i [\beta_n]_i\cos(\theta_s)^i, \tag{44}$$

$$\gamma_n = \sum_i [\gamma_n]_i\cos(\theta_s)^i \qquad \eta_n = \sin(\theta_s)^n\sum_i [\eta_n]_i\cos(\theta_s)^i. \tag{45}$$

For the sake of compactness, the dependencies of the coefficients $[\alpha_n]_i$, $[\beta_n]_i$, $[\gamma_n]_i$, $[\eta_n]_i$ on the incoming and outgoing directions $(\theta_{1,2}, \phi_{1,2})$ are not mentioned explicitly. If the functions are defined as in Eq. (23), the angles would correspond to $(\theta_1, \phi_1) = (\theta_{ex}, \phi_{ex})$ and $(\theta_2, \phi_2) = (\theta_0, \phi_0)$.

Using the above representations Eqs. (42) and (43), the product between the BRDF and the volume scattering phase function can be expanded by rearranging the double series (also referred to as Cauchy-product formula) [14], i.e., $[\sum_{p=0}^{\infty} a_p][\sum_{q=0}^{\infty} b_q] = \sum_{n=0}^{\infty} c_n$ with $c_n = \sum_{k=0}^{n}(a_k b_{n-k})$,

$$\begin{aligned}\mathrm{BRDF}\cdot\hat{p} = \sum_{n=0}^{\infty}\sum_{k=0}^{n}\{&\alpha_{n-k}\gamma_k \\ &+ \beta_{n-k}\gamma_k[\tilde{b}_1\cos(\phi_s) + \tilde{c}_1\sin(\phi_s)]^{n-k} \\ &+ \eta_k\alpha_{n-k}[\tilde{b}_2\cos(\phi_s) + \tilde{c}_2\sin(\phi_s)]^{k} \\ &+ \eta_k\beta_{n-k}[\tilde{b}_1\cos(\phi_s) + \tilde{c}_1\sin(\phi_s)]^{n-k} \\ &\times[\tilde{b}_2\cos(\phi_s) + \tilde{c}_2\sin(\phi_s)]^{k}\}. \end{aligned} \tag{46}$$

Integrating the above representation with respect to ϕ_s, we find for the appearing integrals

$$\int_0^{2\pi}[\tilde{b}_1\cos(\phi_s) + \tilde{c}_1\sin(\phi_s)]^n \mathrm{d}\phi_s \begin{cases} \neq 0 & \text{if} \quad n\ldots\text{even} \\ 0 & \text{if} \quad n\ldots\text{odd} \end{cases}, \tag{47}$$

$$\begin{aligned}&\int_0^{2\pi}[\tilde{b}_1\cos(\phi_s) + \tilde{c}_1\sin(\phi_s)]^k \\ &\quad\times[\tilde{b}_2\cos(\phi_s) + \tilde{c}_2\sin(\phi_s)]^{n-k}\mathrm{d}\phi_s \begin{cases} \neq 0 & \text{if} \quad n\ldots\text{even} \\ 0 & \text{if} \quad n\ldots\text{odd} \end{cases}. \end{aligned} \tag{48}$$

Applying this result to the representation Eq. (46), one can see that in the ϕ_s-integrated product only even coefficients of β_n and η_n or products of the form $\beta_{(\text{even})}\eta_{(\text{even})}$ or $\beta_{(\text{odd})}\eta_{(\text{odd})}$ appear. In terms of the θ_s dependency of the residual terms, we thus find from Eqs. (44) and (45) that they all consist of either powers of $\cos(\theta_s)$ or even powers of $\sin(\theta_s)$, which can consequently always be represented in terms of $\cos(\theta_s)$ using $\sin(\theta_s)^{2n} = [1 - \cos(\theta_s)^2]^n$.

This therefore proves that the ϕ_s-integrated product of the BRDF and $\hat{p}$ as given in Eq. (41) can always be represented in terms of a series expansion in $\cos(\theta_s)$, ensuring the existence of the f_n coefficients needed to compute Eq. (37).

A few well-known analytic phase functions obeying this criterion are the isotropic phase function, the Rayleigh phase function, the Henyey–Greenstein and combined Henyey–Greenstein–Rayleigh phase function [15,16], as well as the Mie scattering phase function in terms of a power series expansion as proposed in [17] or general approximated phase functions using, for example, the G-δ-L method as proposed in [18]. Therein, a solution for the δ part of the phase function can readily be found since the integral Eq. (20) can directly be solved for $\hat{p}(\mu' \to \mu_{ex}) \propto \delta(\mu' - \mu_{ex})\delta(\phi' - \phi_{ex})$.

Furthermore, possible analytic BRDF are, for example, given by the *ideal diffuse (Lambert) BRDF*, arbitrary *cosine lobe models* [19], or the *Lafortune model* [13].

Examples using a Rayleigh and a Henyey–Greenstein phase function for the volume scattering phase function as well as a cosine lobe for the BRDF are given in Appendix A.2.

5. CONCLUSION

It has been shown that the first-order correction to the scattered signal originating from a rough surface covered by a tenuous distribution of particulate media can be evaluated analytically by using approximate functions to represent the surface BRDF and the scattering-phase function of the covering layer.

The gained solution remains applicable for arbitrary choices of surface and covering layer properties as long as the azimuthally averaged product of the used BRDF and the scattering-phase function can be represented in terms of a power series in the scattering angle. Moreover, in Section 4, it was proven that such a representation is always possible as long as the BRDF and the scattering-phase function can be expressed as a power series in a generalized scalar product between an incoming and an outgoing direction.

Therefore, the method is capable of providing a consistent, analytical solution to the first-order interaction contribution of the successive orders of scattering approximation to the RTE for a wide range of possible choices for the scattering characteristics of both the surface and covering layers.

APPENDIX A

A. EXPLICIT SOLUTIONS FOR THE APPEARING INTERACTION INTEGRALS

1. Calculation of Eq. (31)

In order to find the principal value of Eq. (31), we first notice that the antiderivative of the integrand is given by

$$\int \frac{\mu_0^N}{\mu_0 - \mu'}\mathrm{d}\mu' = -\mu_0^N\ln(\mu_0 - \mu') + \text{const.} \tag{A1}$$

Inserting this result in the definition of the principal value in Eq. (27), we find

$$\begin{aligned}\mathcal{P}\int_0^1 \frac{\mu_0^N}{\mu_0 - \mu'}\mathrm{d}\mu' = \mu_0^N\lim_{\epsilon\to 0}[&\ln(\mu_0) + \ln(-\epsilon) \\ &- \ln(\mu_0 - 1) - \ln(\epsilon)]. \end{aligned} \tag{A2}$$

Using the identities $\ln(a \cdot b^{\pm 1}) = \ln(a) \pm \ln(b)$, we find that the limit can readily be evaluated. Thus, the solution to the integral is given by

$$\begin{aligned}\mathcal{P}\int_0^1 \frac{\mu_0^N}{\mu_0 - \mu'}\mathrm{d}\mu' &= \mu_0^N\lim_{\epsilon\to 0}[\ln(-\epsilon\mu_0) - \ln(\epsilon[\mu_0 - 1])] \\ &= \mu_0^N\lim_{\epsilon\to 0}\left[\ln\left(\frac{-\epsilon\mu_0}{\epsilon(\mu_0 - 1)}\right)\right] \\ &= \mu_0^N\ln\left(\frac{\mu_0}{1 - \mu_0}\right). \end{aligned}$$

2. Calculation of Eq. (33)

A solution to Eq. (33) can only be given in terms of the *exponential integral function* $Ei(x)$, which is defined in [12] as

$$Ei(x) = \mathcal{P}\int_{-\infty}^{x} \frac{\exp(t)}{t}\mathrm{d}t \quad \text{with} \quad x > 0. \tag{A3}$$

To identify the integrand as an exponential integral, we split the appearing fraction as follows:

$$\frac{1}{\mu_0 - \mu'} = \frac{1}{\mu'} + \frac{\mu_0}{\mu'(\mu_0 - \mu')}. \tag{A4}$$

Inserting this representation, we find

$$\mathcal{P}\int_0^1 \frac{\mu_0^N}{\mu_0 - \mu'} \exp(-\tau/\mu')\mathrm{d}\mu' = \mu_0^N \mathcal{P}\int_0^1 \frac{\exp(-\tau/\mu')}{\mu'}\mathrm{d}\mu' + \mu_0^N \mathcal{P}\int_0^1 \frac{\mu_0 \exp(-\tau/\mu')}{\mu'(\mu_0 - \mu')}. \tag{A5}$$

The first integral can now directly be interpreted as $Ei(-\tau)$ by substituting $t = -\tau/\mu'$, i.e.,

$$\mathcal{P}\int_0^1 \frac{\exp(-\tau/\mu')}{\mu'}\mathrm{d}\mu' = \left| \begin{array}{l} t = -\tau/\mu' \\ d\mu' = \tau/t^2 dt \end{array} \right| = \mathcal{P}\int_{-\infty}^{-\tau} \frac{\exp(t)}{t}\mathrm{d}t = Ei(-\tau). \tag{A6}$$

In order to find the necessary substitution for the second integral, we notice that

$$\mathcal{P}\int_0^1 \exp[f(x)]\frac{f(x)'}{f(x)}\mathrm{d}x = \mathcal{P}\int_{f(0)}^{f(1)} \frac{e^t}{t}\mathrm{d}t = Ei[f(1)] \quad \text{if} \begin{cases} f(0) = -\infty \\ f(1) \in \mathbb{R} \end{cases},$$

a possible candidate for a function $f(\mu')$, which can be used to identify the second integral of Eq. (A5), is given by

$$f(\mu') = \frac{\tau}{\mu'} - \frac{\tau}{\mu_0} \Rightarrow \frac{f'(\mu')}{f(\mu')} = -\frac{\mu_0}{\mu'(\mu_0 - \mu')}. \tag{A7}$$

Using this function, we therefore find

$$\begin{aligned} &\mathcal{P}\int_0^1 \frac{\mu_0}{\mu'(\mu_0 - \mu')} \exp(-\tau/\mu') \\ &= -\exp\left(-\frac{\tau}{\mu_0}\right)\mathcal{P}\int_0^1 \left[-\frac{\mu_0}{\mu'(\mu_0 - \mu')}\right]\exp\left(-\frac{\tau}{\mu'} + \frac{\tau}{\mu_0}\right) \\ &= -\exp\left(-\frac{\tau}{\mu_0}\right)Ei\left(\tau - \frac{\tau}{\mu_0}\right). \end{aligned} \tag{A8}$$

Combining the results of Eqs. (A6) and (A8), we thus find

$$\mathcal{P}\int_0^1 \frac{\mu_0^N}{\mu_0 - \mu'} \exp\left(-\frac{\tau}{\mu_0}\right)\mathrm{d}\mu' = \mu_0^N\left[Ei(-\tau) - \exp\left(-\frac{\tau}{\mu_0}\right)Ei\left(\tau - \frac{\tau}{\mu_0}\right)\right]. \tag{A9}$$

3. Calculation of Eq. (34)

A solution to Eq. (34) can similarly be given in terms of the *generalized exponential integral function* $E_n(x)$, which is defined in [12] as

$$E_n(x) = \mathcal{P}\int_1^\infty \frac{\exp(-xt)}{t^n}\mathrm{d}t. \tag{A10}$$

The identification of the integral as a *generalized exponential integral function* can readily be performed via

$$\begin{aligned} &\mathcal{P}\int_0^1 \mu_0^{N-k}(\mu')^{k-1} \exp(-\tau/\mu')\mathrm{d}\mu' = \left| \begin{array}{l} t = (\mu')^{-1} \\ d\mu' = -dt/t^2 \end{array} \right| \\ &= \mu_0^{N-k}\mathcal{P}\int_1^\infty \frac{\exp(-\tau t)}{t^{k+1}}\mathrm{d}t = \mu_0^{N-k}E_{k+1}(\tau) \end{aligned} \tag{A11}$$

B. Example

In the following, two examples are shown. First, the volume scattering phase function and the BRDF are given by the Rayleigh phase function in Eq. (A12) and a cosine lobe implemented using a 10 coefficient Legendre series approximation given in Eq. (A13)

$$\hat{p}(\theta_i, \theta_s) = \frac{3}{16\pi}(1 + \cos(\Theta)^2), \tag{A12}$$

$$\begin{aligned} \mathrm{BRDF}(\theta_i, \theta_s) &= \mathrm{Max}[\cos(\Theta')^5, 0] \\ &= \sum_{n=0}^{\infty} \frac{(2n+1)15\sqrt{\pi}}{16\Gamma\left(\frac{7-n}{2}\right)\Gamma\left(\frac{8+n}{2}\right)} P_n(\cos(\Theta')) \end{aligned} \tag{A13}$$

with

$$\cos(\Theta) = \cos(\theta_i)\cos(\theta_s) + \sin(\theta_i)\sin(\theta_s)\cos(\phi_i - \phi_s), \tag{A14}$$

$$\cos(\Theta') = -\cos(\theta_i)\cos(\theta_s) + \sin(\theta_i)\sin(\theta_s)\cos(\phi_i - \phi_s). \tag{A15}$$

For the second example, the scattering distribution of the volume has been changed from the equally forward- and backward-scattering Rayleigh distribution to a primarily forward-scattering Henyey–Greenstein phase function in Eq. (A16) with an asymmetry factor of $t = 0.7$, which has been implemented using a 20 coefficient Legendre series given in Eq. (A17). The used functions are illustrated in Fig. 4, and the resulting distributions are shown in Figs. 5–8.

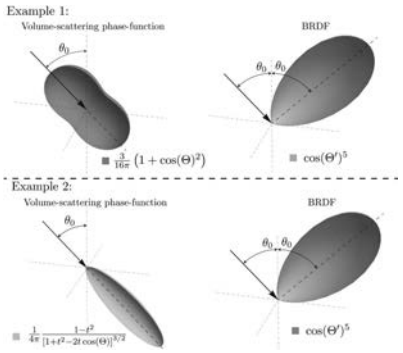

Fig. 4. Illustration of the scattering distributions in Eqs. (A12), (A13), and (A16) as used in their following examples.

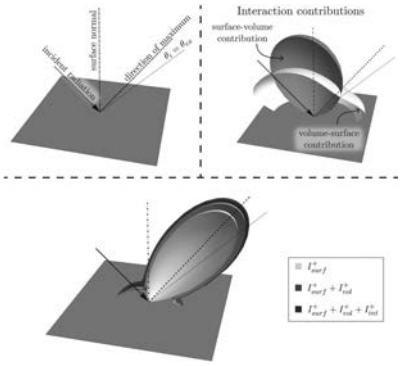

Fig. 5. Visualization of the resulting contributions in Eqs. (17)–(19) to the scattered intensity in linear scale as a function of the outgoing direction (θ_{ex}, ϕ_{ex}) using the phase functions of Fig. 4's Example 1 with $\theta_0 = 45°$, $\tau = 0.7$, and $\omega = 0.3$.

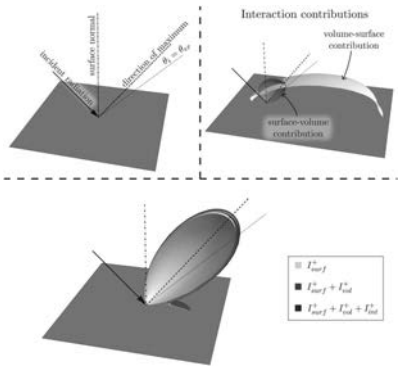

Fig. 6. Visualization of the resulting contributions in Eqs. (17)–(19) to the scattered intensity in linear scale as a function of the outgoing direction (θ_{ex}, ϕ_{ex}) using the phase functions of Fig. 4's Example 2 with $\theta_0 = 45°$, $\tau = 0.7$, and $\omega = 0.3$.

$$\hat{p}(\theta_i, \theta_s) = \frac{1}{4\pi} \frac{1 - t^2}{[1 + t^2 - 2t\cos(\Theta)]^{3/2}} \tag{A16}$$

$$= \frac{1}{4\pi} \sum_{n=0}^{\infty} (2n+1) t^n P_n(\cos(\Theta)). \tag{A17}$$

In the first example, one can see that the interaction contribution is much more significant for the backscattered radiation since the volume contribution is merely negligible for a primarily forward-scattering coverage, and the surface contribution of a cosine lobe decreases rapidly with increasing incidence angle.

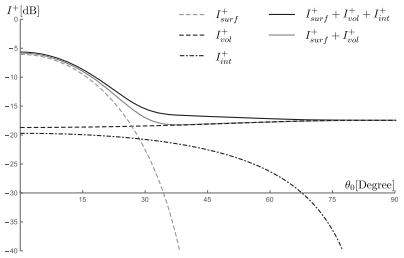

Fig. 7. Illustration of the backscattering contributions [Eqs. (17)–(19) with $\theta_{ex} = \theta_0$ and $\phi_{ex} = \pi$] in decibel scale using the phase functions of Fig. 4's Example 1 with $\tau = 0.7$ and $\omega = 0.3$.

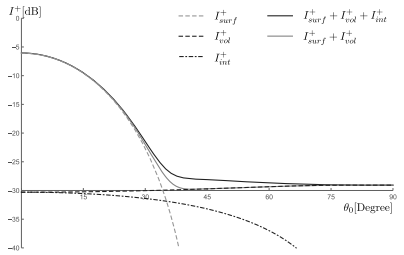

Fig. 8. Illustration of the backscattering contributions [Eqs. (17)–(19) with $\theta_{ex} = \theta_0$ and $\phi_{ex} = \pi$] in decibel scale using the phase functions of Fig. 4's Example 2 with $\tau = 0.7$ and $\omega = 0.3$.

Funding. Seventh Framework Programme (FP7) (606971).

REFERENCES

1. R. Bindlish and A. P. Barros, "Parameterization of vegetation backscatter in radar-based, soil moisture estimation," Remote Sens. Environ. **76**, 130–137 (2001).
2. O. Taconet, D. Vidal-Madjar, C. Emblanch, and M. Normand, "Taking into account vegetation effects to estimate soil moisture from C-band radar measurements," Remote Sens. Environ. **56**, 52–56 (1996).
3. J. Alvarez-Mozos, J. Casali, M. Gonzalez-Audicana, and N. Verhoest, "Assessment of the operational applicability of RADARSAT-1 data for surface soil moisture estimation," IEEE Trans. Geosci. Remote Sens. **44**, 913–924 (2006).
4. H. Lievens and N. Verhoest, "On the retrieval of soil moisture in wheat fields from L-band SAR based on water cloud modeling, the IEM, and effective roughness parameters," IEEE Geosci. Remote Sens. Lett. **8**, 740–744 (2011).

5. W. T. Crow, W. Wagner, and V. Naeimi, "The impact of radar incidence angle on soil-moisture-retrieval skill," IEEE Geosci. Remote Sens. Lett. **7**, 501–505 (2010).
6. A. Fung, *Microwave Scattering and Emission Models and Their Applications* (Artech House, 1994).
7. F. Ulaby, R. Moore, and A. Fung, *Microwave Remote Sensing* (Artech House, 1986), Vol. **3**.
8. E. P. W. Attema and F. T. Ulaby, "Vegetation modeled as a water cloud," Radio Sci. **13**, 357–364 (1978).
9. S. Chandrasekhar, *Radiative Transfer* (Clarendon, 1950).
10. F. E. Nicodemus, J. C. Richmond, J. J. Hsia, I. W. Ginsberg, and T. Limperis, *Geometric Considerations and Nomenclature for Reflectance*, (National Bureau of Standards, 1977).
11. P. Liang, L. E. Pierce, and M. Moghaddam, "Radiative transfer model for microwave bistatic scattering from forest canopies," IEEE Trans. Geosci. Remote Sens. **43**, 2470–2483 (2005).
12. F. W. Olver, D. W. Lozier, R. F. Boisvert, and C. W. Clark, *NIST Handbook of Mathematical Functions*, 1st ed. (Cambridge University, 2010).
13. E. Lafortune, S. Foo, K. Torrance, and D. Greenberg, "Non-linear approximation of reflectance functions," in *Proceedings of Conference on Computer Graphics and Interactive Techniques (SIGGRAPH)* (ACM/Addison-Wesley, 1997), pp. 117–126.
14. G. Arfken, H. Weber, and F. Harris, *Mathematical Methods for Physicists*, 7th ed. (Elsevier, 2013).
15. L. G. Henyey and J. L. Greenstein, "Diffuse radiation in the galaxy," Astrophys. J. **93**, 70–83 (1941).
16. Q. Liu and F. Weng, "Combined Henyey–Greenstein and Rayleigh phase function," Appl. Opt. **45**, 7475–7479 (2006).
17. M. A. Box, "Power series expansion of the Mie scattering phase function," Aust. J. Phys. **36**, 701–706 (1983).
18. Q. Yin and S. Luo, "An approximation frame of the particle scattering phase function with a delta function and a Legendre polynomial series," in *Light, Energy and the Environment* (Optical Society of America, 2015), paper EW3A.3.
19. B. T. Phong, "Illumination for computer generated pictures," ACM Commun. **18**, 311–317 (1975).

Bibliography

[1] E. P. W. Attema and Fawwaz T. Ulaby. Vegetation modeled as a water cloud. *Radio Science*, 13(2):357–364, 1978. ISSN 1944-799X. doi: 10.1029/RS013i002p00357. URL http://dx.doi.org/10.1029/RS013i002p00357.

[2] Brian W. Barrett, Edward Dwyer, and Pádraig Whelan. Soil moisture retrieval from active spaceborne microwave observations: An evaluation of current techniques. *Remote Sensing*, 1(3):210–242, 2009. ISSN 2072-4292. doi: 10.3390/rs1030210. URL http://www.mdpi.com/2072-4292/1/3/210.

[3] G. Macelloni, S. Paloscia, P. Pampaloni, F. Marliani, and M. Gai. The relationship between the backscattering coefficient and the biomass of narrow and broad leaf crops. *IEEE Transactions on Geoscience and Remote Sensing*, 39 (4):873–884, Apr 2001. ISSN 0196-2892. doi: 10.1109/36.917914.

[4] M. Kurum, R. H. Lang, P. E. O'Neill, A. T. Joseph, T. J. Jackson, and M. H. Cosh. A first-order radiative transfer model for microwave radiometry of forest canopies at l-band. *IEEE Transactions on Geoscience and Remote Sensing*, 49 (9):3167–3179, Sept 2011. ISSN 0196-2892. doi: 10.1109/TGRS.2010.2091139.

[5] M. Kurum, P. O'Neill, and R. Lang. Effective albedo of vegetated terrain at l-band. In *Microwave Radiometry and Remote Sensing of the Environment (MicroRad), 2012 12th Specialist Meeting on*, pages 1–4, March 2012. doi: 10.1109/MicroRad.2012.6185252.

[6] Raphael Quast and Wolfgang Wagner. Analytical solution for first-order scattering in bistatic radiative transfer interaction problems of layered media. *Appl. Opt.*, 55(20):5379–5386, Jul 2016. doi: 10.1364/AO.55.005379. URL http://ao.osa.org/abstract.cfm?URI=ao-55-20-5379.

[7] Raphael Quast, Wolfgang Wagner, and F.J.Mahringer. Formulation of the successive orders of scattering series for the radiative transfer equation applied to 2-layered media. (TU Wien Project Thesis), 2015.

[8] S. Chandrasekhar. *Radiative Transfer*. Clarendon Press, 1950.

[9] F.T. Ulaby, R.K. Moore, and A.K. Fung. *Microwave Remote Sensing (Vol. 1-3)*. Artech House, 1986.

[10] Frank W. Olver, Daniel W. Lozier, Ronald F. Boisvert, and Charles W. Clark.

NIST Handbook of Mathematical Functions 1st Edition. Cambridge University Press, 2010. ISBN 0521140633, 9780521140638.

[11] E.P.F. Lafortune, S.C. Foo, K.E. Torrance, and D.P. Greenberg. Non-linear approximation of reflectance functions. *Proceedings of SIGGRAPH'97*, pages 117–126, 1997.

[12] G.B. Arfken, H.J. Weber, and F.E. Harris. *Mathematical Methods for Physicists 7th Edition*. Elsevier Academic Press, 2013. ISBN 9780123846556.

[13] G.E. Thomas and K. Stamnes. *Radiative Transfer in the Atmosphere and Ocean*. Atmospheric and space science. Cambridge University Press, 2002. ISBN 9780521890618. URL `https://books.google.at/books?id=DxR2nEp0CUIC`.

[14] L. G. Henyey and J. L. Greenstein. Diffuse radiation in the galaxy. *Astrophysical Journal*, 93:70–83, Jan 1941. doi: 10.1086/144246.

[15] Vladimir I. Haltrin. One-parameter two-term henyey-greenstein phase function for light scattering in seawater. *Appl. Opt.*, 41(6):1022–1028, Feb 2002. doi: 10.1364/AO.41.001022. URL `http://ao.osa.org/abstract.cfm?URI=ao-41-6-1022`.

[16] Quanhua Liu and Fuzhong Weng. Combined henyey-greenstein and rayleigh phase function. *Appl. Opt.*, 45(28):7475–7479, Oct 2006. doi: 10.1364/AO.45.007475. URL `http://ao.osa.org/abstract.cfm?URI=ao-45-28-7475`.

[17] T. R. Fernandes, R. F. S. Caldeirinha, M. O. Al-nuaimi, and J. Richter. Radiative energy transfer based model for radiowave propagation in inhomogeneous forests. In *IEEE Vehicular Technology Conference*, pages 1–5, Sept 2006. doi: 10.1109/VTCF.2006.54.

[18] J. Richter, M. Al-Nuaimi, and R. Caldeirinha. Phase function measurement for modelling radiowave attenuation and scatter in vegetation based on the theory of radiative energy transfer. In *Personal, Indoor and Mobile Radio Communications, 2002. The 13th IEEE International Symposium on*, volume 1, pages 146–150 vol.1, Sept 2002. doi: 10.1109/PIMRC.2002.1046678.

[19] F. K. Schwering, E. J. Violette, and R. H. Espeland. Millimeter-wave propagation in vegetation: experiments and theory. *IEEE Transactions on Geoscience and Remote Sensing*, 26(3):355–367, May 1988. ISSN 0196-2892. doi: 10.1109/36.3037.

[20] L. O. Reynolds and N. J. McCormick. Approximate two-parameter phase function for light scattering. *J. Opt. Soc. Am.*, 70(10):1206–1212, Oct 1980. doi: 10.1364/JOSA.70.001206. URL `http://www.osapublishing.org/abstract.cfm?URI=josa-70-10-1206`.

[21] Martin Hammer, Anna N Yaroslavsky, and Dietrich Schweitzer. A scattering phase function for blood with physiological haematocrit. *Physics in Medicine and Biology*, 46(3):N65, 2001. URL `http://stacks.iop.org/0031-9155/46/i=3/a=402`.

[22] Jean-Jacques Greffet and Manuel Nieto-Vesperinas. Field theory for generalized bidirectional reflectivity: derivation of helmholtz's reciprocity principle and kirchhoff's law. *J. Opt. Soc. Am. A*, 15(10):2735–2744, Oct 1998. doi: 10.1364/JOSAA.15.002735. URL `http://josaa.osa.org/abstract.cfm?URI=josaa-15-10-2735`.

[23] W. C. Snyder. Reciprocity of the bidirectional reflectance distribution function (brdf) in measurements and models of structured surfaces. *IEEE Transactions on Geoscience and Remote Sensing*, 36(2):685–691, Mar 1998. ISSN 0196-2892. doi: 10.1109/36.662750.

[24] Marc Leroy. Deviation from reciprocity in bidirectional reflectance. *Journal of Geophysical Research: Atmospheres*, 106(D11):11917–11923, 2001. ISSN 2156-2202. doi: 10.1029/2000JD900667.

[25] F. E. Nicodemus, J. C. Richmond, J. J. Hsia, I. W. Ginsberg, and T. Limperis. Geometric considerations and nomenclature for reflectance. *National Bureau of Standards*, 1977.

[26] Hung-Wei Lee, Kun-Shan Chen, Jeng Chuan Wang, Tzong-Dar Wu, Jong-Sen Lee, and J. C. Shi. Extension of advanced integral equation model for calculations of fully polarimetric scattering coefficient from rough surface. In *2007 IEEE International Geoscience and Remote Sensing Symposium*, pages 73–76, July 2007. doi: 10.1109/IGARSS.2007.4422733.

[27] Bui Tuong Phong. Illumination for computer generated pictures. *Communications of the ACM*, 18(6):311–317, June 1975. ISSN 0001-0782. doi: 10.1145/360825.360839.

[28] K. Tomiyasu. Relationship between and measurement of differential scattering coefficient (sigma;0) and bidirectional reflectance distribution function (brdf). *IEEE Transactions on Geoscience and Remote Sensing*, 26(5):660–665, Sep 1988. ISSN 0196-2892. doi: 10.1109/36.7692.

[29] Fred E. Nicodemus. Directional reflectance and emissivity of an opaque surface. *Appl. Opt.*, 4(7):767–775, Jul 1965. doi: 10.1364/AO.4.000767. URL `http://ao.osa.org/abstract.cfm?URI=ao-4-7-767`.

[30] A. Monerris, A. Camps, and M. Vall-llossera. Empirical determination of the soil emissivity at l-band: Effects of soil moisture, soil roughness, vine canopy, and topography. In *2007 IEEE International Geoscience and Remote Sensing Symposium*, pages 1110–1113, July 2007. doi: 10.1109/IGARSS.2007.4422996.

[31] Mehmet Kurum, Peggy E. O'Neill, Roger H. Lang, Alicia T. Joseph, Michael H. Cosh, and Thomas J. Jackson. Effective tree scattering and opacity at l-band. *Remote Sensing of Environment*, 118:1 – 9, 2012. ISSN 0034-4257. doi: http://dx.doi.org/10.1016/j.rse.2011.10.024. URL `//www.sciencedirect.com/science/article/pii/S0034425711003816`.

[32] Z. Bartalis, V. Naeimi, S. Hasenauer, and W. Wagner. Ascat soil moisture product handbook. ascat soil moisture report series, no. 15,. *Institute of Photogrammetry and Remote Sensing, Vienna University of Technolog*, 2008.

[33] Leung Tsang, Jin Au Kong, and Kung-Hau Ding. *Scattering of Electromagnetic Waves: Theories and Applications*. John Wiley & Sons, 2000.

[34] Sanjar Abrarov and Brendan Quine. A rational approximation for efficient computation of the voigt function in quantitative spectroscopy. *Journal of Mathematics Research*, 7(2):163, 2015. ISSN 1916-9809. doi: 10.5539/jmr.v7n2p163.

[35] J. M. Closed form for an orthogonal polynomial integral? MathOverflow. URL `http://mathoverflow.net/q/33613`. URL:http://mathoverflow.net/q/33613 (version: 2014-05-13).